

AD-A183 174

FINAL REPORT
ON

Contract F-49620-84-C-0078

APPLICATION OF COMPUTER METHODS FOR CALCULATION
OF MULTI COMPONENT PHASE DIAGRAMS OF HIGH TEMPERATURE
STRUCTURAL CERAMICS

1 AUGUST 1984 TO 31 JULY 1987

Submitted to

Air Force Office of Scientific Research (AFSC)
Bolling Air Force Base, D.C. 20332
Att. Major Joseph Hager (202-767-4933)

by
Larry Kaufman

ManLabs, Inc.
21 Erie Street
Cambridge, Massachusetts 02139

DTIC
ELECTE
JUL 30 1987
S D

DISTRIBUTION STATEMENT A
Approved for public release;
Distribution Unlimited

REPORT DOCUMENTATION PAGE

**READ INSTRUCTIONS
BEFORE COMPLETING FORM**

1. REPORT NUMBER AFOSR-TR- 87-0920		2. GOVT ACCESSION NO.	3. RECIPIENT'S CATALOG NUMBER
4. TITLE (and Subtitle) APPLICATION OF COMPUTER METHODS FOR CALCULATION OF MULTICOMPONENT PHASE DIAGRAMS OF HIGH TEMPERATURE STRUCTURAL CERAMICS		5. TYPE OF REPORT & PERIOD COVERED FINAL REPORT AUGUST 84 to JULY 87	
7. AUTHOR(s) Larry Kaufman		6. PERFORMING ORG. REPORT NUMBER	
5. PERFORMING ORGANIZATION NAME AND ADDRESS ManLabs, Inc. 21 Erie Street Cambridge, Massachusetts 02139		8. CONTRACT OR GRANT NUMBER(s) F-49620-84-C-0078	
11. CONTROLLING OFFICE NAME AND ADDRESS Air Force Office of Scientific Research Bolling Air Force Base, D.C. 20332		10. PROGRAM ELEMENT, PROJECT, TASK AREA & WORK UNIT NUMBERS 6102F 2306 A2	
14. MONITORING AGENCY NAME & ADDRESS (if different from Controlling Office) AFOSR/NE Bldg 410 Bolling AFB, DC 20332-6448		12. REPORT DATE 31 July 1987	
		13. NUMBER OF PAGES 94	
		15. SECURITY CLASS. (of this report) Unclassified	
		15a. DECLASSIFICATION/DOWNGRADING SCHEDULE	

16. DISTRIBUTION STATEMENT (of this Report)
**Approved for public release,
distribution unlimited**

17. DISTRIBUTION STATEMENT (of the abstract entered in Block 20, if different from Report)

18. SUPPLEMENTARY NOTES

19. KEY WORDS (Continue on reverse side if necessary and identify by block number)
 Data Base' ~~Quasi-binary~~ Thermocalc,
 Phase Diagrams , ~~Quasi-ternary~~ Titanium Carbonitride,
 Structural Ceramics , Germania Ceramics, Yttria Ceramics,
 Thermochemistry, Zirconia Ceramics, Hafnia Ceramics, ←

20. ABSTRACT (Continue on reverse side if necessary and identify by block number)
 A data base is being developed for calculation of quasi-binary and quasi-ternary phase diagrams of ceramic systems. Previous segments of this base cover combinations of Cr_2O_3 , MgO , Al_2O_3 , SiO_2 , CaO , Si_3N_4 , AlN , BeO , Y_2O_3 and Ce_2O_3 . Sixty-six quasi binary and nineteen quasi ternary systems have been calculated. The current work extends the

ABSTRACT (CONCLUDED)

cont'd → base to cover GeO_2 , HfO_2 , ZrO_2 and TiO_2 which are of interest in applications requiring toughness and structural performance at high temperatures. This has been effected by employing available sources of thermochemical and phase diagram data. Recently it has been shown that by alloying GeO_2 with SiO_2 a whole range of glasses can be synthesized with tailor-made coefficients of expansion. Utilization of such compositions offers the possibility of enhancing the high temperature oxidation resistance of ceramic composites in which a mixed GeO_2 - SiO_2 phase with a desired CTE would replace the conventional SiO_2 as a filler. One of the major obstacles in the development of complex composite systems is the lack of phase diagram information which can be used to guide the fabrication and processing of a new material and help to predict its performance. The current methods of employing models to predict high temperature behaviour has proven useful when basic data is unavailable or too costly and time consuming to obtain by conventional means. This method consists of developing a data base of thermochemical and phase diagram information in analytical form and employing computer models to extend the description to binary and ternary systems. This technique was also applied in order to provide information relative to the development of oxidation resistant coatings for superalloys through calculations of the Cr-Si-Ni and Al-Ni-Si systems between 700K and 1500K to establish minimum liquidus temperatures relevant to the silicide coating technology as well as descriptions of the CrO_2 - SiO_2 and NiO- SiO_2 system was provided. Calculations of the Fe-Ni-O, Fe-Cr-O, Ti-C-N and Al_2O_3 - Y_2O_3 - ZrO_2 systems were performed on the new "Thermocalc" system developed at the Royal Institute of Technology in Stockholm. These calculations which were carried out at the Massachusetts Institute of Technology in Cambridge, Massachusetts and at the National Bureau of Standards in Gaithersburg, Maryland at locations which were remote from the "Thermocalc" programs which were stored on VAX computers.

ABSTRACT

A data base is being developed for calculation of quasi-binary and quasi-ternary phase diagrams of ceramic systems. Previous segments of this base cover combinations of Cr_2O_3 , MgO , Al_2O_3 , SiO_2 , CaO , Si_3N_4 , AlN , BeO , Y_2O_3 and Ce_2O_3 . Sixty-six quasi binary and nineteen quasi ternary systems have been calculated. The current work extends the base to cover GeO_2 , HfO_2 , ZrO_2 and TiO_2 which are of interest in applications requiring toughness and structural performance at high temperatures. This has been effected by employing available sources of thermochemical and phase diagram data. Recently it has been shown that by alloying GeO_2 with SiO_2 a whole range of glasses can be synthesized with tailor-made coefficients of expansion. Utilization of such compositions offers the possibility of enhancing the high temperature oxidation resistance of ceramic composites in which a mixed GeO_2 - SiO_2 phase with a desired CTE would replace the conventional SiO_2 as a filler. One of the major obstacles in the development of complex composite systems is the lack of phase diagram information which can be used to guide the fabrication and processing of a new material and help to predict its performance. The current methods of employing models to predict high temperature behaviour has proven useful when basic data is unavailable or too costly and time consuming to obtain by conventional means. This method consists of developing a data base of thermochemical and phase diagram information in analytical form and employing computer models to extend the description to binary and ternary systems. This technique was also applied in order to provide information relative to the development of oxidation resistant coatings for superalloys through calculations of the Cr-Si-Ni and Al-Ni-Si systems between 700K and 1500K to establish minimum liquidus temperatures relevant to the silicide coating technology as well as descriptions of the CrO_2 - SiO_2 and NiO - SiO_2 system was provided. Calculations of the Fe-Ni-O, Fe-Cr-O, Ti-C-N and Al_2O_3 - Y_2O_3 - ZrO_2 systems were performed on the new "Thermocalc" system developed at the Royal Institute of Technology in Stockholm. These calculations which were carried out at the Massachusetts Institute of Technology in Cambridge, Massachusetts and at the National Bureau of Standards in Gaithersburg, Maryland at locations which were remote from the "Thermocalc" programs which were stored on VAX computers.

TABLE OF CONTENTS

	page number
I INTRODUCTION AND SUMMARY	1
II CALCULATION OF THE Cr-Si-Ni, Al-Ni-Si CrO ₂ -SiO ₂ and NiO-SiO ₂ PHASE DIAGRAMS	4
III CALCULATION OF QUASIBINARY AND QUASI- TERNARY CERAMIC SYSTEMS	20
IV CALCULATION OF MULTICOMPONENT CERAMIC PHASE DIAGRAMS	52
V CALCULATION OF METAL-OXYGEN, METAL-CARBO- NITRIDE AND CERAMIC PHASE DIAGRAMS WITH THE THERMOCALC SYSTEM	73

I INTRODUCTION AND SUMMARY

A data base is being developed for calculation of quasi-binary and quasi-ternary phase diagrams of ceramic systems. Previous segments of this base cover combinations of Cr_2O_3 , MgO , Al_2O_3 , SiO_2 , CaO , Si_3N_4 , AlN , BeO , Y_2O_3 and Ce_2O_3 . Lattice Stability, Solution and Compound Phase Parameters have been derived covering the liquid, spinel, corundum, perilase, cristobalite, tridymite, quartz, hexagonal and beta prime phases which appear in the binary systems composed of pairs of these compounds. Compound phases formed from specific binary combinations of these compounds (i.e. $\text{MgO Cr}_2\text{O}_3$) have been characterized. This description is based on observed thermochemistry and phase diagrams for the binary systems of interest. Selected ternary systems have been computed based on the foregoing data base for comparison with experimental sections in order to illustrate the usefulness of the data base. To date, sixty-six quasi binary and nineteen quasi ternary systems have been calculated. The current work extends the base to cover GeO_2 , HfO_2 , ZrO_2 and TiO_2 . The components are of particular interest in applying ceramic systems in applications requiring toughness and structural performance at high temperatures. This has been effected by employing available sources of thermochemical and phase diagram data. High temperature ceramics have received increased attention during the last few years for structural, thermal protection and engine applications. SIALONS and combinations of zirconia and hafnia with Al_2O_3 , SiC and Si_3N_4 have been shown to develop strength and toughness. This has opened the door to a whole range of new uses for these materials. Recently Slichting and co-workers have shown that by alloying GeO_2 with SiO_2 a whole range of glasses can be synthesized with tailor-made coefficients of expansion. Utilization of such compositions offers the possibility of enhancing the high temperature oxidation resistance of ceramic composites in which a mixed GeO_2 - SiO_2 phase with a desired CTE would replace the conventional SiO_2 as a filler. This kind of compositing would open an entire spectrum of new opportunities for synthesis of high temperature ceramics. One of the major obstacles in the development of complex composite systems is the lack of phase diagram information which can be

used to guide the fabrication and processing of a new material and help to predict its performance. The current methods of employing models to predict high temperature behaviour has proven useful when basic data is unavailable or too costly and time consuming to obtain by conventional means. This method consists of developing a data base of thermochemical and phase diagram information in analytical form and employing computer models to extend the description to binary and ternary systems. Recently J. Lorenz et al. applied this method successfully to SiC-ZrO_2 and $\text{SiC-ZrO}_2\text{-Al}_2\text{O}_3\text{-SiO}_2$ in order to evaluate composition effects and identify fabrication conditions. In the present work, the data base has been expanded by analyzing the following quasi-binary systems: $\text{GeO}_2\text{-HfO}_2$, $\text{GeO}_2\text{-TiO}_2$, $\text{GeO}_2\text{-Al}_2\text{O}_3$, $\text{GeO}_2\text{-MgO}$, $\text{GeO}_2\text{-CaO}$, $\text{GeO}_2\text{-SiO}_2$, $\text{TiO}_2\text{-MgO}$, $\text{HfO}_2\text{-SiO}_2$, $\text{HfO}_2\text{-MgO}$, $\text{HfO}_2\text{-CaO}$, $\text{Al}_2\text{O}_3\text{-HfO}_2$, $\text{HfO}_2\text{-Y}_2\text{O}_3$, $\text{HfO}_2\text{-TiO}_2$, $\text{Ce}_2\text{O}_3\text{-Al}_2\text{O}_3$, $\text{ZrO}_2\text{-HfO}_2$, $\text{ZrO}_2\text{-SiO}_2$, $\text{ZrO}_2\text{-CaO}$, $\text{Y}_2\text{O}_3\text{-CaO}$, $\text{Y}_2\text{O}_3\text{-MgO}$, $\text{TiO}_2\text{-Al}_2\text{O}_3$, $\text{TiO}_2\text{-SiO}_2$, $\text{TiO}_2\text{-CaO}$ and $\text{TiO}_2\text{-Y}_2\text{O}_3$. These results when combined with earlier findings were employed to compute a range of isothermal sections in the following quasi ternary systems sufficient to define their characteristics: $\text{MgO-TiO}_2\text{-SiO}_2$, $\text{MgO-SiO}_2\text{-GeO}_2$, $\text{GeO}_2\text{-MgO-CaO}$, $\text{HfO}_2\text{-CaO-MgO}$, $\text{HfO}_2\text{-SiO}_2\text{-ZrO}_2$, $\text{HfO}_2\text{-CaO-Y}_2\text{O}_3$, $\text{HfO}_2\text{-MgO-Y}_2\text{O}_3$, $\text{HfO}_2\text{-CaO-ZrO}_2$, $\text{SiO}_2\text{-HfO}_2\text{-Y}_2\text{O}_3$, $\text{MgO-SiO}_2\text{-HfO}_2$, $\text{TiO}_2\text{-Al}_2\text{O}_3\text{-MgO}$, $\text{Al}_2\text{O}_3\text{-TiO}_2\text{-SiO}_2$, $\text{TiO}_2\text{-Al}_2\text{O}_3\text{-HfO}_2$ and $\text{MgO-SiO}_2\text{-TiO}_2$.

The coupled thermochemical/phase diagram technique was also applied in order to provide information relative to the development of oxidation resistant coatings for superalloys. Thus, calculations of the Cr-Si-Ni and Al-Ni-Si systems between 700K and 1500K in order to establish minimum liquidus temperatures relevant to the silicide coating technology. In addition a description of the $\text{CrO}_2\text{-SiO}_2$ and NiO-SiO_2 system was provided.

Finally, calculations of the Fe-Ni-O, Fe-Cr-O, Ti-C-N and $\text{Al}_2\text{O}_3\text{-Y}_2\text{O}_3\text{-ZrO}_2$ systems were performed on the new "Thermocalc" system developed at the Royal Institute of Technology in Stockholm. These calculations which were carried out at the Massachusetts Institute of Technology in Cambridge, Massachusetts and at the National Bureau of Standards in Gaithersberg, Maryland at locations which were remote from the "Thermocalc" programs which were stored on VAX computers. This work serves to illustrate how modern computing systems for calculating multicomponent phase diagrams can be used effectively to deal with a wide variety of practical problems.

The following personnel have been active in this program: L. Kaufman, D. Birnie, V. Farber, J. Pershan, E.P. Warekois, P. Neshe, J. Smith, D. Hay, M. Grujicic and W.S. Owen. The technical lectures and papers listed below were presented in connection with work performed under this contract.

1. "Calculation of Quasibinary and Quasiternary Ceramic Systems" CALPHAD XIV, M.I.T. Cambridge, MA June 1985.
2. "Calculation of Ternary Isothermal Sections in Ni-Cr-Al and Ni-Cr-Si Systems" CALPHAD XIV, M.I.T. Cambridge, MA June 1985.
3. "Binary Common Ion Alkali Halide Mixtures-Solid/Liquid Equilibria in Systems Showing Isodimorphism" CALPHAD (1986) vol. 10, No. 2 pp. 163-174.
4. "CALPHAD Generated Multicomponent Phase Diagrams for Elements II Through VI" Annual Meeting TMS-ASM, New Orleans, LA March 1986.
5. "Calculation of Multicomponent Ceramic Phase Diagrams" L. Kaufman CALPHAD XV London, England July 1986.
6. "Calculation of Quasibinary and Quasiternary Ceramic Systems" L. Kaufman, ASM symposium on USER APPLICATIONS OF PHASE DIAGRAMS, Orlando, Florida September 1986, Published July 1987.
7. "Calculation of Multicomponent Ceramic Phase Diagrams" L. Kaufman CALPHAD XVI Irsee, West Germany May 1987.
8. "Calculation of Multicomponent Ceramic Phase Diagrams" L. Kaufman, International Conference on Electronic Structure and Phase Stability of Advanced Ceramic Systems" Argonne National Laboratory Argonne Illinois, August (1987). Proceedings to be published in Physica B (1988)

II CALCULATION OF THE Cr-Si-Ni, Al-Ni-Si, CrO₂-SiO₂, and NiO-SiO₂ PHASE DIAGRAMS

Silicide coatings being considered for application to superalloy systems for special applications. Whenever such coatings are applied and the system heated the interactions between coating and base alloy can produce instabilities which reflect the phase diagram formed along the join between coating and base in specific directions. In order to gain some insight into such reactions the Cr-Si-Ni, Al-Ni-Si, CrO₂-SiO₂ and NiO-SiO₂ phase diagrams were computed along lines described earlier (1,2). The results are shown in Tables 1 and 2 and Figures 1-10 for the metallic systems and Table 3 and Figures 11 and 12 for the oxide systems. The metallic systems are based on the previous descriptions of the metal-silicon systems (3) and the Cr-Ni (4) and Ni-Al (5) systems. Tables 1 and 2 show that all of compound phases were considered to be ideal solutions and that only the ternary sigma phase was added to the Cr-Si-Ni system. Reference to Figures 1-5 shows that an extensive liquid zone exists at 1500K but this zone is virtually eliminated at 1300K. The equilibria calculated below 1300K is in agreement with experimental finding (6-8). The Al-Ni-Cr results in Figures 6-10 show extensive liquid fields at 1100K. The calculated equilibria at low temperature is in agreement with experimental results (9,10).

The calculated CrO₂-SiO₂ and NiO-SiO₂ phase diagrams shown in Figures 11 and 12 show liquids above 1880 and 1900K respectively.

TABLE 1

SUMMARY OF COMPOUND PARAMETERS FOR UNSTABLE COUNTER PHASES AND COMPOUND INTERACTION PARAMETERS IN THE Cr-Si-Ni System.

<u>Compound Chemistry</u>	<u>Name</u>	<u>Base Phase</u>	<u>C_{jk}</u> Joules/ g.at	<u>CAB</u> Joules/ g.at
(Cr,Ni) _{.75} Si _{.25}	W	B	0	0
(Cr,Ni) _{.625} Si _{.375}	U	B	0	0
(Cr,Ni) _{.5} Si _{.5}	Q	B	(Cr _{.5} Si _{.5} and Ni _{.5} Si _{.5} are stable)	0
(Cr,Ni) _{.667} Si _{.333}	Z	B	0	0
(Ni,Cr) _{.333} Si _{.667}	R	A	0	0
(Ni,Cr) _{.6} Si _{.4}	P	A	0	0
(Ni,Cr) _{.667} Si _{.333}	H	A	0	0
(Ni,Cr) _{.714} Si _{.286}	T	A	0	0
(Ni,Cr) _{.75} Si _{.25}	X	A	0	0
Cr _{.61} Si _{.11} Ni _{.28}	Sigma	B	C=13807 + 8.368T	
(Ternary Phase)(Melting Point 1522 ^o K, Entropy of Fusion=13.26 J/g.at ^o K)				

TABLE 2

SUMMARY OF COMPOUND PARAMETERS FOR UNSTABLE COUNTER PHASES AND COMPOUND INTERACTION PARAMETERS IN THE Al-Ni-Si System

<u>Compound Chemistry</u>	<u>Name</u>	<u>Base Phase</u>	<u>C_{jk}</u> Joules/ g.at	<u>CAB</u> Joules/ g.at
(Al,Si) _{.75} Ni _{.25}	V	A	0	0
(Al,Si) _{.6} Ni _{.4}	S	A	0	0
Ni _{.75} (Al,Si) _{.25}	X	A	(Ni _{.75} Al _{.25} and Ni _{.75} Si _{.25} are stable)	0
Ni _{.333} (Si,Al) _{.667}	R	A	0	0
Ni _{.5} (Si,Al) _{.5}	Q	B	0	0
Ni _{.6} (Si,Al) _{.4}	P	A	0	0
Ni _{.667} (Si,Al) _{.333}	H	A	0	0
Ni _{.714} (Si,Al) _{.286}	T	A	0	0

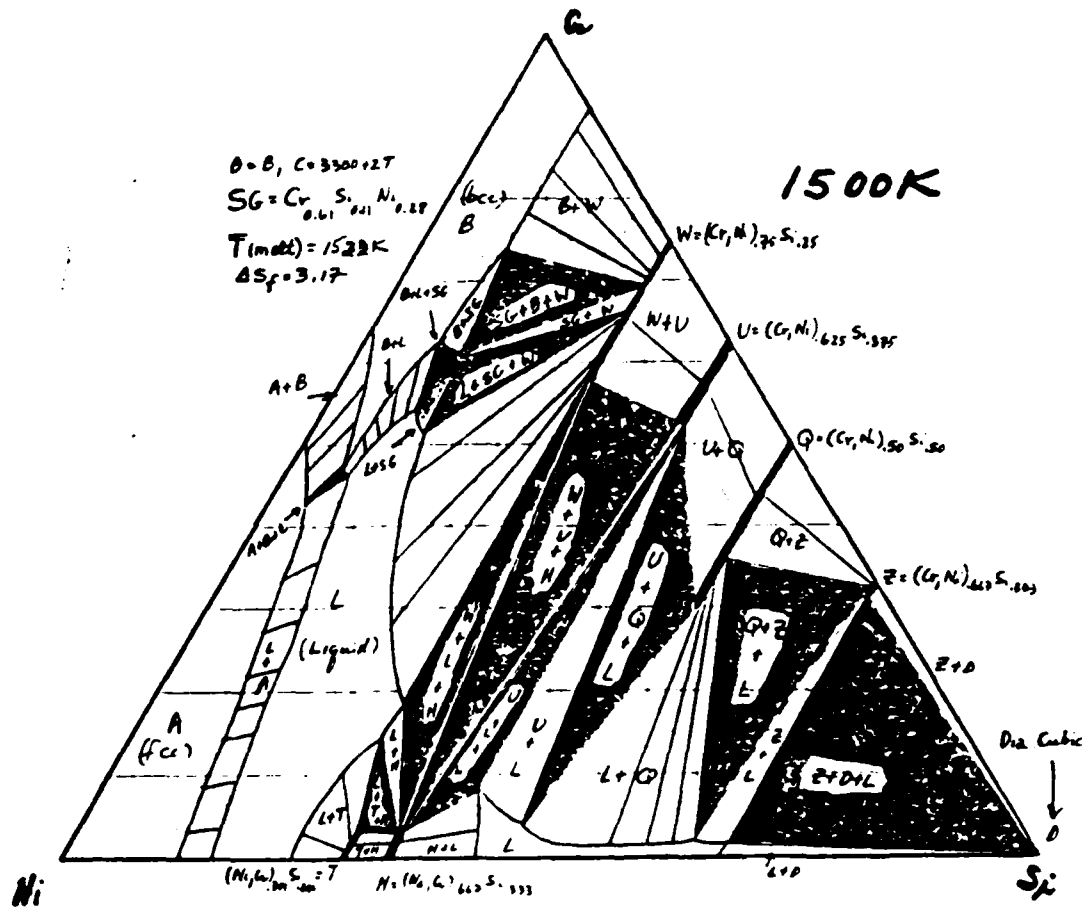


Figure 1 Calculated Isothermal Section in the Cr-Si-Ni System at 1500K

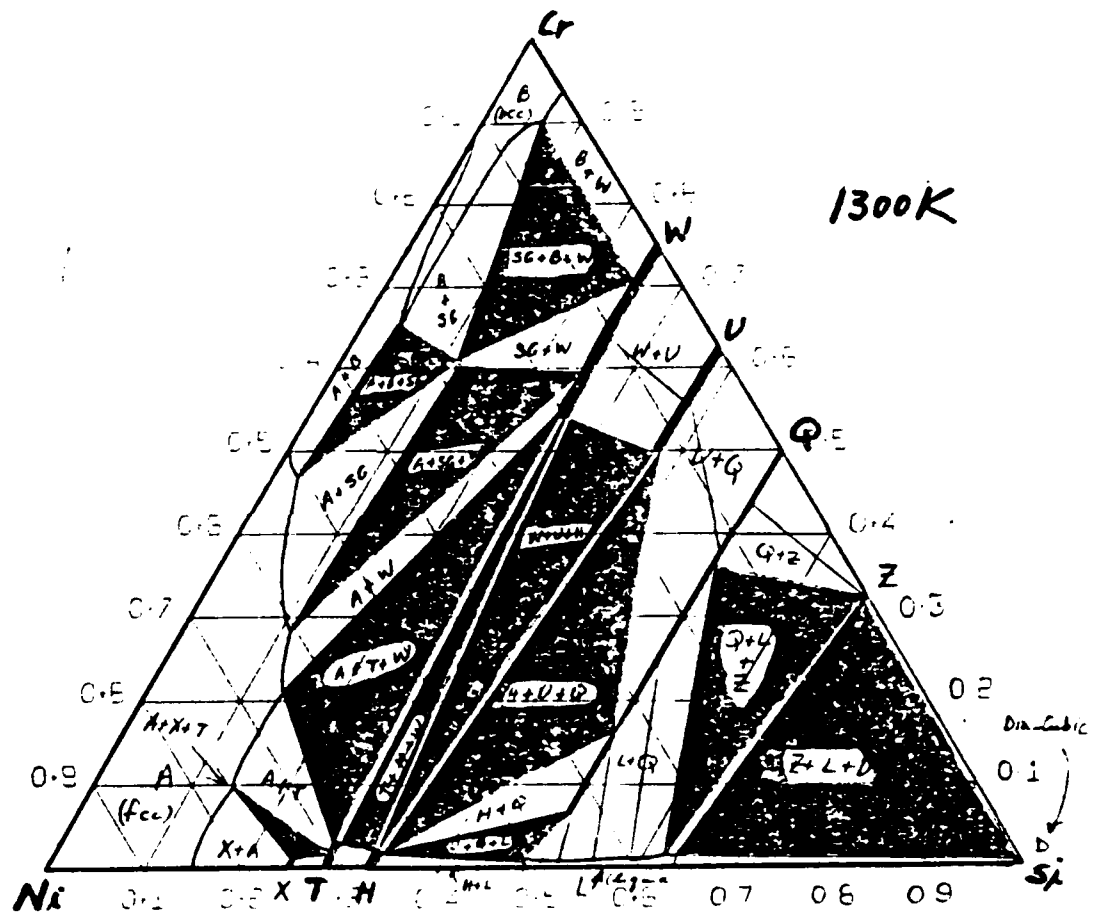


Figure 2 Calculated Isothermal Section in the Cr-Si-Ni System at 1300i.

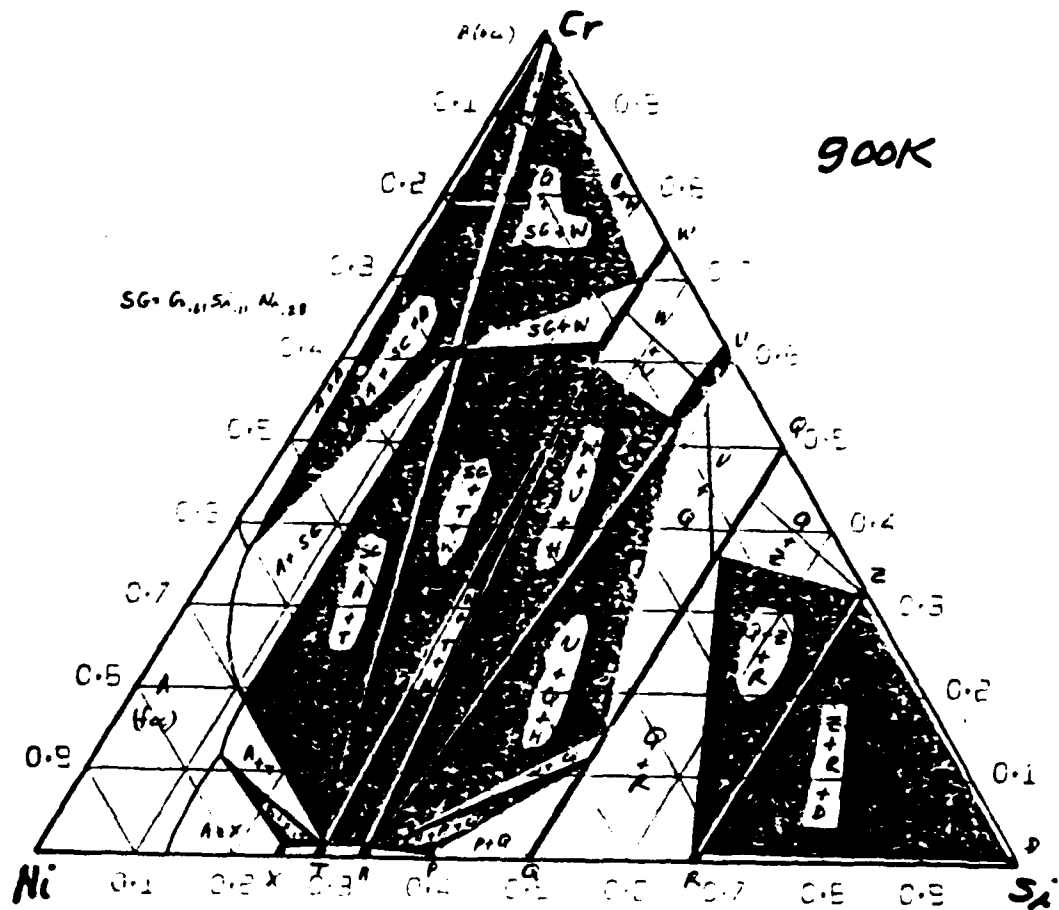


Figure 4 Calculated Isothermal Section in the Cr-Si-Ni System at 900K

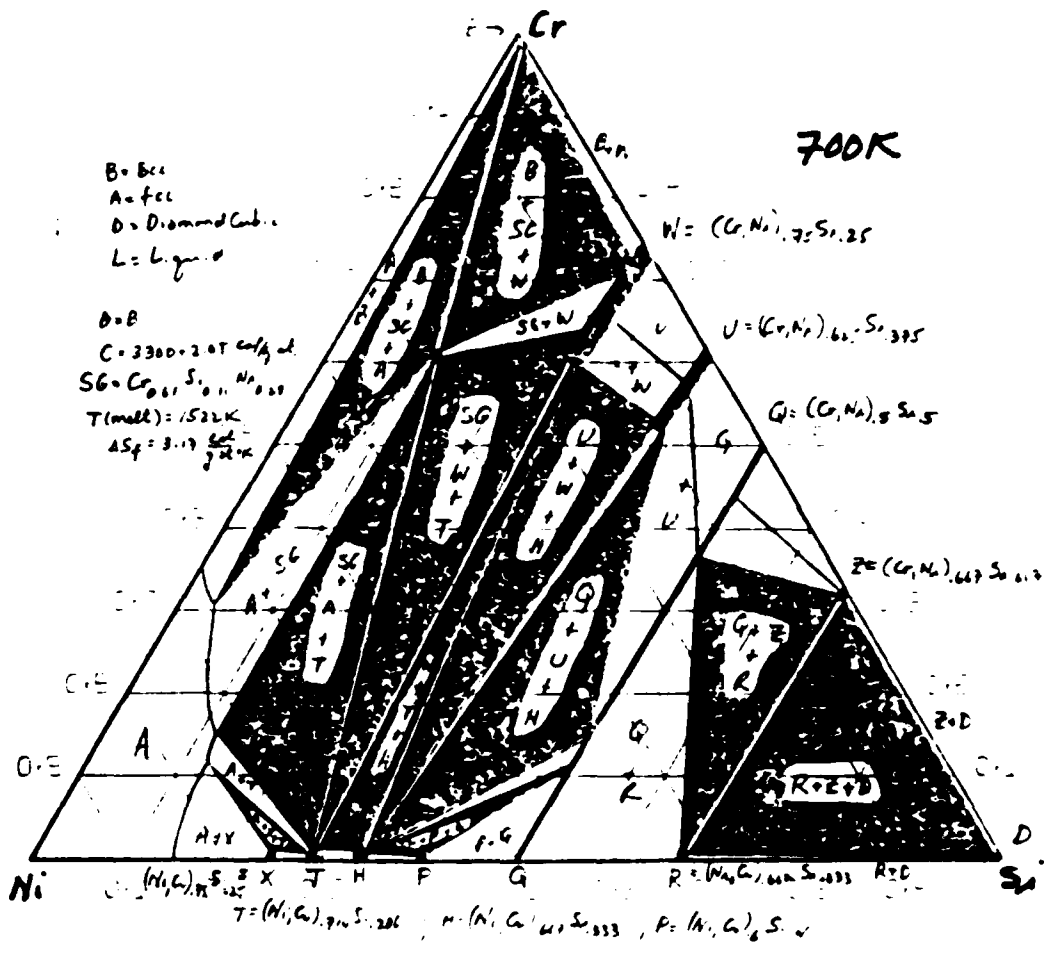


Figure 5 Calculated Isothermal Section in the Cr-Si-Ni System at 700i

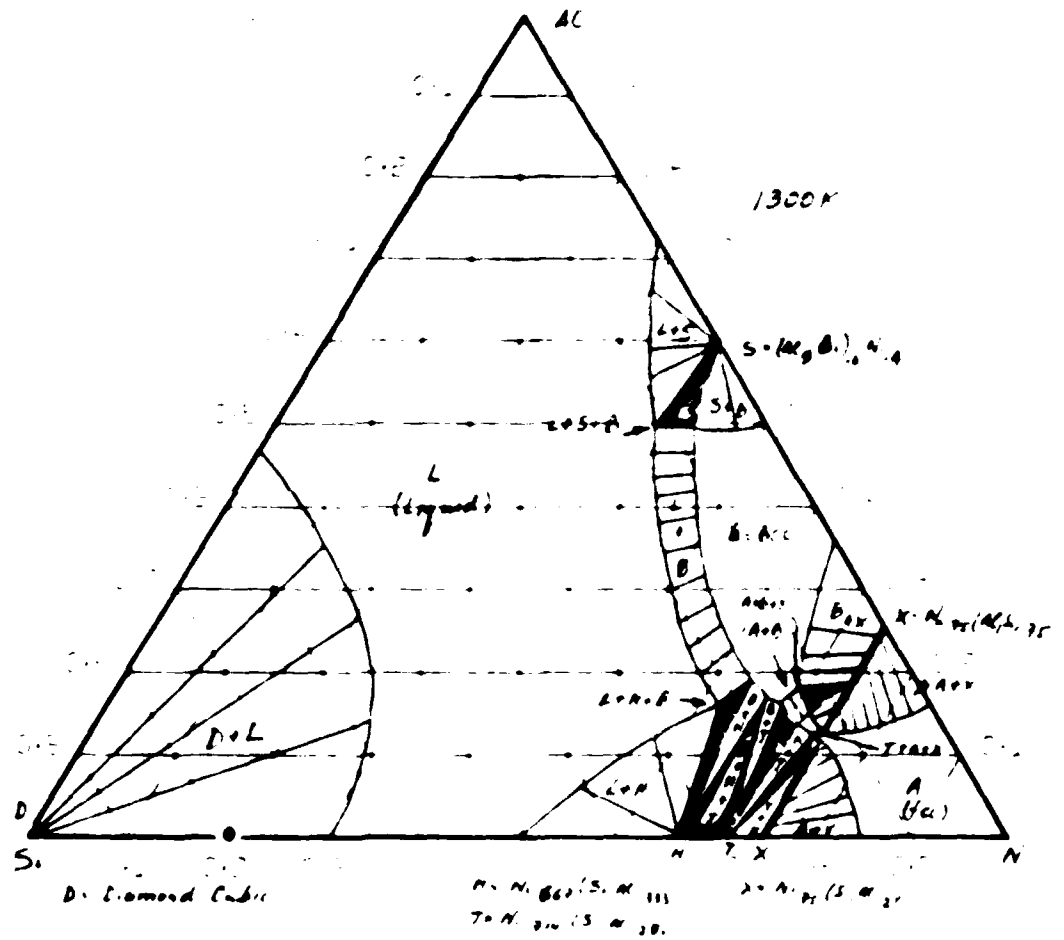


Figure 7 Calculated Isothermal Section in the Al-Ni-Si System at 1300K

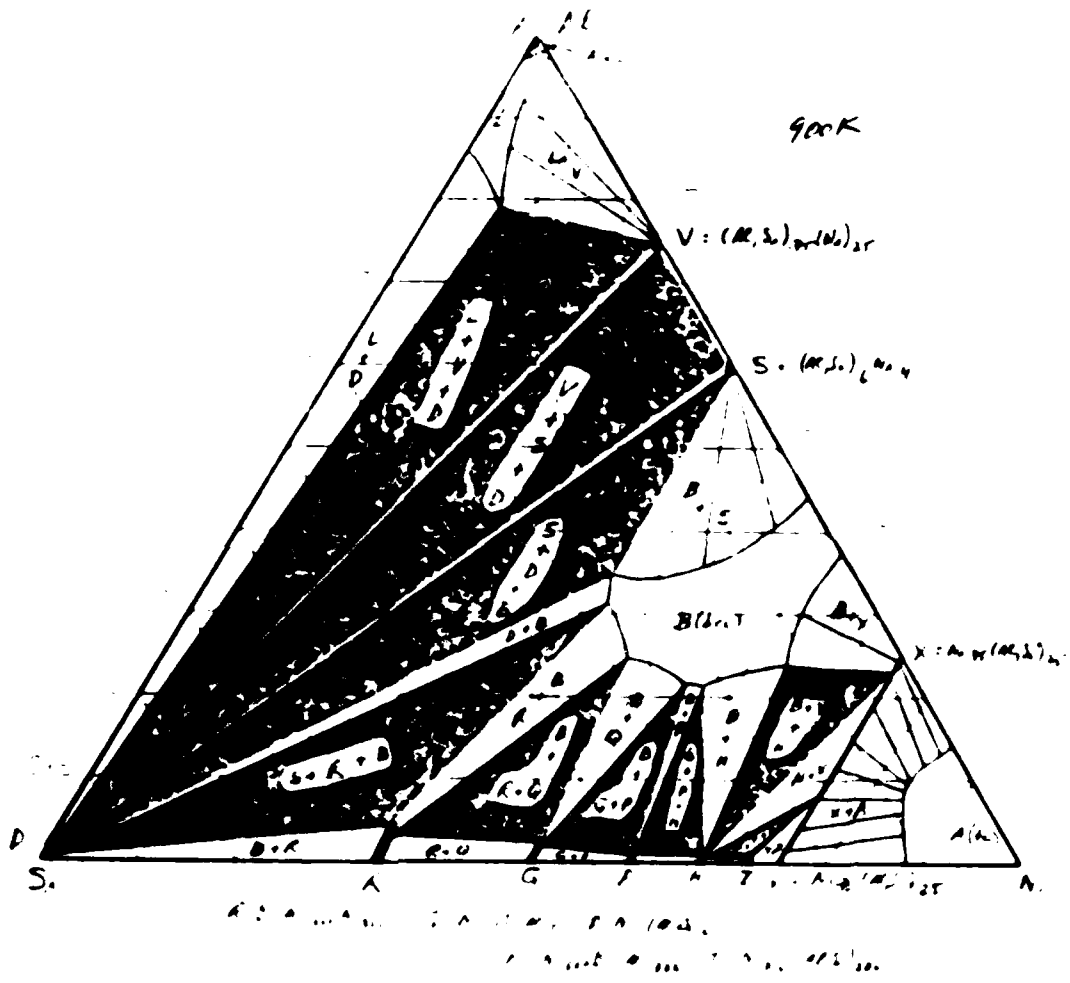


Figure 1. Calculated phase diagram for the Al-Ni-Si system at 900K.

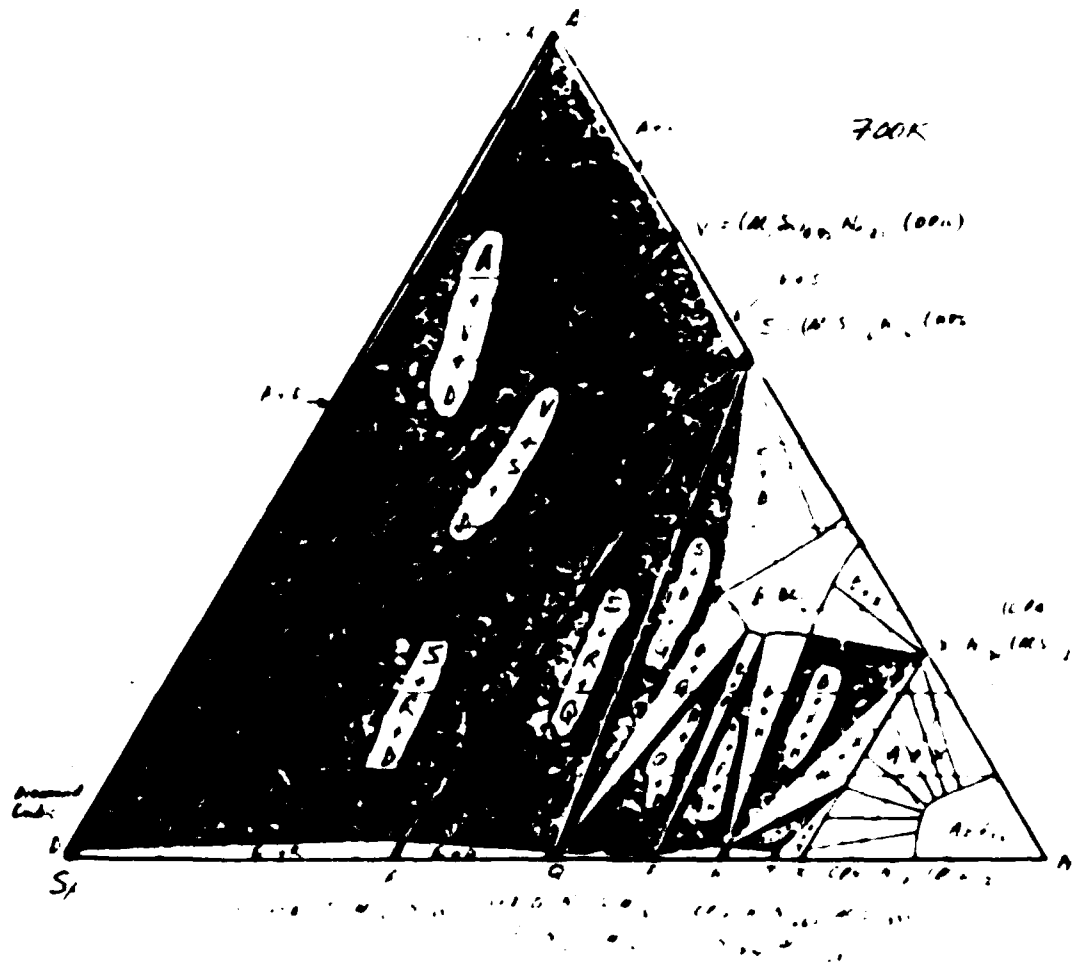


Figure 1. Ternary phase diagram of the Al-Fe-S system.

TABLE 3

SUMMARY OF LATTICE STABILITY, SOLUTION AND COMPOUND PARAMETERS FOR THE $\text{CrO}_2\text{-SiO}_2$ AND NiO-SiO_2 SYSTEMS (Units in J/g.at and J/g.at^oK)

CO = $1/3\text{CrO}_2$, NO= $1/2\text{NiO}$, CO= $1/3\text{CrO}_2$, L=Liquid, C=Corundum, X=Crystoballite, T=Trydimite, P=Periclase

COCOLC=34351-13.47T	NONOLP=25158-11.30T
COCOLX= -1.67T	NONOLX= -1.67T
SOSOLC= -2.09T	NONOLT= -2.01T
SOSOLP= -2.09T	

SOLUTION PARAMETER

LCOSO=LSOCO=68200		0<XNO<0.43
CCOSO=CSOCO=151879	LSONO=33472	LNOSO=379070-225.94T
XCOSO=XSOCO=151879	XSONO=115688-41.8T	XNOSO=400000-225.94T
TCOSO=TSOCO=151879	TSONO=115688-41.8T	TNOSO=400000-225.94T
		0.43<XNO<1.0
	LSONO=147310-97.15T	LNOSO=228166-97.15T
	PSONO=189150-97.15T	PNOSO=270006-97.15T

COMPOUND PARAMETER

FA=Payalite=($\text{SO}_{.429}\text{NO}_{.571}$)= $1/7(\text{SiO}_2 \cdot 2\text{NiO})$
 Base=P, Compound Parameter=198711-102.34T

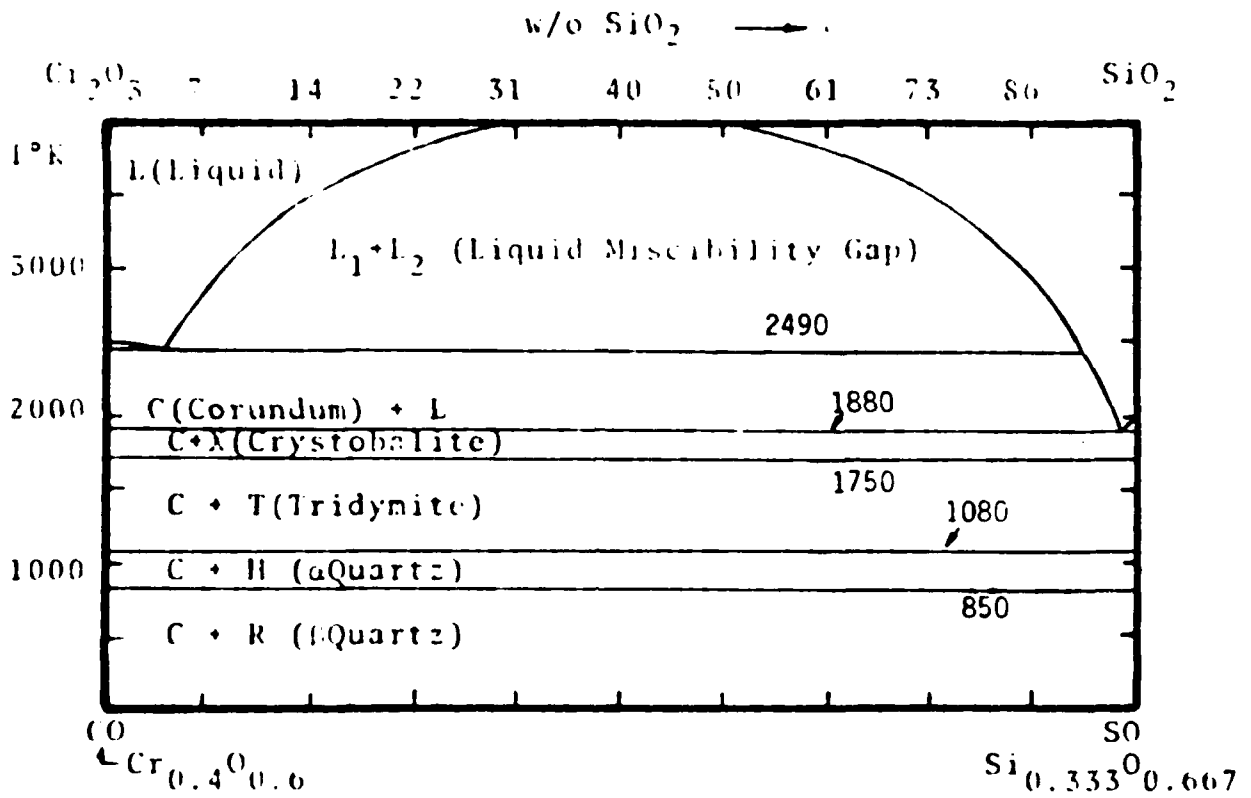


Figure 11. Calculated $\text{Cr}_{0.4}\text{O}_{0.6}-\text{Si}_{0.333}\text{O}_{0.667}$ Phase Diagram

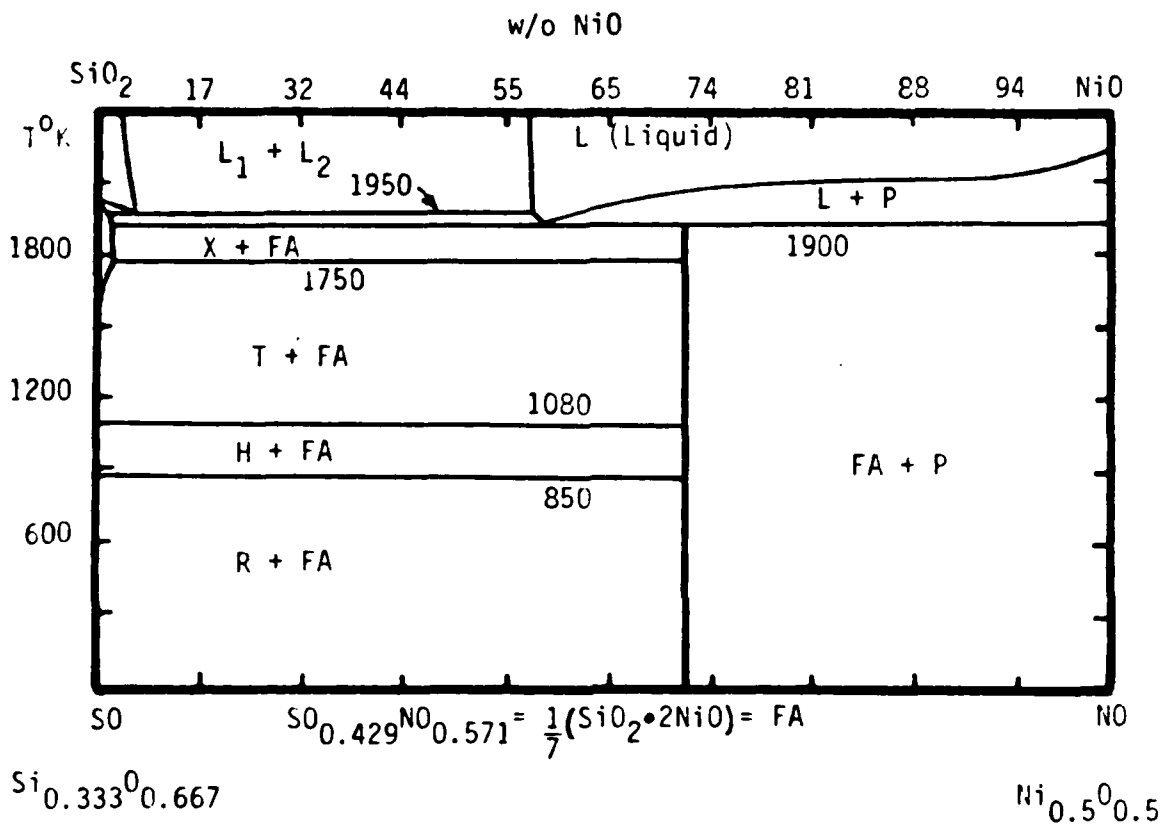


Figure 12 Calculated $\text{Si}_{0.333}\text{O}_{0.667} - \text{Ni}_{0.5}\text{O}_{0.5}$ Phase Diagram

REFERENCES

1. L. Kaufman and H. Nesor, Met. Trans. 5a 1617, 1623(1974) and 6A 2115, 2123(1975).
2. L. Kaufman and H. Nesor, CALPHAD 2 35(1978), 3 27, 279(1979).
3. L. Kaufman , CALPHAD 3 45(1979).
4. L. Kaufman, CALPHAD 1 7 (1977).
5. L. Kaufman and H. Nesor, CALPHAD 2 295 (1978).
6. T.G. Chart, F.H. Putland and A.T. Dinsdale, CALPHAD 1 40 (1980)
7. L.A. Miroshnikov, F.A. Sidorenko and A.N. Bortnik Tr. Ural'sk. Politekhn In-Ta No.186
8. E.I. Gladyshevski and L.K. Borusevich J. Neorg. Chimi 8 1915 (1963)
9. S. Ochai and T. Suzuki, Bulletin of Precision Machinery and Electronics Yokahoma, Japan No.52 p.41 (1983).
10. S. Ochia, Y. Oya and T. Suzuki, Acta Met. 32 289(1983)

III. CALCULATION OF QUASIBINARY AND QUASITERNARY CERAMIC SYSTEMS

by

Larry Kaufman
ManLabs, Inc.

21 Erie Street, Cambridge, Massachusetts 02139

(Presented October 1986, ASM Symposium on USER APPLICATIONS OF PHASE
DIAGRAMS, Orlando Florida Proceedings to be published in 1987)

ABSTRACT

A data base is being developed for calculation of quasi-binary and quasi-ternary phase diagrams of ceramic systems. Previous segments of this base cover combinations of Cr_2O_3 , MgO , Al_2O_3 , SiO_2 , CaO , Si_3N_4 , AlN , BeO , Y_2O_3 and Ce_2O_3 . Lattice Stability, Solution and Compound Phase Parameters have been derived covering the liquid, spinel, corundum, periclase, cristobalite, tridymite, quartz, hexagonal and beta prime phases which appear in the binary systems composed of pairs of these compounds. Compound phases formed from specific binary combinations of these compounds (i.e. $\text{MgO}\cdot\text{Cr}_2\text{O}_3$) have been characterized. This description is based on observed thermochemistry and phase diagrams for the binary systems of interest. Selected ternary systems have been computed based on the foregoing data base for comparison with experimental sections in order to illustrate the usefulness of the data base. The present paper extends the data base to cover GeO_2 , HfO_2 , ZrO_2 and TiO_2 . The components are of

particular interest in recent developments of structural high temperature ceramics and applications requiring unusual toughness. (6). In order to expand the data base nineteen quasi-binary systems have been analyzed and ten quasi-ternary systems have been calculated over a wide range of temperatures. These samples demonstrate the capability of the data base and computational model for dealing with phase equilibria in multicomponent oxide systems over a wide range of conditions and compositions of practical interest.

INTRODUCTION

Previous papers in the current series (1-5) provide descriptive information for computing condensed phase equilibria in ceramic systems. In view of current interest in applying ceramic systems in applications requiring toughness and structural performance at high temperatures the present data base is being extended to cover GeO_2 , HfO_2 , ZrO_2 and TiO_2 . This has been effected by employing

available sources (7-9) of thermochemical and phase diagram data. High temperature ceramics have received increased attention during the last few years for structural, thermal protection and engine applications. SIALONS and combinations of zirconia and hafnia with Al_2O_3 , SiC and Si_3N_4 have been shown to develop strength and toughness. This has opened the door to a whole range of new uses for these materials. Recently Slichting and co-workers (10-11) have shown that by alloying GeO_2 with SiO_2 a whole range of glasses can be synthesized with tailor-made coefficients of expansion. Utilization of such compositions offers the possibility of enhancing the high temperature oxidation resistance of ceramic composites in which a mixed GeO_2 - SiO_2 phase with a desired CTE could replace the conventional SiO_2 as a filler. This kind of compositing would open an entire spectrum of new opportunities for synthesis of high temperature ceramics. One of the major obstacles in the development of complex composite systems is the lack of phase diagram information which can be used to guide the fabrication and processing of a new material and help to predict its performance. The current methods of employing models to predict high temperature behaviour has proven useful when basic data is unavailable or too costly and time consuming to obtain by conventional means. This method consists of developing a data base of thermochemical and phase diagram information in analytical form and employing computer models to extend

the description to binary and ternary systems. Recently J. Lorenz et al. (12) applied this method successfully to SiC-ZrO_2 and $\text{SiC-ZrO}_2\text{-Al}_2\text{O}_3\text{-SiO}_2$ in order to evaluate composition effects and identify fabrication conditions. In the present paper, the data base has been expanded by analyzing the following quasi-binary systems: $\text{GeO}_2\text{-HfO}_2$, $\text{GeO}_2\text{-TiO}_2$, $\text{GeO}_2\text{-Al}_2\text{O}_3$, $\text{GeO}_2\text{-MgO}$, $\text{GeO}_2\text{-CaO}$, $\text{GeO}_2\text{-SiO}_2$, $\text{TiO}_2\text{-MgO}$, $\text{HfO}_2\text{-SiO}_2$, $\text{HfO}_2\text{-MgO}$, $\text{HfO}_2\text{-CaO}$, $\text{Al}_2\text{O}_3\text{-HfO}_2$, $\text{HfO}_2\text{-Y}_2\text{O}_3$, HfO-TiO_2 , $\text{Ce}_2\text{O}_3\text{-Al}_2\text{O}_3$, $\text{ZrO}_2\text{-HfO}_2$, $\text{ZrO}_2\text{-SiO}_2$, $\text{ZrO}_2\text{-CaO}$, $\text{Y}_2\text{O}_3\text{-CaO}$ and $\text{Y}_2\text{O}_3\text{-MgO}$. These results when combined with earlier findings (1-5) were employed to compute a range of isothermal sections in the following quasi-ternary systems sufficient to define their characteristics: $\text{MgO-TiO}_2\text{-SiO}_2$, $\text{MgO-SiO}_2\text{-GeO}_2$, $\text{GeO}_2\text{-MgO-CaO}$, $\text{HfO}_2\text{-CaO-MgO}$, $\text{HfO}_2\text{-SiO}_2\text{-ZrO}_2$, $\text{HfO}_2\text{-CaO-Y}_2\text{O}_3$, $\text{HfO}_2\text{-MgO-Y}_2\text{O}_3$, $\text{HfO}_2\text{-CaO-ZrO}_2$, $\text{SiO}_2\text{-HfO}_2\text{-Y}_2\text{O}_3$ and $\text{MgO-SiO}_2\text{-HfO}_2$.

LATTICE STABILITY VALUES

Table 1 defines the lattice stability values employed in the current study. Data for the stable forms were taken from Kubaschewski and Alcock (7). The remaining values were adopted along with the lines employed previously. As shown in Table 1 the present analysis is based on one gram atom of compound and/or solution phase. Moreover, dissociation of the components or vaporization is not considered!

TABLE 1

(CONCLUDED)

SUMMARY OF LATTICE STABILITY PARAMETERS

(All units in Joules per gram atom (mole of atoms), T in Kelvin).

P = Periclase, C = Corundum, S = Spinel, X = Crystobalite
 Tr = Tridymite, H = Hexagonal (quartz), R(SO) = Triclinic (quartz)

R = Rutile (TO) A = Cubic (HO and ZO)
 T = Tetragonal (HO and ZO) H = Monoclinic (HO and ZO)
 Y = High Temperature YO R = Low Temperature YO
 L = Liquid

DODOLR =	- 16.23 T	MOMOLH =	- 8.37 T
DOROLA =	8732 - 13.731T	MOMOLR =	- 10.42 T
DODOPA =	-31016	MOMOPA =	-31016
DODOAM =	16736 - 2.134T	MOMOLA =	16682 - 15.387T
DODOAT =	-22594	MOMOAM =	16736 - 2.134T
DODOLR =	5439 - 8.36RT	MOMOAT =	-22594
DODOLY =	2929 - 6.694T	MOMOLR =	13389 - 10.042T
DODOLR =	- 10.41RT	MOMOLY =	10878 - 8.36RT
TOTOLR =	14539 - 10.54 T	YOYOLY =	22694 - 8.36RT
TOTOLR =	22313 - 10.42 T	YOYOLR =	26878 - 10.042T
TOTOHR =	7774 - 0.12 T	YOYOLA =	22615 - 9.932T
TOTOLP =	- 9.37 T	YOYOAM =	-16736 - 2.134T
TOTOLT =	3527 - 11.757T	YOYOTM =	-836R - 1.381T
TOTOLA =	1017 - 11.757T	YOYOLP =	- 12.552T
TOTOTM =	-12259	YOYOLR =	- 10.41RT
TOTOLC =	- 10.208T	ZOZOLA =	28008 - 9.832T
TOTOLX =	- 1.674T	ZOZOAT =	1987 - 0.753T
TOTOYL =	- 8.36RT	ZOZOAM =	2008 - 1.381T
TOTOLR =	6862 - 9.205T	ZOZOLP =	- 8.36RT
AOAOHR =	- 10.54 T	SOSOLR =	-4790 - 5.69 T
AOAOLA =	- 9.832T	SOSOLT =	- 2.092T
AOAOLY =	- 10.585T	SOSOLA =	- 2.092T
AOAOLR =	- 8.36RT	SOSOLR =	- 2.092T
AOAOLR =	- 10.41RT		
CECELC =	- 10.208T		

TABLE 1

SUMMARY OF LATTICE STABILITY PARAMETERS

(All units in Joules per gram atom (mole of atoms), T in Kelvin).

P = Periclase, C = Corundum, S = Spinel, X = Crystobalite
 Tr = Tridymite, H = Hexagonal (quartz), R(SO) = Triclinic (quartz)

R = Rutile (TO) A = Cubic (HO and ZO)
 T = Tetragonal (HO and ZO) H = Monoclinic (HO and ZO)
 Y = High Temperature YO R = Low Temperature YO
 L = Liquid

CO = 1/3CaO ₂	HO = 1/3HF ₂	TO = 1/3TiO ₂	AO = 1/5Al ₂ O ₃
MO = 1/2MgO	DO = 1/2CaO	SO = 1/5SiO ₂	YO = 1/5Y ₂ O ₃
CF = 1/3CeO ₂	ZO = 1/3ZrO ₂		
COOOLR =	(1/3)CeO ₂ (liquid) - (1/3)GeO ₂ (hexagonal)		
COOOLP =	(1/3)CeO ₂ (liquid) - (1/3)GeO ₂ (rutile)		
COOOLM =	(1/3)CeO ₂ (hexagonal) - (1/3)GeO ₂ (rutile)		
COOOLR =	COOOLH + COOOLM		
COOOLH =	14644 - 10.54T	HOHOLA =	34865 - 11.00 T
COOOLP =	22087 - 16.21T	HOHOAT =	2239 - 0.753T
COOOLM =	7481 - 5.69T	HOHOLT =	37104 - 11.753T
COOOLA =	- 11.00T	HOHOTM =	2724 - 1.381T
COOOLT =	- 11.57T	HOHOLM =	39828 - 13.134T
COOOLH =	- 11.14T	HOHOLX =	- 2.092T
COOOLC =	- 10.21T	HOHOLP =	- 8.36RT
COOOLP =	- 9.37T	HOHOLC =	- 10.208T
COOOLM =	7108 - 5.40T	HOHOLA =	30711 - 10.376T
COOOLX =	- 1.67T	HOHOLY =	23849 - 9.196T
COOOLT =	- 2.01T	HOHOLR =	21882 - 10.42 T
COOOLR(SO) =	315 - 0.79T		
COOOLTR =	14644 - 8.54T		

* These differences specify the free energy of one phase (i.e. liquid) minus the free energy of the second phase (i.e. hexagonal) for a compound.

BINARY SYSTEMS

Tables 2-4 and Figures 1-19 summarize the results for the binary systems listed above. The solution phases are described as subregular solutions along the lines of Equations (1) and (2) of reference 4. When the subregular parameters are equal (i.e. GO-HO in Table 2) the solutions are regular, degenerating to ideal solutions for the liquid in HO-MO or all of the HO-ZO phases. The compound phases are defined at fixed compositions (i.e. Equations 3-6 of reference 4) in terms of the compound parameter and the base phase. The latter values are listed in Table 3 for the compounds of interest while Table 4 shows the Gibbs energy of formation for these compounds from the component oxides. Figure 1 shows the calculated GO-HO ($1/2\text{GeO}_2$ - $1/2\text{HfO}_2$) system derived from the description contained in Tables 1-4. This phase diagram was taken to compare with the analogous (SO-HO) case given by Figure 4443 (8). The system exhibits very little mutual solubility in the solid phase and an equimolar compound $\text{GO}_{.5}\text{HO}_{.5}$. The GO-TO case shown in Figure 2 is based on the experimental phase diagram in Figure 358 (8). The system is characterized by a miscibility gap ($R_1 + R_2$) in the rutile solid solution. The GO-AO system in Figure 3 is based on the experimental diagram given in Figure 4372 (8) and the earlier analog SO-AO analysis (2). This system exhibits little solubility in the solid and a single compound analogous to the SO-AO rutile. The calculated GO-MO phase diagram is shown in Figure 4 and is

based on the experimental phase diagram in Figure 264 (f) and the analogous SO-MO results (2). This system exhibits a liquid miscibility gap and a number of compound phases which have similar stoichiometry to the SO-MO compounds Enstatite (E) and Fosterite (F). The GO-DO ($1/3\text{GeO}_2$ - $1/2\text{CaO}$) case shown in Figure 5 is based on the experimental diagram given in Figure 4309 (8). Figure 6 shows the GO-SO phase diagram ($1/3\text{GeO}_2$ - $1/3\text{SiO}_2$) which is based upon the experimental diagram in Figure 357 (8). The latter is restricted to the low temperature range, however it is sufficient to permit definition of the solution phase parameters listed in Table 2. The system is distinguished by a large range of solid solution within the H phase which is a stable form of GeO_2 and SiO_2 . This continuous solid solution is undoubtedly the basis of Slichting's finding that permitted a continuous variation in the coefficient of thermal expansion between the low values characteristics of SiO_2 to the GeO_2 value, more compatible with the expansion coefficients exhibited by metals. The TO-MO diagram shown in Figure 7 is based on the experimental diagram given in Figure 4336 (8). The SO-HO phase diagram calculated on the basis of the parameters listed in Tables 1-3 and shown in Figure 8 exhibits little solubility in the solid and one equimolar compound in keeping with Figure 4443 (8). The $1/3\text{HfO}_2$ - $1/2\text{MgO}$ (HO-MO) case displayed in Figure 9 shows some solubility in the cubic structure based on HfO_2 and no compounds. This phase diagram was defined on the basis

TABLE 2
(Continued)

QUASIBINARY SOLUTION PARAMETERS FOR OXIDE SYSTEMS (All units in Joules per gram atom (mole of atoms), T in Kelvin)		QUASIBINARY SOLUTION PARAMETERS FOR OXIDE SYSTEMS (All units in Joules per gram atom (mole of atoms), T in Kelvin)	
LGHO = 16736	LHGO = 16736	LSGO = 4184 + 12.552T	LGSO = 4184 + 12.552T
AGHO = 62760	AHGO = 62760	HSGO = 4184 + 12.552T	HGSO = 4184 + 12.552T
TGHO = 62760	THGO = 62760	PSGO = 4184 + 12.552T	PGSO = 4184 + 12.552T
MGOH = 62760	MHGO = 62760	XSGO = 83680	XGSO = 83680
HGOH = 62760	HGOH = 62760	TSGO = 83680	TGSO = 83680
RGHO = 62760	RHGO = 62760	RSGO = 41840	RGSO = 41840
LGTO = 22292	LTGO = - 5908 + 3.347T	LTMO = - 45187 + 26.36T	LMTO = 1883 - 13.39T
HGTO = 18828	HTGO = - 9372 + 3.347T	PTMO = 83680	PMTO = 83680
PGTO = 52300 - 20.92T	RTGO = 19246	RTMO = 41840	RMTO = 41840
LGAO = 21221	LAO = 21221	LHOS = 46024	LHOS = 46024
HGAO = 41840	HAO = 41840	XHOS = 62760	XHOS = 62760
RGAO = 41840	RAO = 41840	AHOS = 125520	AHOS = 125520
CGAO = 83680	CAO = 83680	THOS = 125520	THOS = 125520
LGOM = - 29288 + 18.41T	LGOM = - 216731 + 60.25T	MHOS = 125520	MHOS = 125520
0 ≤ X _{MO} ≤ 0.4	0 ≤ X _{MO} ≤ 0.4	LMOM = 0	LMOM = 0
LGOM = -104265 + 35.15T	LGOM = - 104265 + 35.15T	AMOM = 8368	AMOM = - 29288
0.4 ≤ X _{MO} ≤ 1.0	0.4 ≤ X _{MO} ≤ 1.0	TMOM = 8368	TMOM = - 29288
PGOM = - 20585 + 35.15T	PGOM = - 20585 35.15T	MMOM = 46024	MMOM = 46024
HGOM = - 12552 + 18.41T	HGOM = - 12.552 + 60.25T	PMOM = 83680	PMOM = 83680
0 ≤ X _{DO} ≤ 0.4	0 ≤ X _{DO} ≤ 0.4	LDOM = - 25104 + 9.20T	LDOM = -112968 + 41.84T
LGOD = - 43179 + 20.92T	LGOD = - 226020 + 62.76T	ADOM = - 12552	ADOM = -142256 + 41.84T
0 ≤ X _{DO} ≤ 0.4	0 ≤ X _{DO} ≤ 0.4	TDOM = 8368	TDOM = - 29288
LGOD = -116315 + 37.66T	LGOD = - 116315 + 37.66T	MDOM = 46024	MDOM = 46024
0.4 ≤ X _{DO} ≤ 1.0	0.4 ≤ X _{DO} ≤ 1.0	PDOM = 83680	PDOM = 83680
PGOD = 62.760	PGOD = 62.760	LMOH = 17573	LMOH = 39748
HGOD = - 43179 + 20.92T	HGOD = - 226020 + 62.76T	AMOH = 62760	AMOH = 62760
LYOD = 27196	LYOD = 27196	TMOH = 62760	TMOH = 62760
YOYD = 35564	YOYD = 35564	MMOH = 62760	MMOH = 62760
MOYD = 35564	MOYD = 35564	PMOH = 62760	PMOH = 62760
PYOD = 81680	PYOD = 81680	LMOH = 17573	LMOH = 39748

TABLE 2
(Concluded)

QUANTITARY SOLUTION PARAMETERS FOR OXIDE SYSTEMS
(All units in Joules per gram atom (mole of atoms), T in Kelvin)

LYMO	-3975	-2.51T	LYMO	= 16527 + 3.67T
TYMO	2510	+ 7.11T	TYMO	= 11715 + 0.618T
MYMO	816R		MYMO	= -10042 + 8.786T
AYMO	-1674	+ 7.11T	AYMO	= -10042 + 8.79T
YMOV	7113	+ 8.168T	YMOV	= 7113 + 8.168T
BYMO	-2243	+ 11.96T	BYMO	= -2243 + 11.97T
LYTO	-816R		LYTO	= -836R
AYTO	-12552		AYTO	= -12552
TYTO	-12552		TYTO	= -12552
MYTO	-12552		MYTO	= -12552
BYTO	-816R		BYTO	= -836R
LYFA	27196		LYFA	= 27196
TYFA	8168R		TYFA	= 8168R
MYFA	8168R		MYFA	= 8168R
LYZO	0		LYZO	= 0
AYZO	0		AYZO	= 0
TYZO	0		TYZO	= 0
MYZO	0		MYZO	= 0
LYSO	80040	- 15.61T	LYSO	= 80040 - 15.61T
AYSO	125520		AYSO	= 125520
TYSO	125520		TYSO	= 125520
MYSO	62760		MYSO	= 62760
BYSO	125520		BYSO	= 125520
LYPO	-37474	+ 16.226T	LYPO	= -6066R + 10.842T
TYPO	8168R		TYPO	= 8168R
MYPO	-54392	+ 16.216T	MYPO	= -54392 + 16.216T
TYPO	-64107	+ 16.216T	TYPO	= -64107 + 16.216T
MYPO	-16716	+ 16.216T	MYPO	= -16716 + 16.216T
LYVO	27196		LYVO	= 27196
TYVO	35568		TYVO	= 35568
MYVO	35568		MYVO	= 35568

TABLE 3

SUMMARY OF COMPOUND PARAMETERS FOR BINARY SYSTEMS
(All units in Joules per gram atom (mole of atoms) T in Kelvin)

Compound	Name	Stoichiometry	Stability	Base	Compound/Percentage (Joules/g.at.)
(1/6)(GeO ₂ , MnO ₂)	S	Ge _{0.5} Mn _{0.5}	stable	M	66964
(1/21)(2GeO ₂ , 3Al ₂ O ₃)	M	Ge _{0.286} Al _{0.714}	stable	C	64634 - 5.21T
(1/5)(MgO, GeO ₂)	F	Ge _{0.6} Mg _{0.4}	stable	P	-39719 + 60.75T
(1/7)(GeO ₂ , 2MgO)	F	Ge _{0.429} Mg _{0.571}	stable	P	-53631 + 66.60T
(1/11)(GeO ₂ , 2MgO)	X	Ge _{0.273} Mg _{0.727}	stable	P	-61137 + 62.37T
(1/14)(4GeO ₂ , CaO)	M	Ge _{0.857} Ca _{0.143}	stable	P	-28108 + 75.00T
(1/8)(2GeO ₂ , CaO)	R	Ge _{0.75} Ca _{0.25}	stable	R	-33129 + 76.10T
(1/5)(CaO, GeO ₂)	F	Ge _{0.6} Ca _{0.4}	stable	P	-59320 + 62.03T
(1/12)(2GeO ₂ , 3CaO)	T	Ge _{0.5} Ca _{0.5}	stable	P	-69287 + 61.38T
(1/7)(GeO ₂ , 2CaO)	F	Ge _{0.429} Ca _{0.571}	stable	P	-74834 + 61.55T
(1/9)(GeO ₂ , 3CaO)	V	Ge _{0.333} Ca _{0.667}	stable	P	-84701 + 60.00T
(1/8)(2TiO ₂ , MgO)	W	Ti _{0.75} Mg _{0.25}	stable	R	56811 + 5.06T
(1/5)(TiO ₂ , MgO)	V	Ti _{0.6} Mg _{0.4}	stable	P	48606 + 3.01T
(1/7)(TiO ₂ , 2MgO)	U	Ti _{0.429} Mg _{0.571}	stable	P	34593 + 0.00T
(1/6)(SiO ₂ , MnO ₂)	S	Si _{0.5} Mn _{0.5}	stable	M	64601 - 4.18T
(1/25)(7MnO ₂ , 2CaO)	P	Mn _{0.84} Ca _{0.16}	stable	A	35564 + 10.00T
(1/5)(MnO ₂ , CaO)	O	Mn _{0.6} Ca _{0.4}	stable	A	9701 + 32.22T
(1/6)(MnO ₂ , TiO ₂)	S	Mn _{0.5} Ti _{0.5}	stable	T	30074 + 17.00T
(1/10)(Cr ₂ O ₃ , Al ₂ O ₃)	P	Cr _{0.5} Al _{0.5}	stable	V	61538 + 7.24T
(1/30)(CeAl ₁₁ O ₁₉)	O	Ce _{0.083} Al _{0.917}	stable	C	20619 + 25.00T
(1/4)(ZrO ₂ , SiO ₂)	O	Zr _{0.5} Si _{0.5}	stable	M	102600 - 22.51T
(1/14)(2ZrO ₂ , CaO)	V	Zr _{0.857} Ca _{0.143}	stable	A	30125 + 17.20T
(1/5)(ZrO ₂ , CaO)	O	Zr _{0.6} Ca _{0.4}	stable	A	21664 + 20.87T

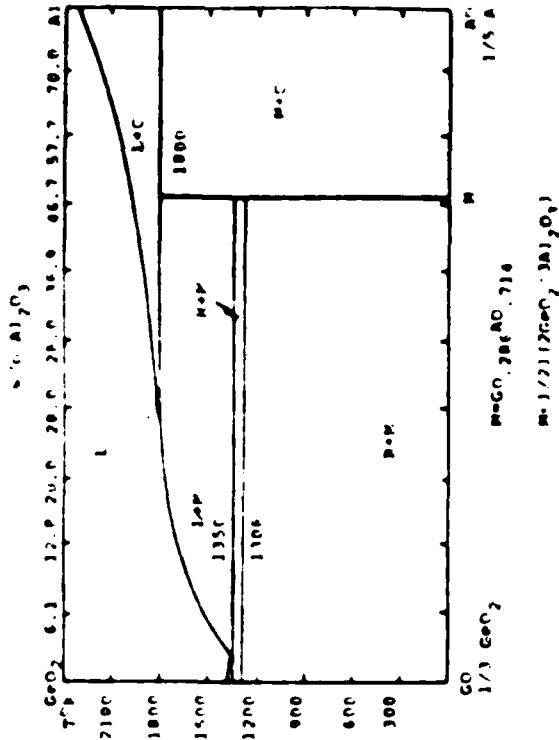


Figure 3. Calculated GeO₂-Al₂O₃ Phase Diagram.

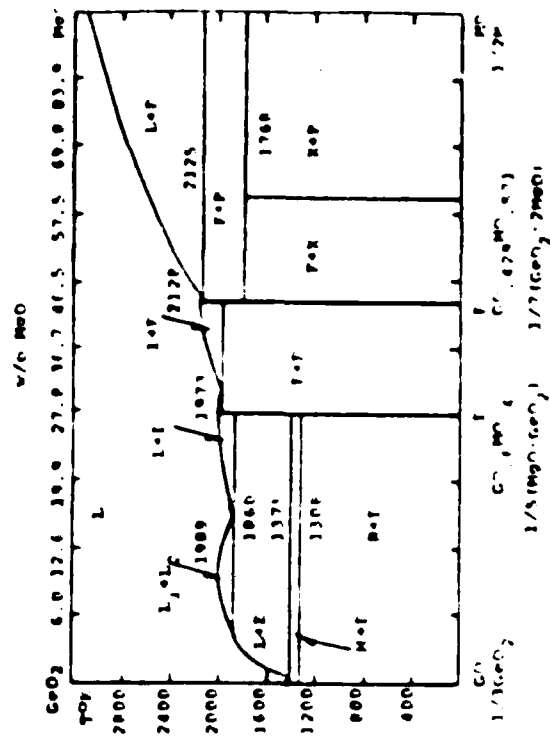


Figure 4. Calculated GeO₂-MnO Phase Diagram.

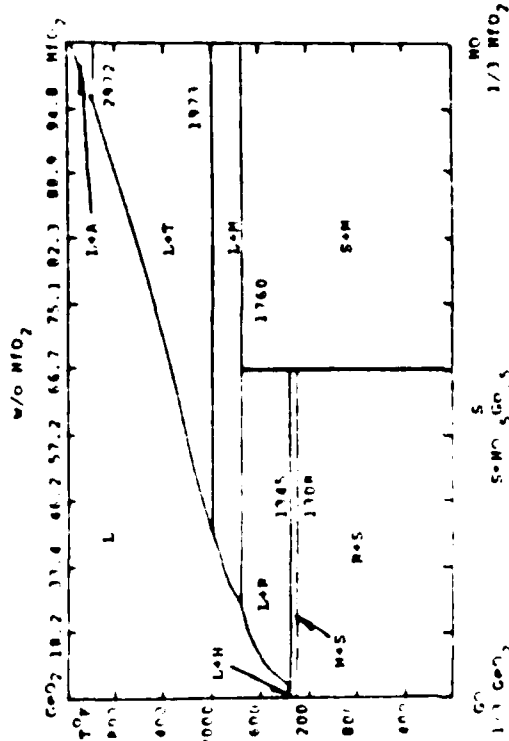


Figure 5. Calculated GeO₂-MnO Phase Diagram.

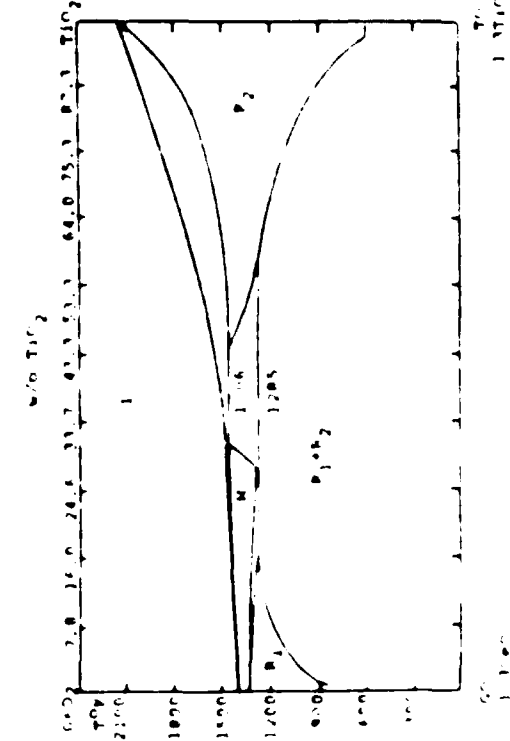


Figure 6. Calculated GeO₂-TiO₂ Phase Diagram.

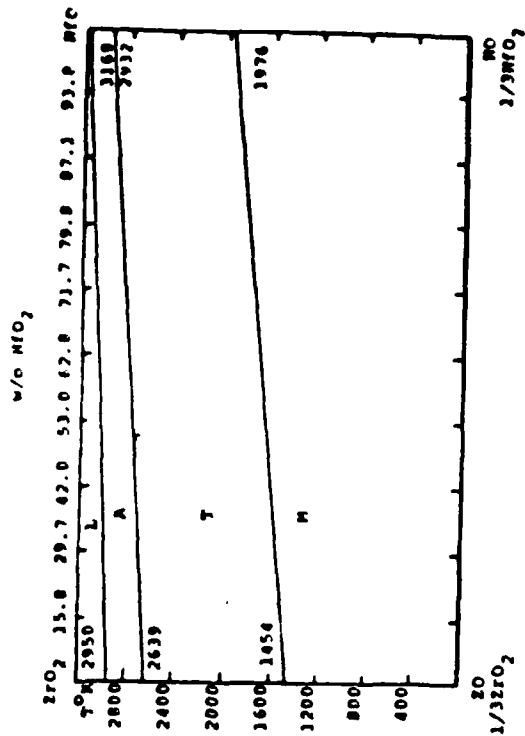


Figure 15. Calculated ZrO_2 - MfO_2 Phase Diagram.

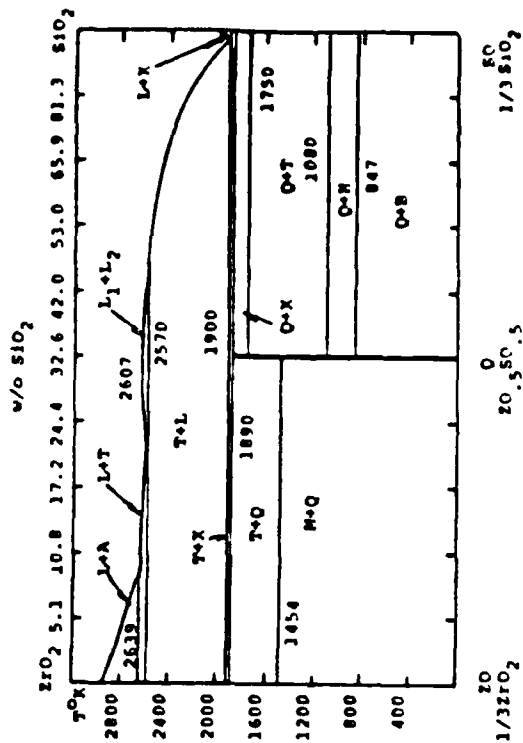


Figure 16. Calculated ZrO_2 - SiO_2 Phase Diagram.

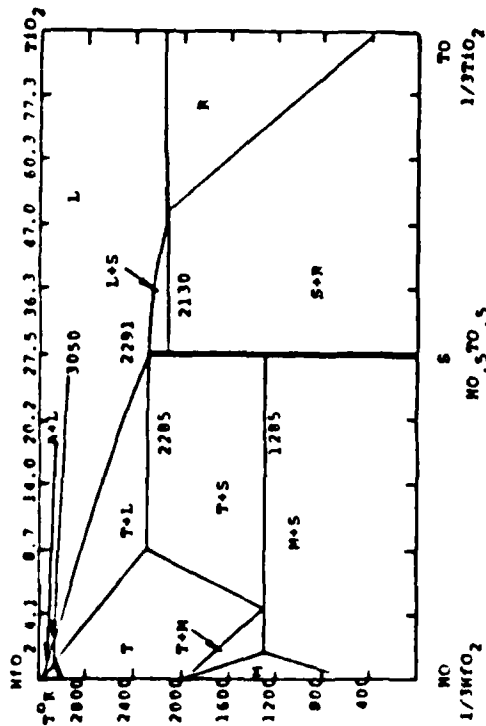


Figure 13. Calculated MfO_2 - TiO_2 Phase Diagram.

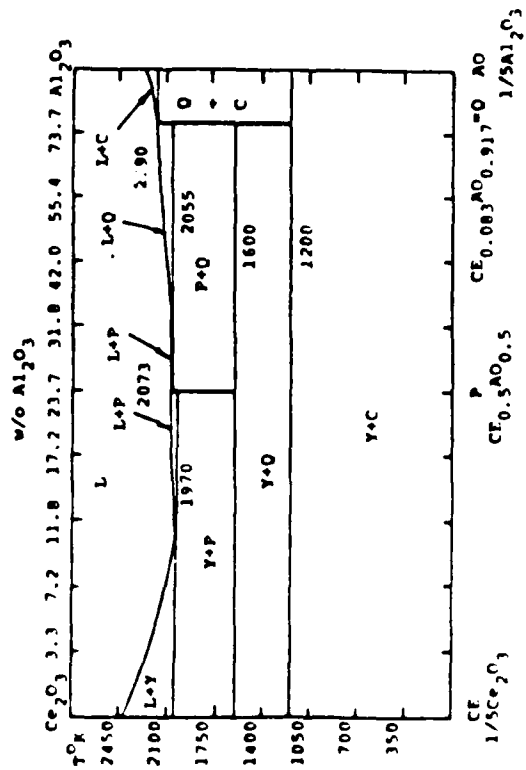


Figure 14. Calculated Ce_2O_3 - Al_2O_3 Phase Diagram.

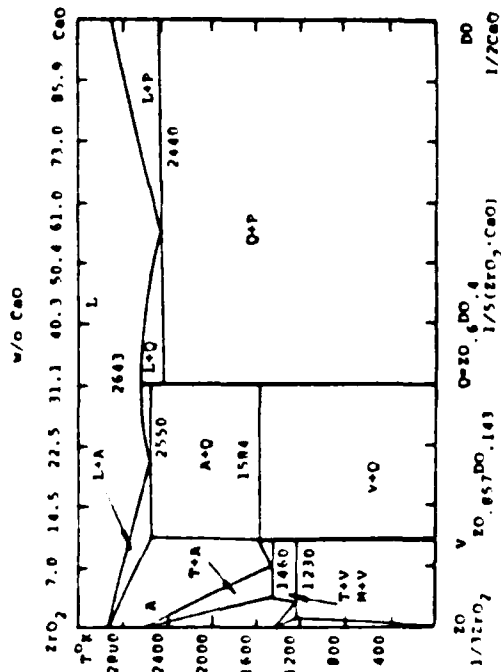


Figure 17. Calculated $\text{ErO}_2\text{-CaO}$ Phase Diagram.

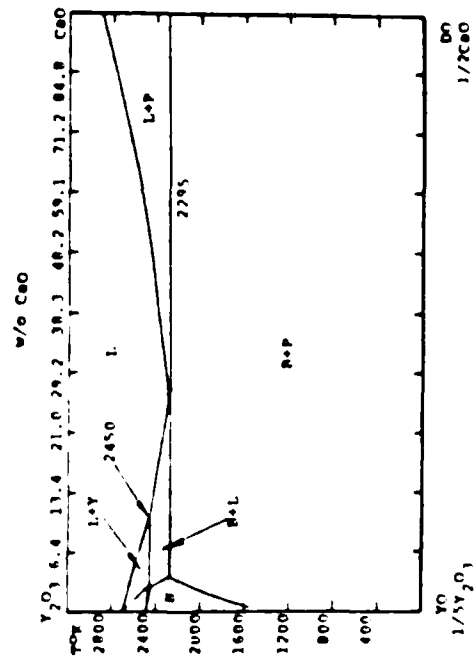


Figure 18. Calculated $\text{Y}_2\text{O}_3\text{-CaO}$ Phase Diagram.

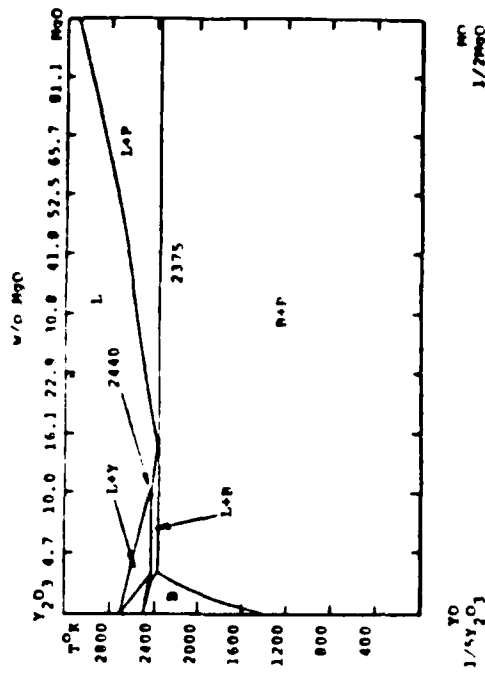


Figure 19. Calculated $\text{Y}_2\text{O}_3\text{-MgO}$ System.

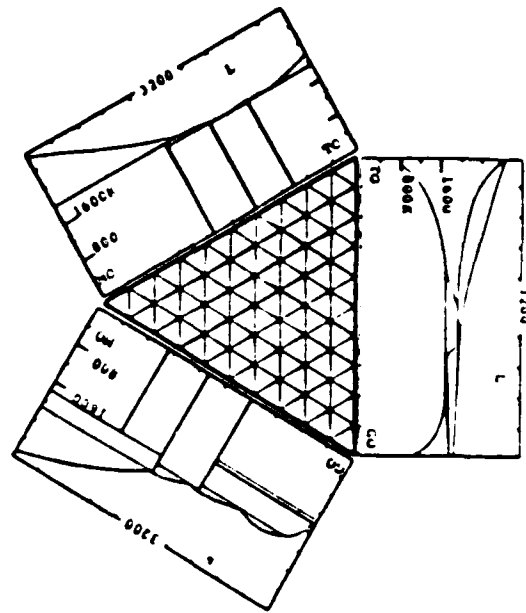


Figure 20. Calculated Isothermal Sections in the $\text{MgO-Y}_2\text{O}_3\text{-3CaO-4BaO-11CeO}_2$ System.

of Figure 5159 (9). By contrast the $\text{HfO}_2\text{-CaO}$ system in Figure 10, while similar to the $\text{HfO}_2\text{-MgO}$ case exhibits two compounds designated R and C. This phase diagram is based on the work of Senft and Stubican (13). The HO-AO case in Figure 11 is based on the analogous ZO-AO system, Figure 4378 (8), showing little solubility in the solid phase and no compounds. A very extensive range of solubility in both the cubic structure based on HfO_2 and that based on Y_2O_3 is illustrated in the HO-YO case shown in Figure 12 which is derived from Figure 4436 (8). Inspection of Table 2 shows that this system is defined by solution phase parameters which tend to be positive over most of the temperature range of interest. This is in keeping with the absence of compound phases and the observation that the dominant A solid solution phase decomposes. This will be discussed further in the calculation of the $\text{SiO}_2\text{-HfO}_2\text{-Y}_2\text{O}_3$ system in the next section of this paper. Figure 13 shows the $\text{HfO}_2\text{-TiO}_2$ system based upon the analogous ZO-TO case shown in Figure 4452 (8). This system exhibits solid phase solubility in the cubic phase based on HfO_2 and the rutile phase based on TiO_2 . In addition an equimolar compound in this system is stable and melts congruently. Figure 14 shows the calculated CE-AO($1/5\text{Ce}_2\text{O}_3\text{-}1/5\text{Al}_2\text{O}_3$) system which is based on Figures 356 and 4366 in reference (8). The system contains two compounds designated as F and C in Figure 14 which decomposes into Ce_2O_3 and Al_2O_3 at low temperature. The $\text{ZrO}_2\text{-HfO}_2$ system is shown in Figure 15 which is based on Figure 4444 (8). The calculated phase

diagram is based on assuming ideal solutions for each of the solution phases as can be seen in Table 2. Figure 16 displays the calculated ZO-SO phase diagram which is derived from Figure 2400 (8) and the above noted HO-SO analysis. This system is characterized by a symmetrical miscibility gap, little solubility in the solid phases and an equimolar compound which decomposes prior to melting into tetragonal ZrO_2 and crystalite. The ZO-DO system shown in Figure 17 is based on Figure 5392 (9). It is quite similar to the HO-DO system in Figure with two compound phases and some solid phase solubility especially in the cubic phase. The YO-DO and YO-MO diagrams shown in Figures 18 and 19 complete the set of systems considered here. The YO-MO($1/5\text{Y}_2\text{O}_3\text{-}1/2\text{MgO}$) case in Figure 19 is based on Figure 5156 (9). Neither system contains compounds or substantial solubility in the solid. Examination of Table 2 shows that most of the solution phases exhibit small interaction parameters except for those cases where limited solubility occurs leading to large positive interaction parameters.

TERNARY SYSTEMS

The description of the foregoing systems combined with those presented earlier (1-5) have been employed to calculate isothermal sections in ten quasi-ternary systems over a wide range of temperatures. The results of these calculations are presented in Figures 20-31. In each case the component quasi-binary systems are

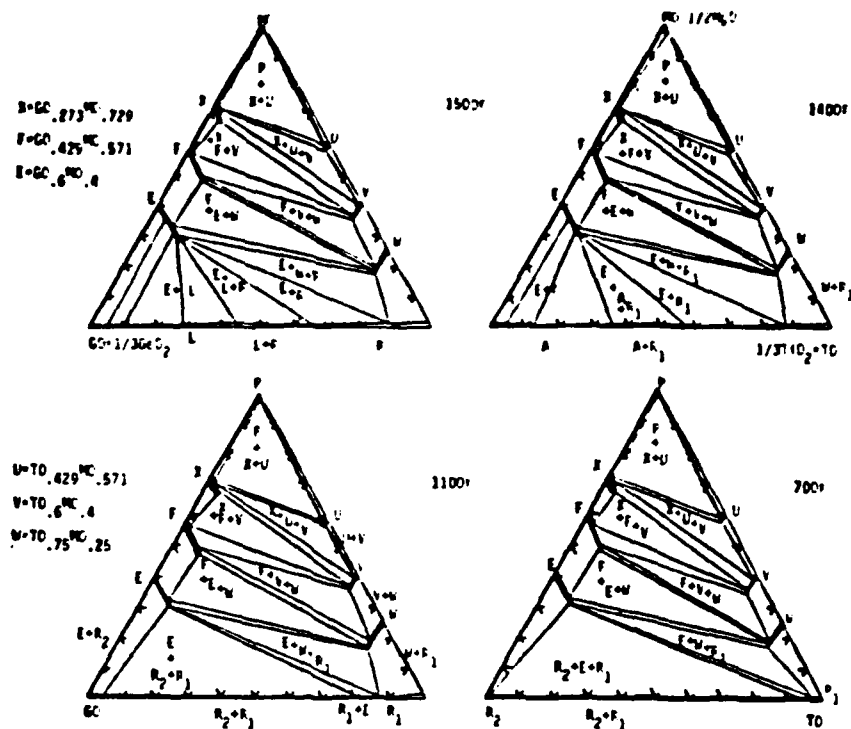


Figure 23. Calculated Isothermal Sections in Mg-TO-Ge

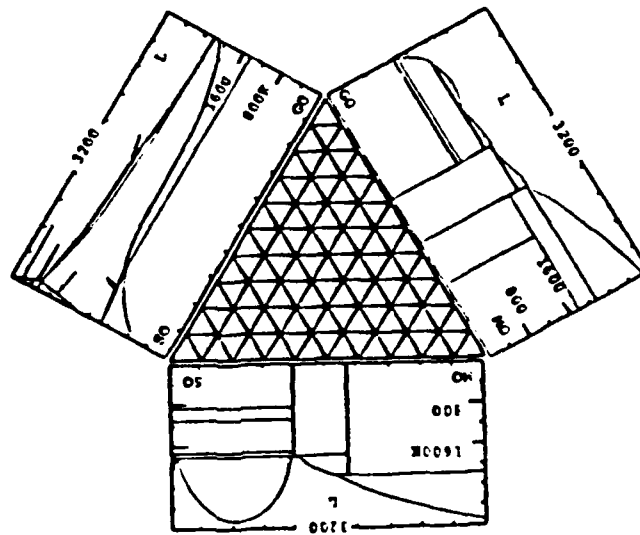


Figure 24. Calculated Isothermal Sections in the $Ge(1/3GeO_2)-Mg(1/2MgO)-Si(1/3SiO_2)$ system.

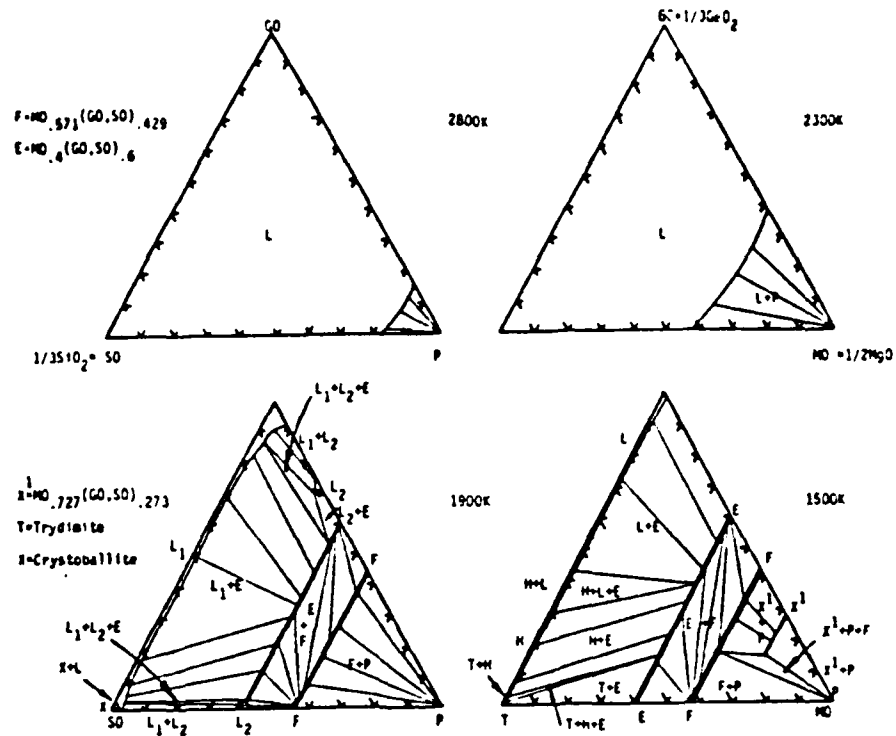


Figure 25. Calculated Isothermal Sections in GeO-MgO-SiO₂

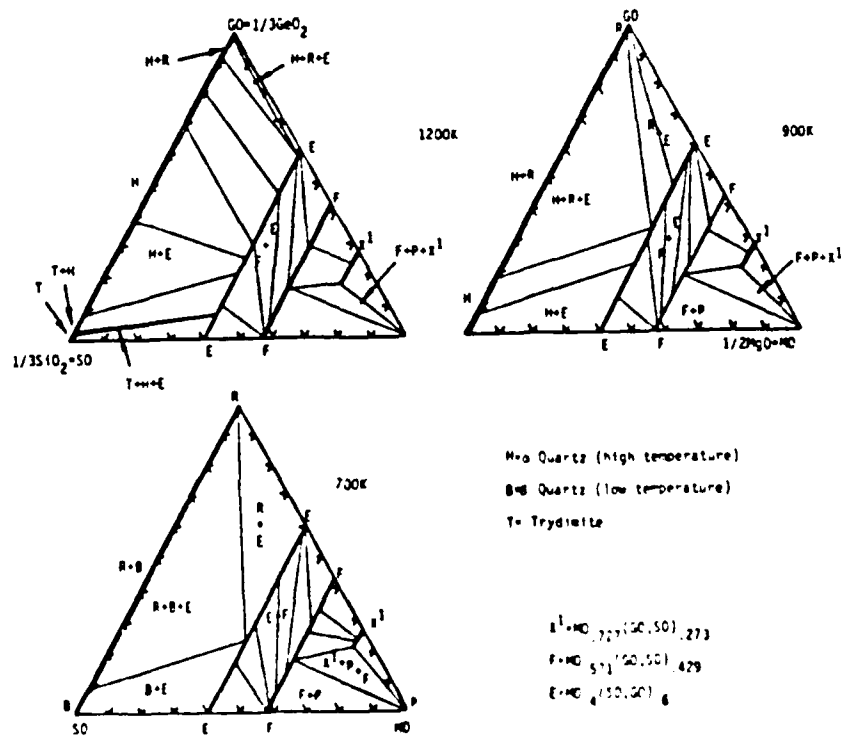


Figure 26. Calculated Isothermal Sections in SiO₂-MgO-SiO₂

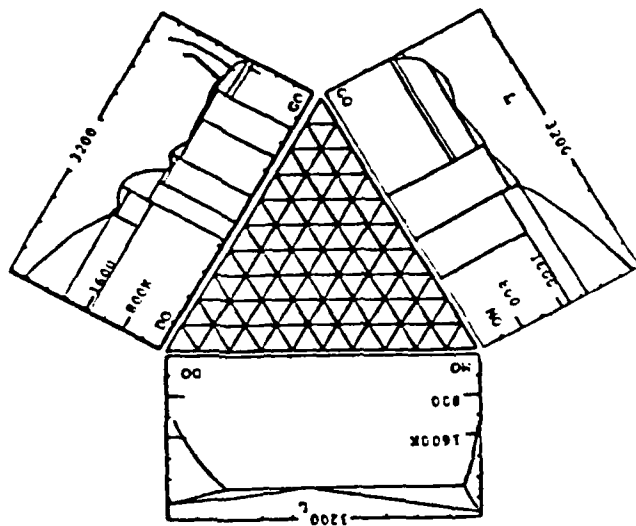


Figure 27 Calculated Isothermal Sections in the GO (1/3 GeO₂) - MO (1/2 MgO) - DO (1/2 CaO) System.

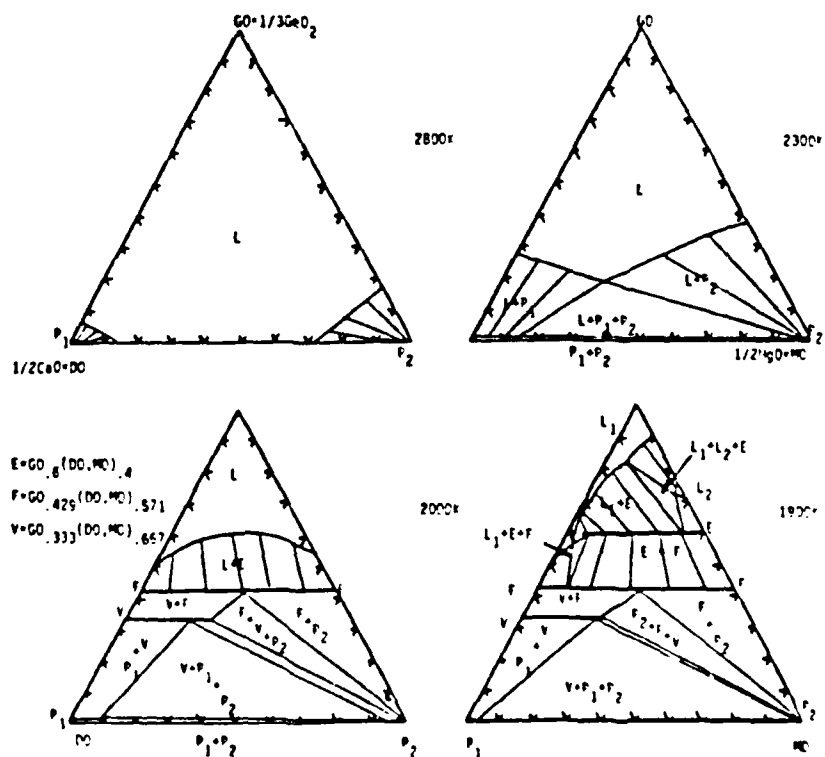


Figure 28 Calculated Isothermal Sections in GO-MO-DO

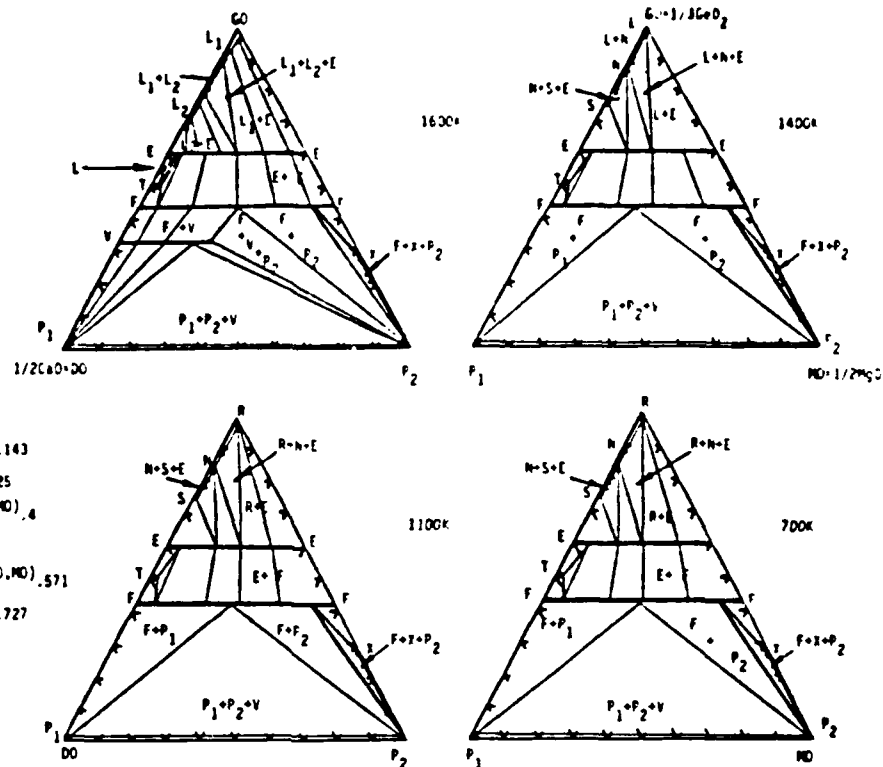


Figure 29. Calculated Isothermal Sections in GO-MD-DO

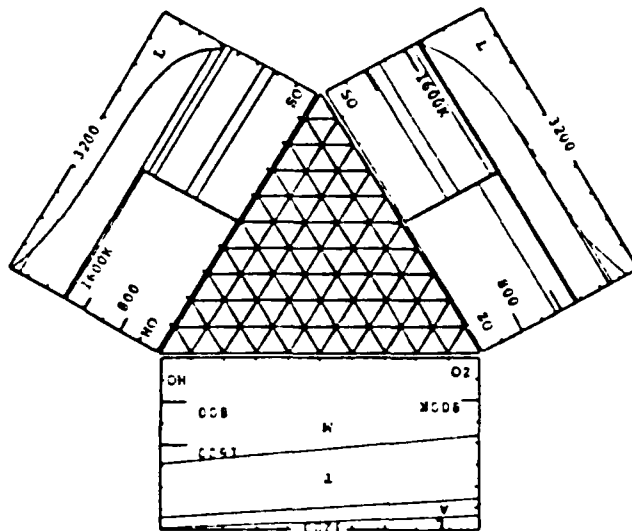


Figure 30. Calculated Isothermal Sections in the $SrO-35xO_2-20yO_2-MO_{11/3}HfO_2$ System

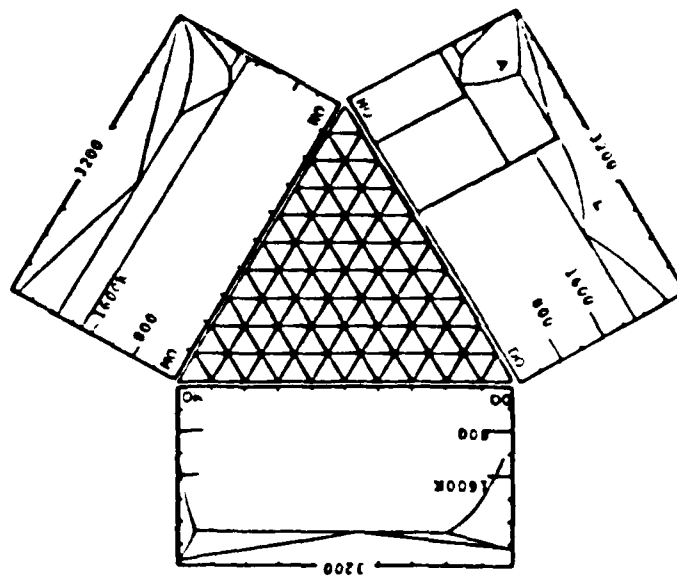


Figure 33. Calculated Isothermal Sections in the $\text{NO}(1/3 \text{MnO}_2) - \text{DC}(1/2 \text{CaO}) - \text{MO}(1/2 \text{MgO})$

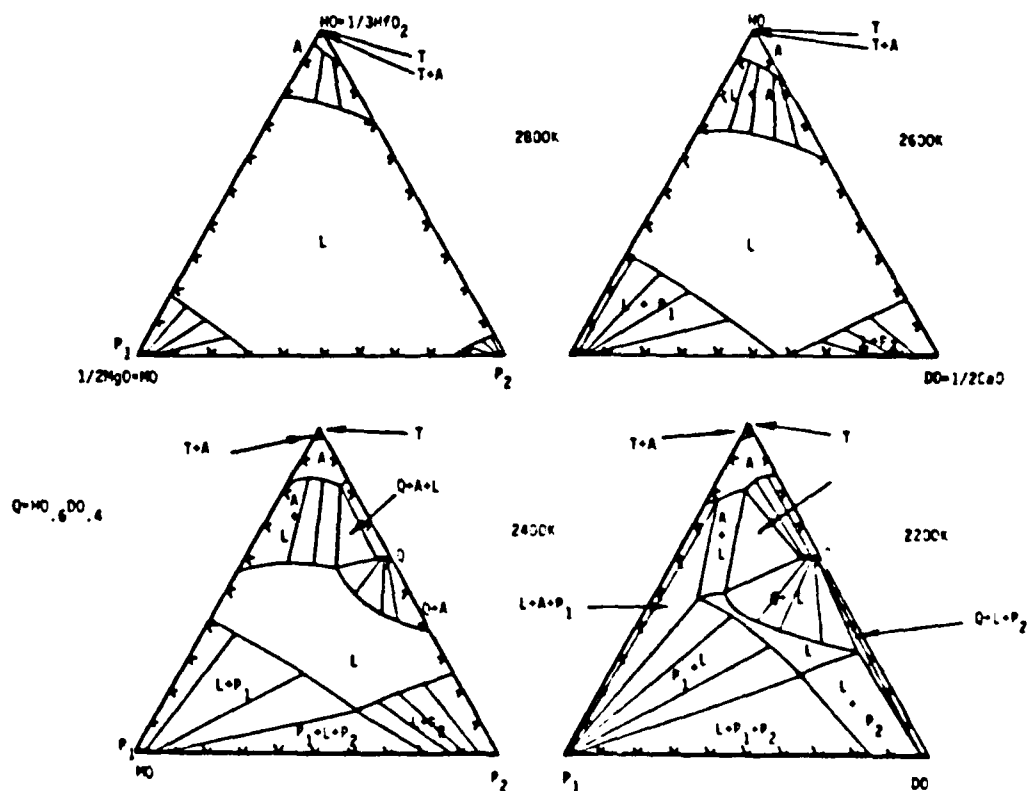


Figure 34. Calculated Isothermal Sections in MO-DO-MN

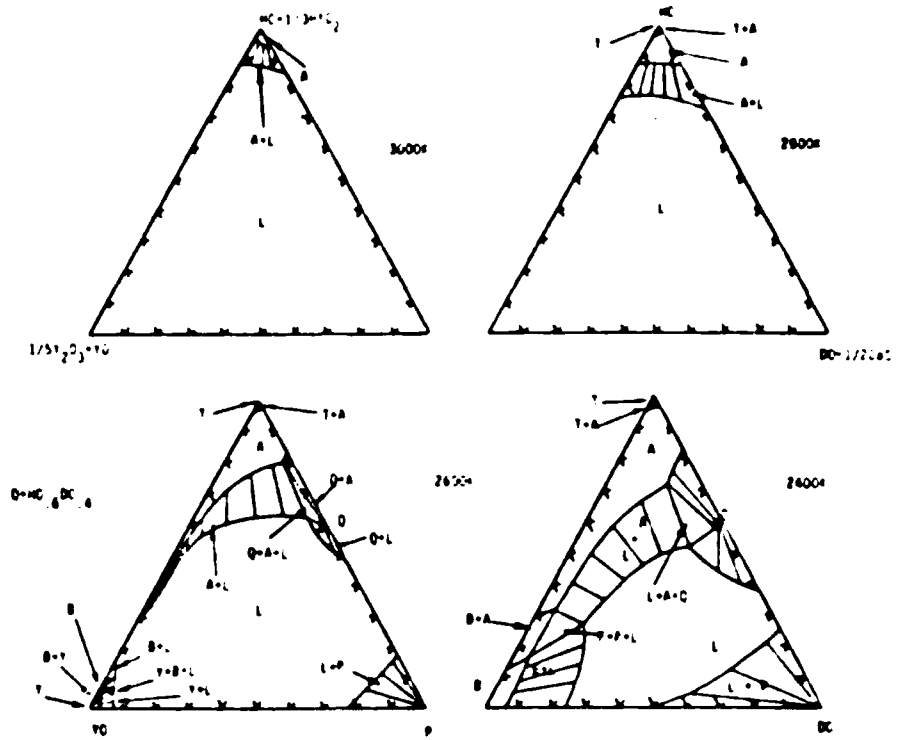


Figure 37 Calculated Isothermal Sections in MC-DC-YO

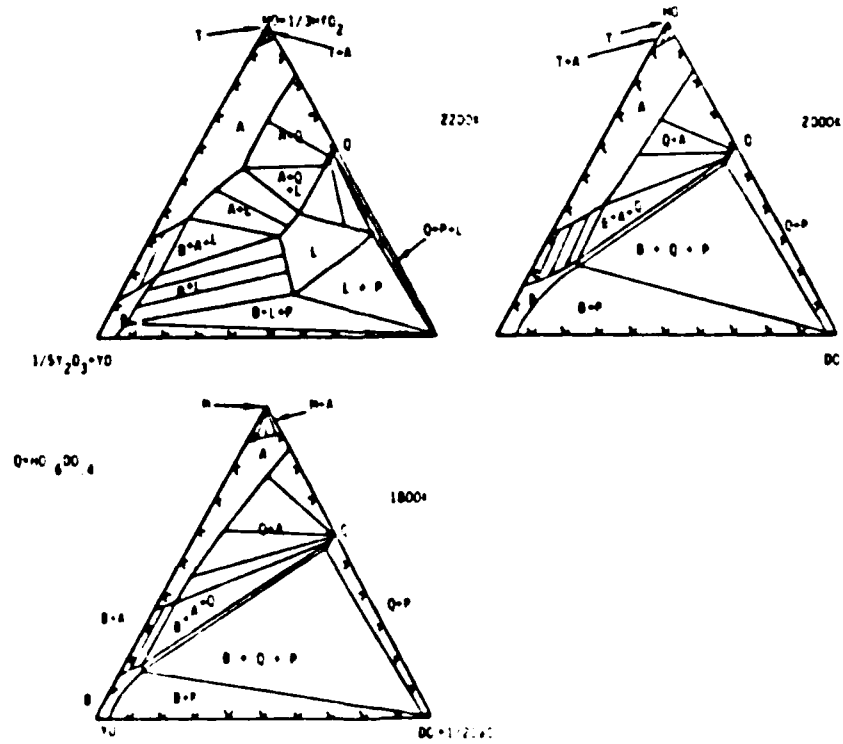


Figure 38 Calculated Isothermal Sections in MC-DC-YO

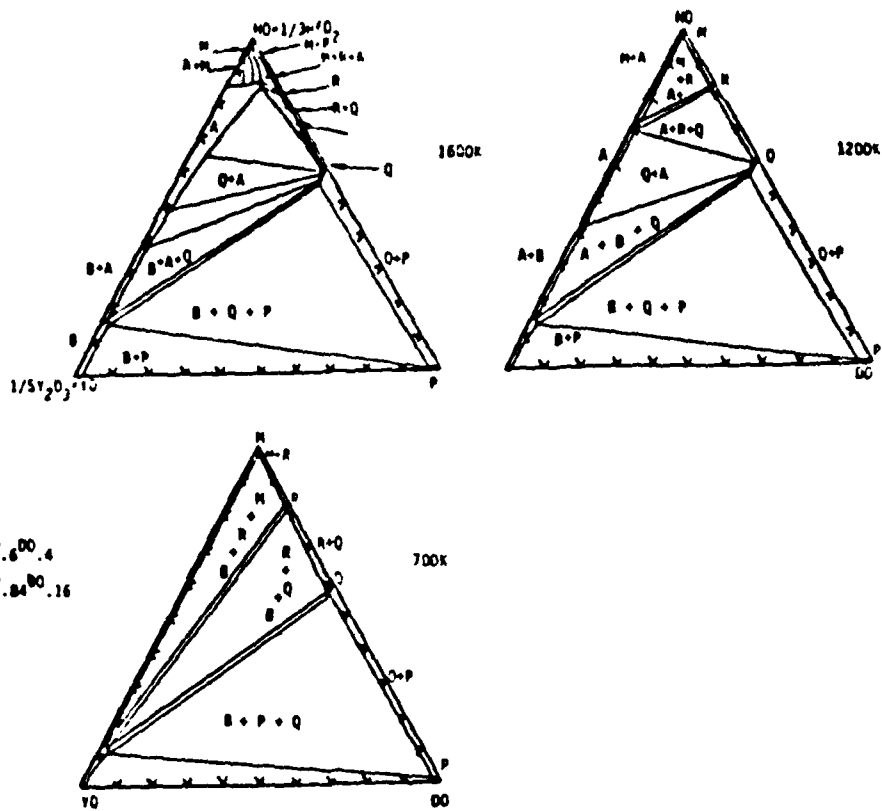


Figure 39. Calculated Isothermal Sections in MO-DO-YO

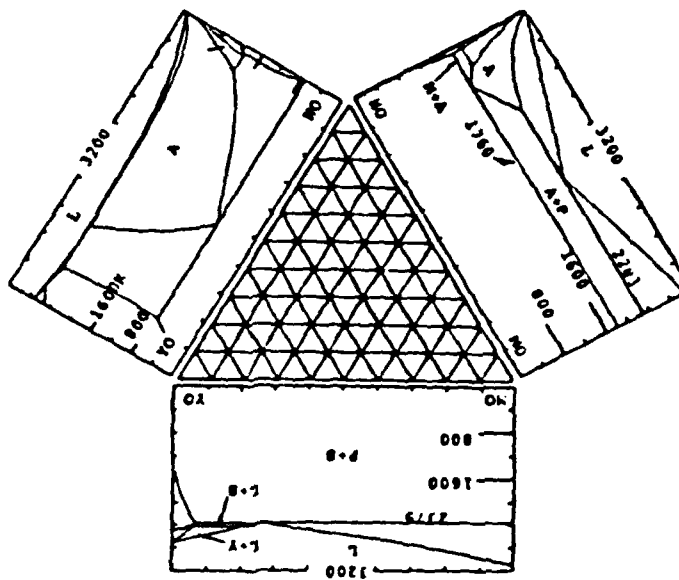


Figure 40. Calculated Isothermal Sections in the $MO(1/3HfO_3)$ - $MO(1/2MgO)$ - $YO(1/3Y_2O_3)$ system

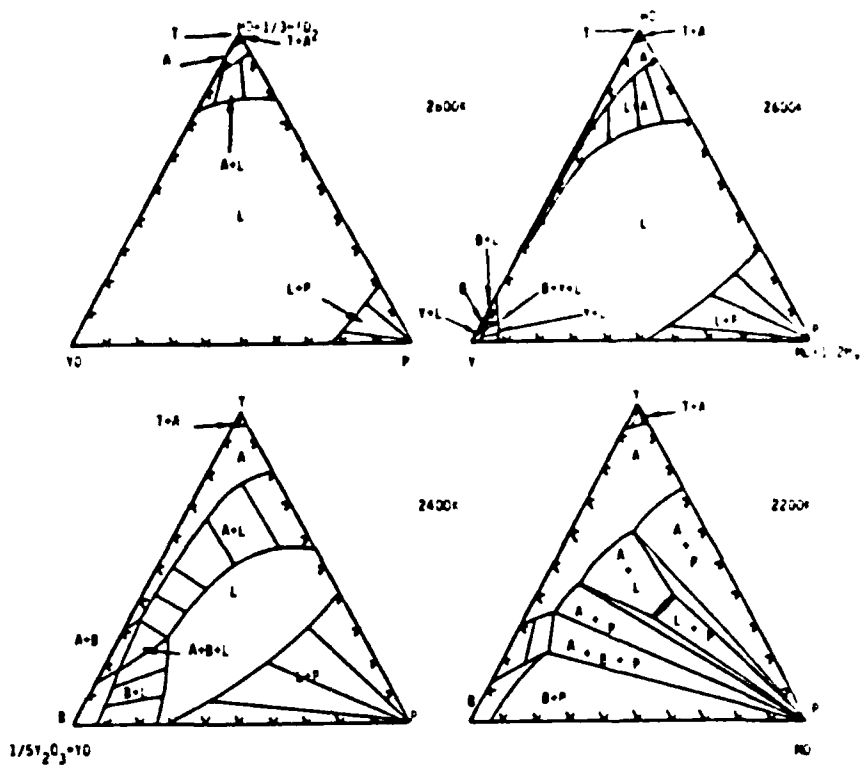


Figure 41. Calculated Isothermal Sections in MC-MD-YO

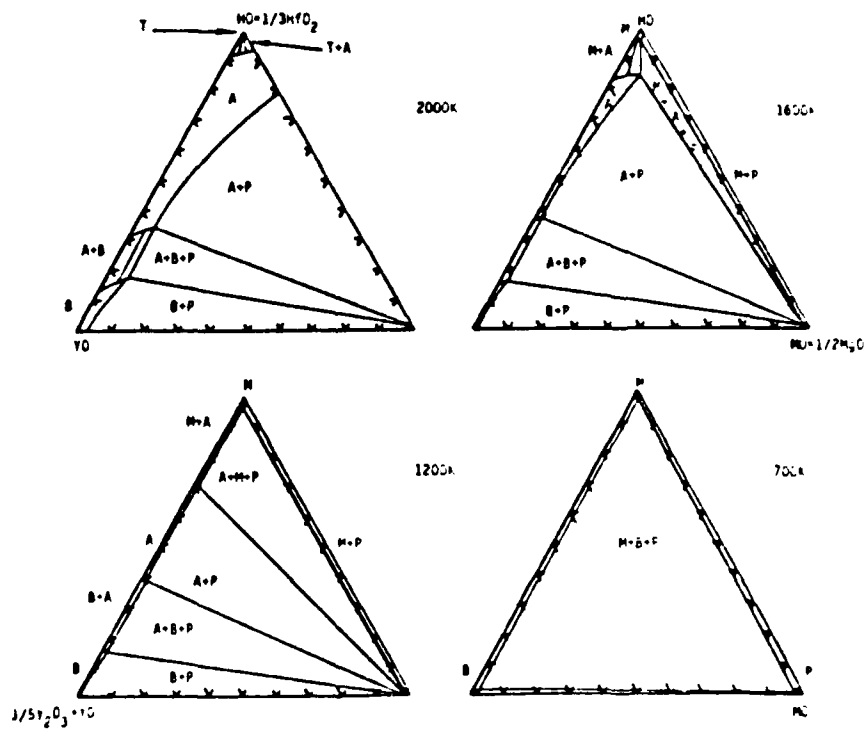


Figure 42. Calculated Isothermal Sections in MD-MU-YO

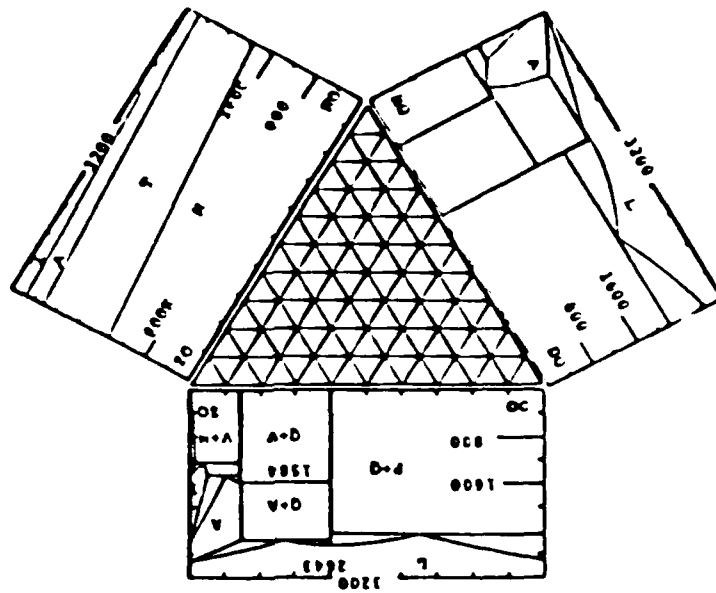


Figure 43. Calculated Isothermal Sections in the $MO(1/3MgO) - DC(1/2CaO) - EC(1/3ZrO_2)$ System

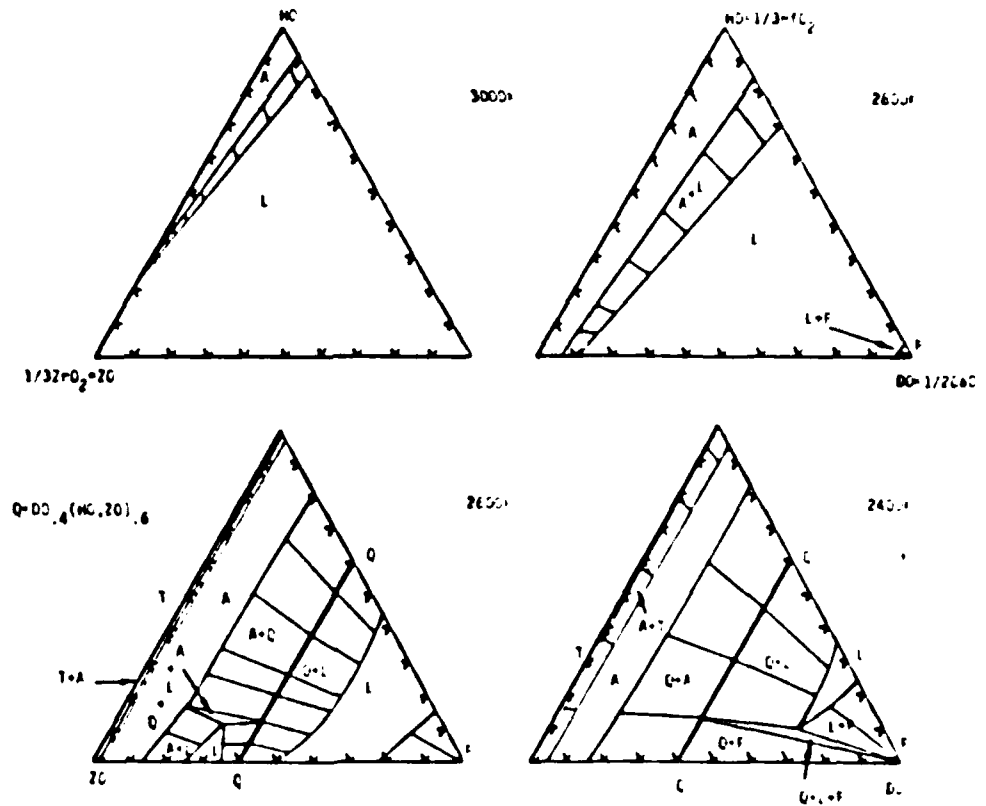


Figure 44. Calculated Isothermal Sections in MO-DC-ZO

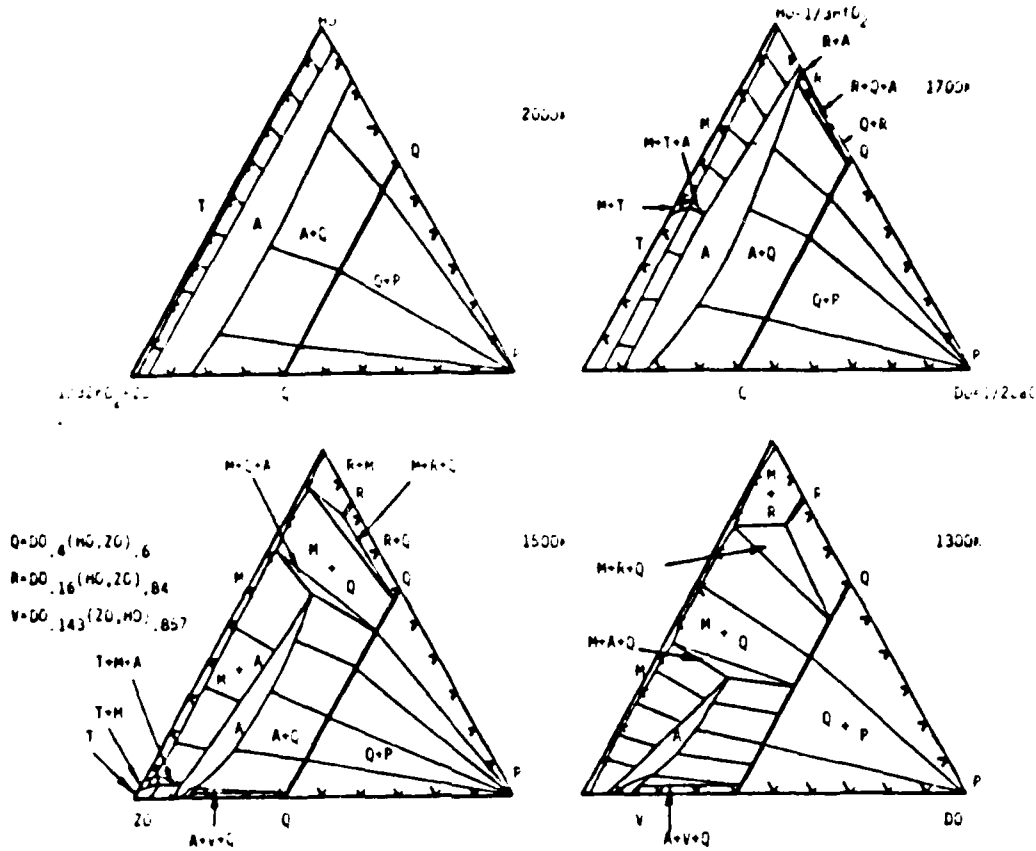


Figure 45. Calculated Isothermal Sections in MO-DO-ZO

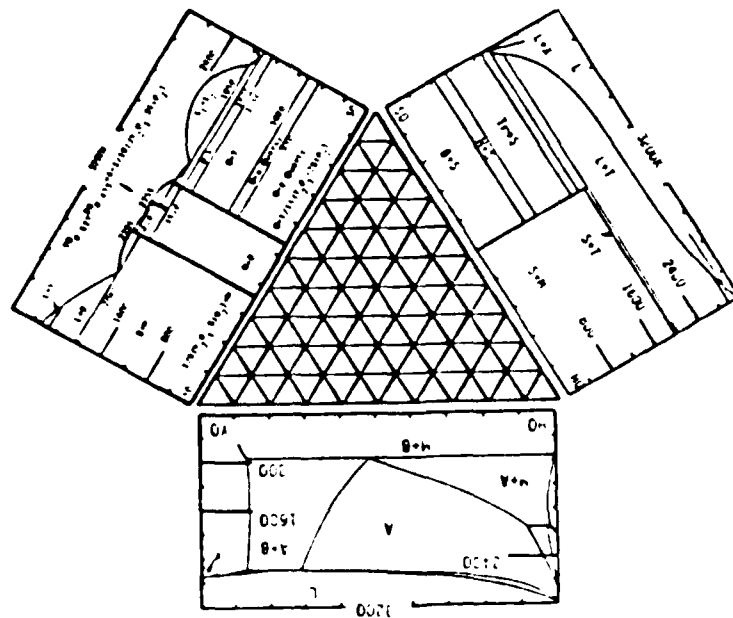


Figure 46. Calculated Isothermal Sections in the $SO(1/3510_2)-MO(1/3510_2)-VO(1/5120_3)$ System.

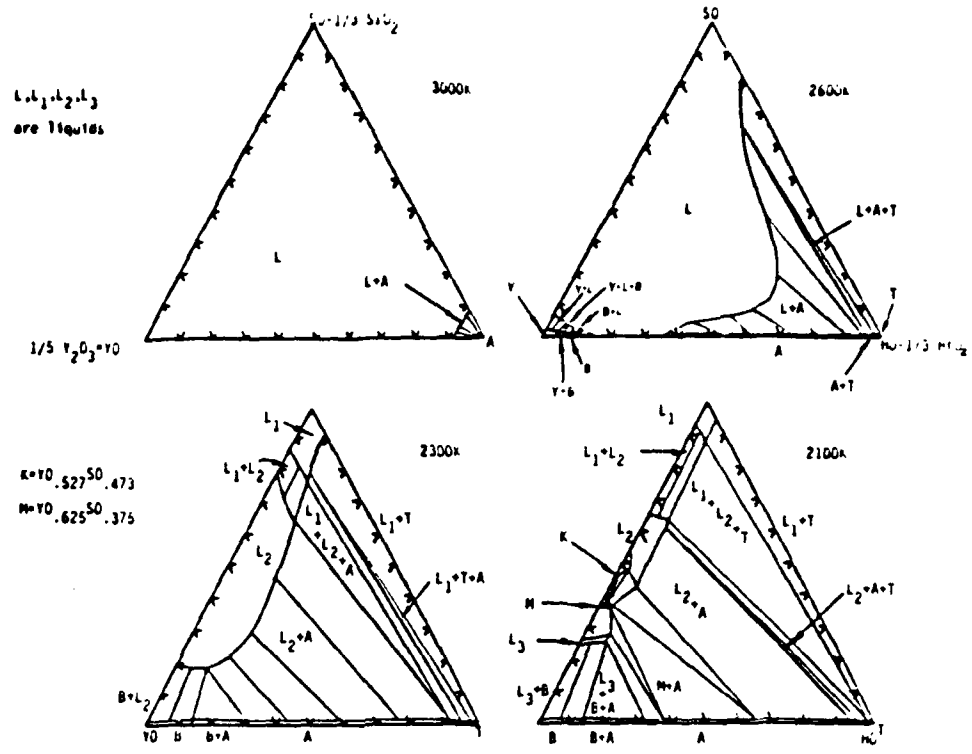


Figure 47. Calculated Isothermal Sections in SO-H₂O-YO

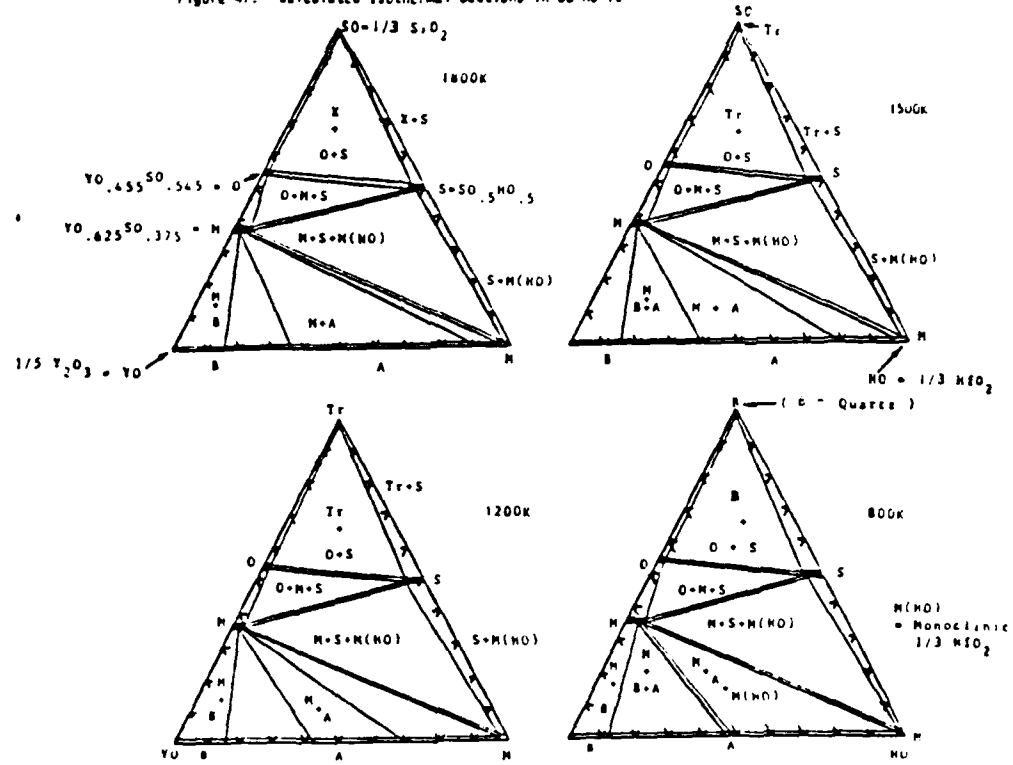


Figure 48. Calculated Isothermal Sections in SO-H₂O-YO

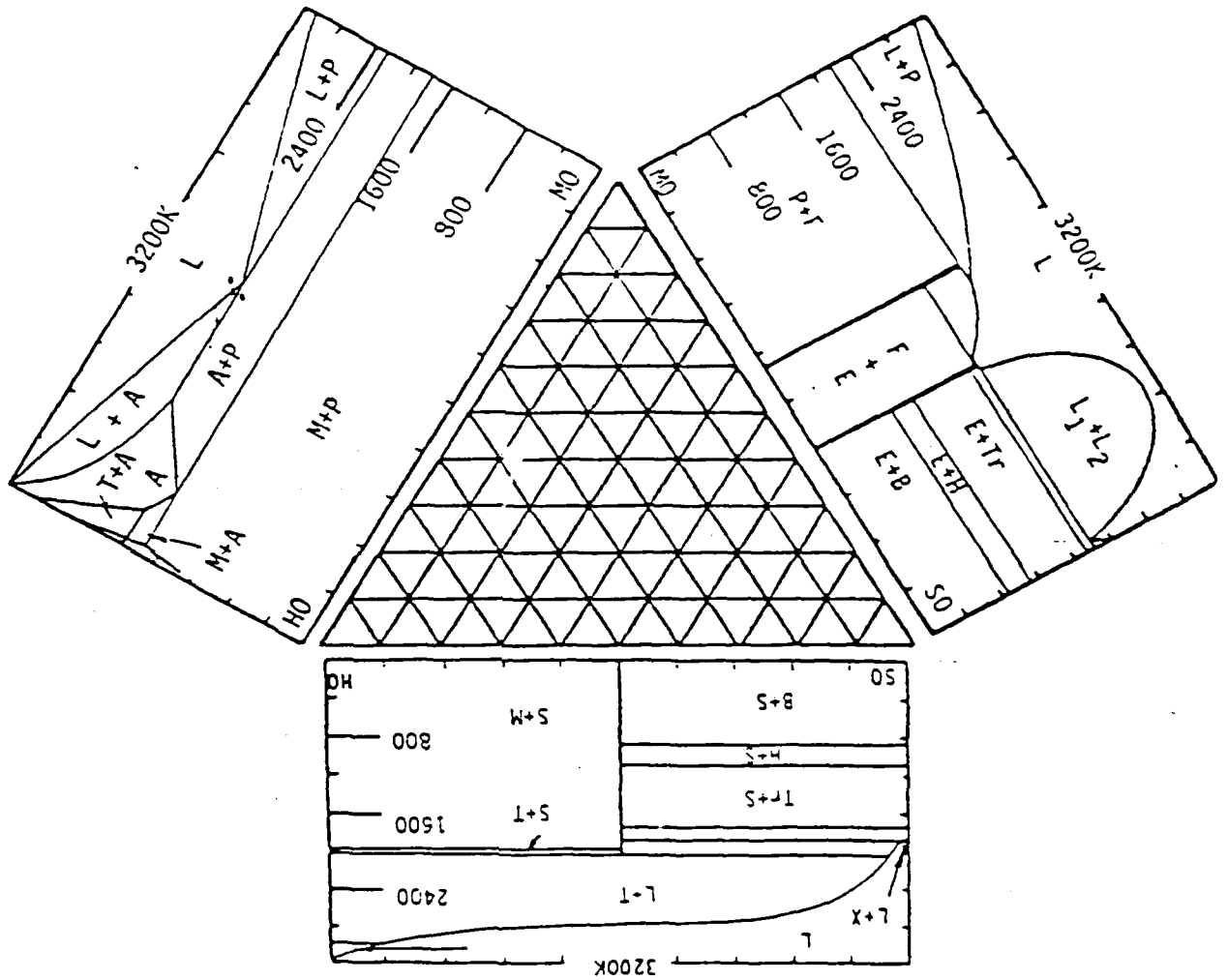


Figure 49. Calculated Isothermal Sections in the MO(1/2MgO)-SO(1/3SiO₂)-HO(1/3HfO₂) System.

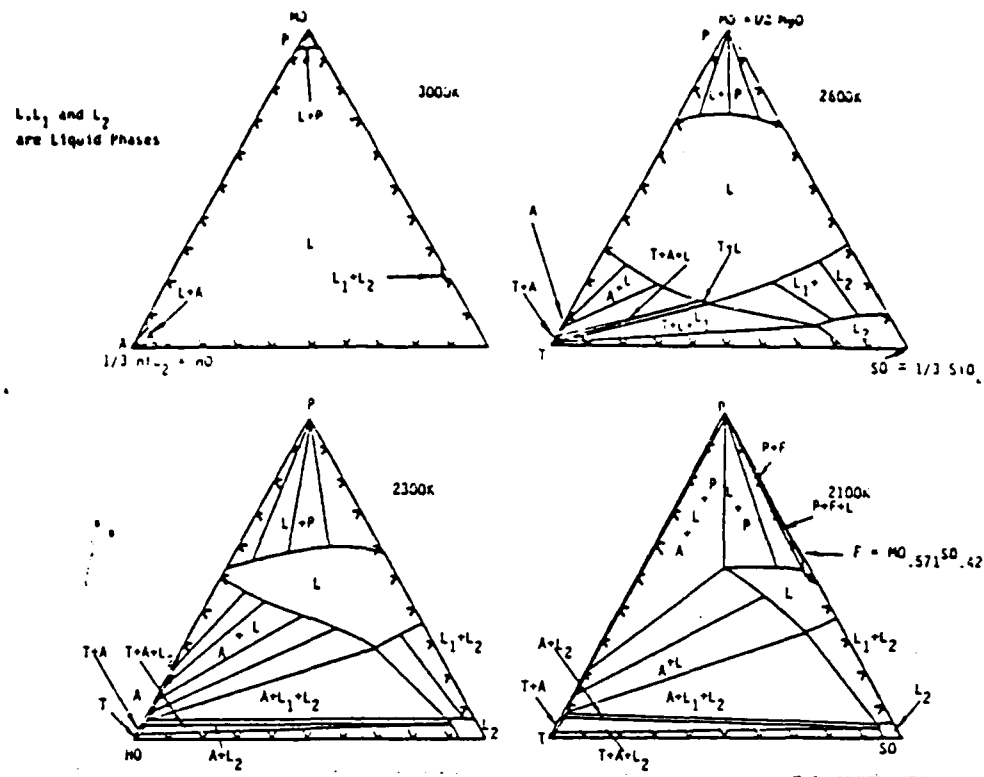


Figure 50. Calculated Isothermal Sections in Mg-SiO-HO

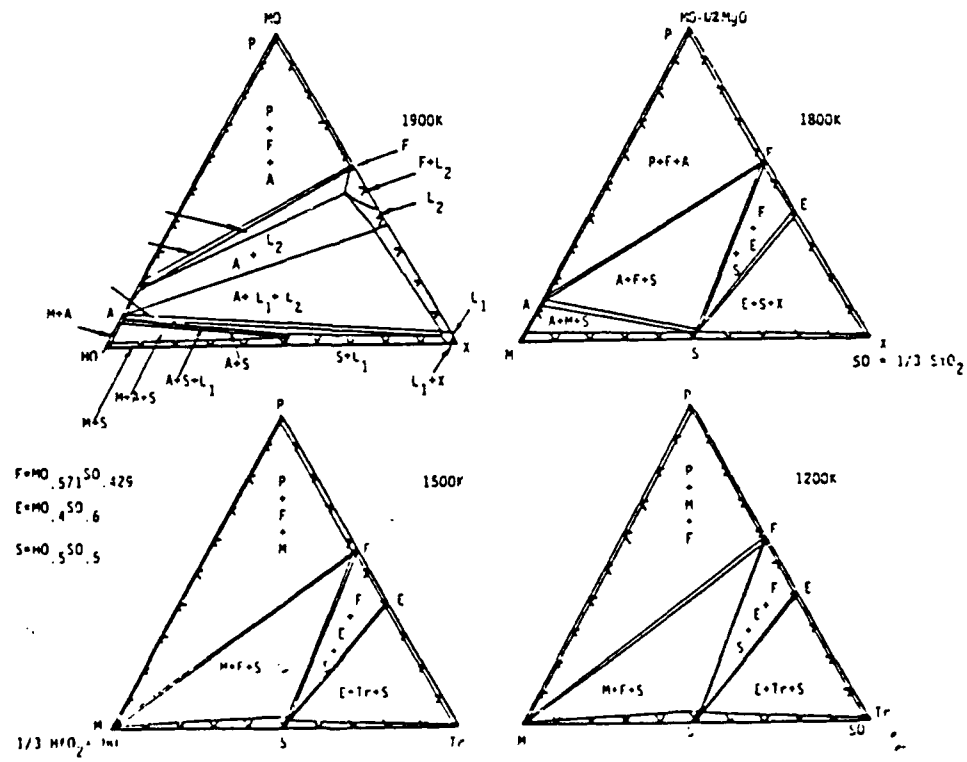


Figure 51. Calculated Isothermal Sections in Mg-SiO-HO

arranged in the appropriate ternary orientation to permit interpretation of the ternary sections. Thus the analysis of the MO-TO-GO case begins with Figure 20 showing the component quasi-binary systems. The calculated isothermal sections for this system between 2800°K and 700°K are shown in Figures 21-23. Figure 720 (8) shows a set of compatibility relations for this system. Examination of Figures 21-23 show how the phase fields covered by the liquid shrinks as the temperature is reduced with the final bit of liquid disappearing between 1600°K and 1590°K in Figure 22. The isothermal sections calculated at 1500°K and below, in Figure 23, agree with the experimental compatibility relations noted above in Figure 720 (8). The extension of the binary description into the ternary is performed along the lines suggested by Equations (7) - (11) in reference (4). Tables 3 and 5 contain all of the required descriptive data. Reference to Table 5 shows that in most cases the counterphase parameter is equal to zero. Two obvious exceptions are the $SO_{.5}(HO,ZO)_{.5}$ and $DO_{.4}(HO,ZO)_{.6}$ cases where the counterphase is stable and can be located in Table 3. In the other five cases where the counterphase is characterized by finite values of the counterphase parameter i.e. in GO-MO-SO and GO-MO-DO, the specific values were chosen to conform to available experimental data. In all cases, the ternary compound parameter, CAB, was set equal to zero except for the MO-TO-GO discussed above. In this case the values chosen were selected to conform to the published

compatibility results given in Figure 720 (8). Figures 24-26 display the calculated isothermal sections for the GO-MO-SO system. The sections at 1200°K and 900°K are in agreement with the compatibility relations shown in Figure 717 (8). The high temperature equilibria is dominated by the liquid miscibility gap entering from the GO-MO edge and the Enstatite ($E = MO_{.4}(GO,SO)_{.6}$) and Fosterite ($F = MO_{.571}(GO,SO)_{.429}$) compounds. The calculated isothermal sections in the GO-MO-DO system shown in Figures 27-29 were derived on the basis of the compatibility diagram in Figure 2470 (8). These are similar to the GO-MO-SO case in that the high temperature equilibria is dominated by the E and F phases. In each of the foregoing systems very little solid solubility is suggested. The SO-ZO-HO ($SiO_2-ZrO_2-HfO_2$) system shown in Figures 30-32 is of specific interest in high temperature thermal protection systems due to low diffusivity for oxygen in silica. However the system is dominated by liquid miscibility gaps and the equimolar compound, Q, which does not appear to possess very high stability (see Tables 3-5). The HO-DO-MO case in Figures 33-35 shows some solid solubility in the cubic A phase at high temperatures in the HO corner of the phase diagram. The calculations suggest that the liquid phase will disappear just below 2200°K. The analog HO-DO-YO and HO-MO-YO systems shown in Figures 36-38 and 39-41 both show extensive ranges of solid solubility in the cubic A and B phases which enter the ternary from the HO-YO edge. In both cases liquid phase is still present at

2200°K. However the liquid is just barely stable in the HO-MO-YO case at 2200°K. In both these systems it is likely that quenching from the high temperature cubic A region could permit retention of this phase at low temperatures. Figures 43-45 show the calculated isothermal sections in the HO-DO-ZO ($1/3\text{HfO}_2-1/2\text{CaO}-1/32\text{rO}_2$) system. Experimental sections are displayed in Figures 5392 A and B (9). Although the general features of the calculations and observations are in agreement a number of subtle differences appear which stem from differences in the binary and unary systems. To start with, the experimental diagram in Figure 5392 (9) appears to have combined the M/T transition in HfO_2 . Thus in comparison with Figure 15 or Figure 4444 (8) where an M/T transition is shown at 1976°K and a T/A transition shown at 2932°K, Figure 5392 B (9) shows a M(T)/A transition in HfO_2 near 2273°K. A second difference is that while Figure 15 and Figure 4444 (8) show narrow two-phase fields in HO-ZO Figure 5392 shows a wide two-phase field. Nevertheless the remaining features of the ternary sections are in general agreement. At high temperatures extensive solid solubility is present in cubic A phase leading to opportunities for retention on quenching and the equilibria is dominated by the Q phase $\text{DO}_{.4}(\text{HO},\text{ZO})_{.6}$ with no liquid present below 2300°K. Figures 46-48 show the calculated sections in SO-HO-YO. Vertical sections across the join HO-O and HO-M are shown in Figures 5440 and 5441 (9). Although there is general agreement between the calculated and

experimental results with respect to disappearance of the liquid phase near 2100°K in the HO-M join and 1800°K on the HO-O join, the calculations do not show the wide range of stability in the ternary for the cubic A phase indicated by the experimental diagram in Figures 5440 and 5441 (9). It would appear that the experimental results must reflect "quenching-in" of the high temperature form or difficulty in recognizing the O, M or Q phases experimentally. In view of the forgoing discussion of the heat of formation of the A phase in the HO-YO system presented earlier it is very unlikely that this phase could extend into the ternary to the extent suggested by Figures 5440 and 5441 (9) without precipitation of $\text{Y}_2\text{Si}_2\text{O}_7$, Y_2SiO_5 or HfSiO_2 . Figures 49-51 display the calculated MO-SO-HO sections which is dominated by miscibility gaps in the liquid phase at high temperatures and the E, F and S compound phases at low temperatures. Little solubility is suggested in the solid phases.

SUMMARY

The forgoing set of binary and ternary examples show how model calculations of ceramic phase diagrams can be performed in order to guide development of new structural systems and to evaluate existing experimental data. It also provides a means for planning future experimental studies.

ACKNOWLEDEMENT

This research was sponsored by the Air Force Office of Scientific Research, Bolling Air Force Base, D.C. 20332 under Contract F49620-84-C-0078.

REFERENCES

1. Kaufman, L. and Nesor, H. CALPHAD 2 35 (1978).
2. Kaufman, L. and Nesor, H. CALPHAD 3 27 (1979).
3. Kaufman, L. and Nesor, H. CALPHAD 3 279 (1979).
4. Kaufman, L., Hayes, F. Birnie, D., CALPHAD 5 163 (1981).
5. Kaufman, L., Hayes, F. Birnie, D., High Temperatures - High Pressures 14 619 (1982).
6. Gulati, S. T., Hansson, J. N. and Helfinstine, J. D. Metal Progress Feb. 1984 p. 21.
7. Kubashewski, O. and Alcock, C.B. "Metallurgical Thermochemistry Pergamon Press, Oxford (1979).
8. Levin, E. M., Robbins, C.R. and McMurdie, H. F. Phase Diagrams for Ceramists", American Ceramics Society, Columbus, Ohio (1964), (1969), (1975).
9. Roth, R. S., Negas, T. and Cook, L. "Phase Diagrams for Ceramists," American Ceramics Society, Columbus, Ohio (1981).
10. Fitzer, E., Neumann, S. and Slichting, J. Glastechn. Ber. (1983).
11. Slichting, J. and Neumann, S. Jnl. of Non-Crystalline Solids 48 185 (1982).
12. Lorentz, J., Lukas, H. L., Hucke, E. E. and Gaukler, L.J., CALPHAD 7 125 (1983).
13. Senft, G. and Stubican, V. S. Mat. Res. Bull. 18, 1163 (1983).

IV. CALCULATION OF MULTICOMPONENT CERAMIC PHASE DIAGRAMS

Larry Kaufman

ManLabs, Inc., 21 Erie Street
Cambridge, Massachusetts, U.S.A., 02139

(Presented at the International Conference on "Electronic Structure and Phase Stability" Argonne National Laboratory, Argonne, Illinois, August 1987. Proceedings to be published in Physica B 1988)

A data base is being developed for calculation of quasi-binary and quasi-ternary phase diagrams of ceramic systems. Previous segments of this base cover combinations of Cr_2O_3 , MgO , Al_2O_3 , SiO_2 , CaO , Si_3N_4 , AlN , BeO , Y_2O_3 and Ce_2O_3 . Lattice Stability, Solution and Compound Phase Parameters have been derived covering the liquid, spinel, corundum, periclase, cristobalite, tridymite, quartz, hexagonal and beta prime phases which appear in the binary systems composed of pairs of these compounds. Compound phases formed from specific binary combinations of these compounds (i.e. $\text{MgO}\cdot\text{Cr}_2\text{O}_3$) have been characterized. This description is based on observed thermochemistry and phase diagrams for the binary systems of interest. Selected ternary systems have been computed based on the foregoing data base for comparison with experimental sections in order to illustrate the usefulness of the data base. To date, sixty six quasi binary and nineteen quasi ternary systems have been calculated. The most recent set of papers extend the base to cover GeO_2 , HfO_2 , ZrO_2 and TiO_2 . The components are of particular

interest in recent developments of structural high temperature ceramics and applications requiring unusual toughness. The current work deals with four quasi binary systems and four quasi ternary systems which have been calculated over a wide range of temperatures. These samples demonstrate the capability of the data base and computational model for dealing with phase equilibria in multicomponent oxide systems over a wide range of conditions and compositions of practical interest.

INTRODUCTION

Previous papers in the current series (1-6) provide descriptive information for computing condensed phase equilibria in ceramic systems. In view of current interest in applying ceramic systems in applications requiring toughness (7) and structural performance at high temperatures the present data base is being extended to cover GeO_2 , HfO_2 , ZrO_2 and TiO_2 . This has been effected by employing available sources (8-10) of thermochemical and phase diagram data. High temperature ceramics have received increased attention during the last few years for structural, thermal protection and engine applications. SIALONS and combinations of zirconia and hafnia with Al_2O_3 , SiC and Si_3N_4 have been shown to develop strength and toughness. This has opened the door to a whole range of new uses for these materials. Recently Slichting and co-workers (11,12) have shown that by alloying GeO_2 with SiO_2 a whole range of glasses can be synthesized with tailor-made coefficients of expansion. Utilization of such compositions offers the possibility of enhancing the high temperature oxidation resistance of ceramic composites in which a mixed GeO_2 - SiO_2 phase with a desired CTE could replace the conventional SiO_2 as a filler. This kind of compositing would open an entire spectrum of new opportunities for synthesis of high

temperature ceramics. One of the major obstacles in the development of complex composite systems is the lack of phase diagram information which can be used to guide the fabrication and processing of a new material and help to predict its performance. The current methods of employing models to predict high temperature behaviour has proven useful when basic data is unavailable or too costly and time consuming to obtain by conventional means. This method consists of developing a data base of thermochemical and phase diagram information in analytical form and employing computer models to extend the description to binary and ternary systems. Recently J. Lorenz et al. (13) applied this method successfully to SiC-ZrO₂ and SiC-ZrO₂-Al₂O₃-SiO₂ in order to evaluate composition effects and identify fabrication conditions. In the present paper, the data base has been expanded by analyzing the following quasi-binary systems: TiO₂-Al₂O₃, TiO₂-SiO₂, TiO₂-CaO, and TiO₂-Y₂O₃. These results when combined with earlier findings (1-6) were employed to compute a range of isothermal sections in the following quasi ternary systems sufficient to define their characteristics: TiO₂-Al₂O₃-MgO, Al₂O₃-TiO₂-SiO₂, TiO₂-Al₂O₃-HfO₂ and MgO-SiO₂-TiO₂.

LATTICE STABILITY VALUES

Table 1 defines the lattice stability values employed in the current study. Data for the stable forms were taken from Kubaschewski and Alcock (8). The remaining values were adopted along with the lines employed previously. As shown in Table 1 the present analysis is based on one gram atom of compound and/or solution phase. Moreover, dissociation of the components or vaporization is not considered!

TABLE 1

SUMMARY OF LATTICE STABILITY PARAMETERS

(All units in Joules per gram atom (mole of atoms), T in Kelvins).

P = Periclase, C = Corundum, S = Spinel, X = Cristobalite
 Tr = Tridymite, H = Hexagonal(α quartz), B(SO) = Trigonal(β quartz)

F = Rutile (TO)

A = Cubic (HO and ZO)

T = Tetragonal (HO and ZO)

M = Monoclinic (HO and ZO)

Y = High Temperature YO

B = Low Temperature YO

L = Liquid

GO = $1/3\text{GeO}_2$ HO = $1/3\text{HfO}_2$ TO = $1/3\text{TiO}_2$ AO = $1/5\text{Al}_2\text{O}_3$ MO = $1/2\text{MgO}$ DO = $1/2\text{CaO}$ SO = $1/3\text{SiO}_2$ YO = $1/5\text{Y}_2\text{O}_3$ CE = $1/3\text{CeO}_2$ ZO = $1/3\text{ZrO}_2$ GOGOLH* = $(1/3)\text{GeO}_2$ (liquid) - $(1/3)\text{GeO}_2$ (hexagonal)GOGOLR = $(1/3)\text{GeO}_2$ (liquid) - $(1/3)\text{GeO}_2$ (rutile)GOGOHR = $(1/3)\text{GeO}_2$ (hexagonal) - $(1/3)\text{GeO}_2$ (rutile)

GOGOLR = GOGOLH + GOGOHR

GOGOLH = 14644 - 10.54T

HOHOLA = 34865 - 11.00 T

GOGOLR = 22087 - 16.23T

HOHOAT = 2239 - 0.753T

GOGOHR = 7443 - 5.69T

HOHOLT = 37104 - 11.753T

GOGOLA = - 11.00T

HOHOTM = 2724 - 1.381T

GOGOLT = - 11.57T

HOHOLM = 39828 - 13.134T

GOGOLM = - 13.14T

HOHOLX = - 2.092T

GOGOLC = - 10.21T

HOHOLP = - 8.368T

GOGOLP = - 8.37T

HOHOLC = - 10.209T

GOGOBR = 7109 - 5.40T

HOHOLB = 30711 - 10.376T

GOGOLX = - 1.67T

HOHOLY = 23849 - 9.396T

GOGOLTr = - 2.01T

HOHOLR = 21882 - 10.42 T

GOGOHB(SO) = 335 - 0.29T

GOGOTrH = 14644 - 8.54T

* These differences specify the free energy of one phase (i.e. liquid) minus the free energy of the second phase (i.e. hexagonal) for a compound.

BINARY SYSTEMS

Tables 2-4 and Figures 1-4 summarize the results for the binary systems listed above. The solution phases are described as subregular solutions along the lines of Equations (1) and (2) of reference 4. When the subregular parameters are equal (i.e. $TC-YO$, R , Y and B) the solution is regular. The compound phases are defined at fixed compositions (i.e. Equations 3-6 of reference 4) in terms of the compound parameter and the base phase. The latter values are listed in Table 3 for the compounds of interest while Table 4 shows the Gibbs energy of formation for these compounds from the component oxides. Figure 1 shows the calculated $TO-AO$ ($1/3 TiO_2-1/5 Al_2O_3$) system derived from the description contained in Tables 1-4 in conformity with Figure 316 of reference 9. There is one quasi binary compound phase, designated as D , which transforms on heating above 2000K to a different structure, E . Figure 2 shows the calculated $TO-SO$ ($1/3 TiO_2-1/3 SiO_2$) system based on Tables 1-4 which agrees with the experimental diagram in Figure 113 (9). Figure 3 displays the calculated $TO-DO$ phase diagram ($1/3 TiO_2-1/2 CaO$) based on Tables 1-4 in agreement with the experimental results shown in Figures 239, 4312 and 4553 (9). The final quasi binary in this group shown in Figure 4 is the calculated $TO-YO$ ($1/3 TiO_2-1/5 Y_2O_3$) system based on the parameters listed in Tables 1-4. These parameters were derived from the values given earlier for the $HO-YO$ system (6).

TERNARY SYSTEMS

The description of the forgoing systems combined with those presented earlier (1-6) have been employed to calculate isothermal sections in four quasi-ternary systems over a wide range of temperatures. The results of these calculations are presented in

TABLE 2

QUASIBINARY SOLUTION PARAMETERS FOR OXIDE SYSTEMS

(All units in Joules per gram atom (mole of atoms), T in Kelvins)

LTOAO =	5335 + 13.60T	LAOTO =	7008 + 13.60T
RTOAO =	62760	RAOTO =	62760
CTOAO =	62760	CAOTO =	62760
LTOSO =	51463	LSOTO =	43095
FTOSO =	62760	RSOTO =	62760
XTOSO =	62760	XSOTO =	62760
TTOSO =	62760	TSOTO =	62760
LTODD =	-127194 + 50.208T	LDOTO =	-127194 + 50.208T
RTODD =	41840	RDOTO =	41840
PTODD =	83680	PDOTO =	83680
LTOYO =	14016 + 4.184T	LYOTO =	14016 + 4.184T
RTOYO =	20920	RYOTO =	20920
YTOYO =	20920	YYOTO =	20920
BTOYO =	20920	BYOTO =	20920

TABLE 3

SUMMARY OF COMPOUND PARAMETERS FOR BINARY SYSTEMS

(All units in Joules per gram atom (mole of atoms) T in Kelvins)

<u>Compound</u>	<u>Name</u>	<u>Stoichiometry</u>	<u>Stability</u>	<u>Base</u>	<u>Compound/Parameter</u> (Joules/g.at.)
(1/8)(Al ₂ O ₃ .TiO ₂)	D	TO _{.375} AO _{.625}	stable (below 2000†)	C	81755 - 4.184T
(1/8)(Al ₂ O ₃ .TiO ₂)	F	TO _{.375} AO _{.625}	stable (above 2000†)	C	-16004 + 44.000T
(1/5)(TiO ₂ .CaO)	U	TO _{.6} DO _{.4}	stable	F	8786 + 37.032T
(1/17)(3TiO ₂ .4CaO)	V	TO _{.529} DO _{.471}	stable	F	-5021 + 33.432T
(1/12)(TiO ₂ .3CaO)	V	TO _{.4} DO _{.6}	stable	F	-10042 + 33.432T

TABLE 4

CALCULATED FREE ENERGY OF FORMATION OF COMPOUND PHASES
(A) units in Joules per gram atom (mole of atoms) T in Kelvins)

Compound	Name	Stoichiometry	Free Energy of Formation, ΔG_f [298K] from Component Compounds
(1/6)(Al ₂ O ₃ ·7TiO ₂)	D	TO _{.375} AO _{.625} stable below 2000K	-9272 + 4.0E1T
(2/3)(Al ₂ O ₃ ·7TiO ₂)	E	TO _{.375} AO _{.625} stable above 2000K	13606 - 7.373T
(1/5)(TiO ₂ ·CaO)	U	TO _{.6} DO _{.4}	-16175 - 3.95T
(1/5)(TiO ₂ ·CaO)	U	TO _{.6} DO _{.4}	ΔH_f (experimental) = -16150 ± 516
(1/17)(3TiO ₂ ·4CaO)	V	TO _{.529} DO _{.471}	-17451 + 3.03T
(1/17)(3TiO ₂ ·4CaO)	V	TO _{.529} DO _{.471}	ΔH_f (experimental) = -17472
(1/12)(2TiO ₂ ·3CaO)	W	TO _{.5} DO _{.5}	-17397 + 3.0E1T
(1/12)(2TiO ₂ ·3CaO)	W	TO _{.5} DO _{.5}	ΔH_f (experimental) = -17431

TABLE 5

SUMMARY OF COUNTERPHASE STOICHIOMETRY AND PARAMETERS
EMPLOYED IN TERNARY CALCULATIONS

System	Stable Phase (Name)	BASE	COUNTERPHASE	BASE	COUNTERPHASE Parameter (Joules/g. at.)
TO-AO-MO	TO _{.75} MO _{.75}	(W) F	AO _{.75} MO _{.25}	F	0
	TO _{.6} MO _{.4}	(V) P	AO _{.6} MO _{.4}	P	0
	TO _{.429} MO _{.571}	(U) F	AO _{.429} MO _{.571}	F	0
	TO _{.375} AO _{.625}	(D) C	MO _{.375} AO _{.625}	C	0
	TO _{.375} AO _{.625}	(D) C	MO _{.375} AO _{.625}	C	0
	MO _{.286} AO _{.714}	(SP) S	MO _{.286} TO _{.714}	S	0
AO-TO-SO	TO _{.375} AO _{.625}	(D) C	SO _{.375} AO _{.625}	C	0
	TO _{.375} AO _{.625}	(E) C	SO _{.375} AO _{.625}	C	0
	SO _{.286} AO _{.714}	(M) C	TO _{.286} AO _{.714}	C	0
TO-AO-TI	MO _{.5} TO _{.5}	(S) T	AO _{.5} TO _{.5}	T	0
	TO _{.375} AO _{.625}	(D) C	MO _{.375} AO _{.625}	C	0
	TO _{.375} AO _{.625}	(E) C	MO _{.375} AO _{.625}	C	0
MO-SO-TI	TO _{.75} MO _{.25}	(F) F	SO _{.75} MO _{.25}	F	(ICAF = -25104)
	TO _{.6} MO _{.4}	(V) F	SO _{.6} MO _{.4}	F	(ICAF = -58576)
	TO _{.429} MO _{.571}	(U) F	SO _{.429} MO _{.571}	F	0
	TO _{.375} MO _{.625}	(E) F	SO _{.375} MO _{.625}	F	0
	TO _{.375} MO _{.625}	(E) F	SO _{.375} MO _{.625}	F	(ICAF = -40840)

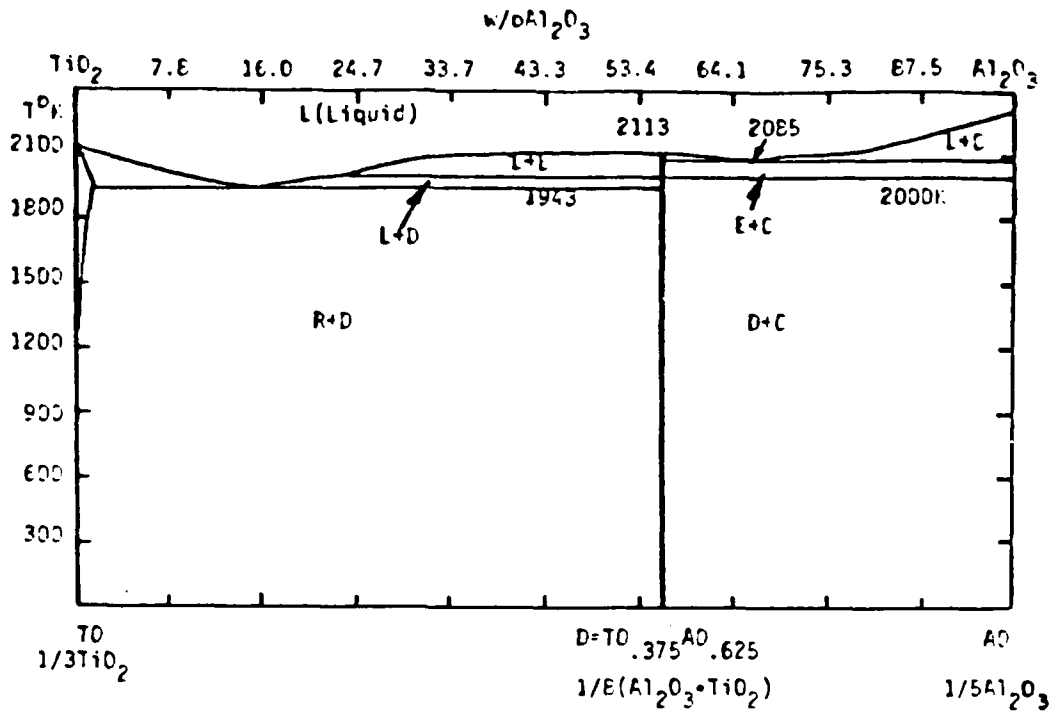


Figure 1. Calculated TiO₂-Al₂O₃ Phase Diagram.

E = High Temperature form of D

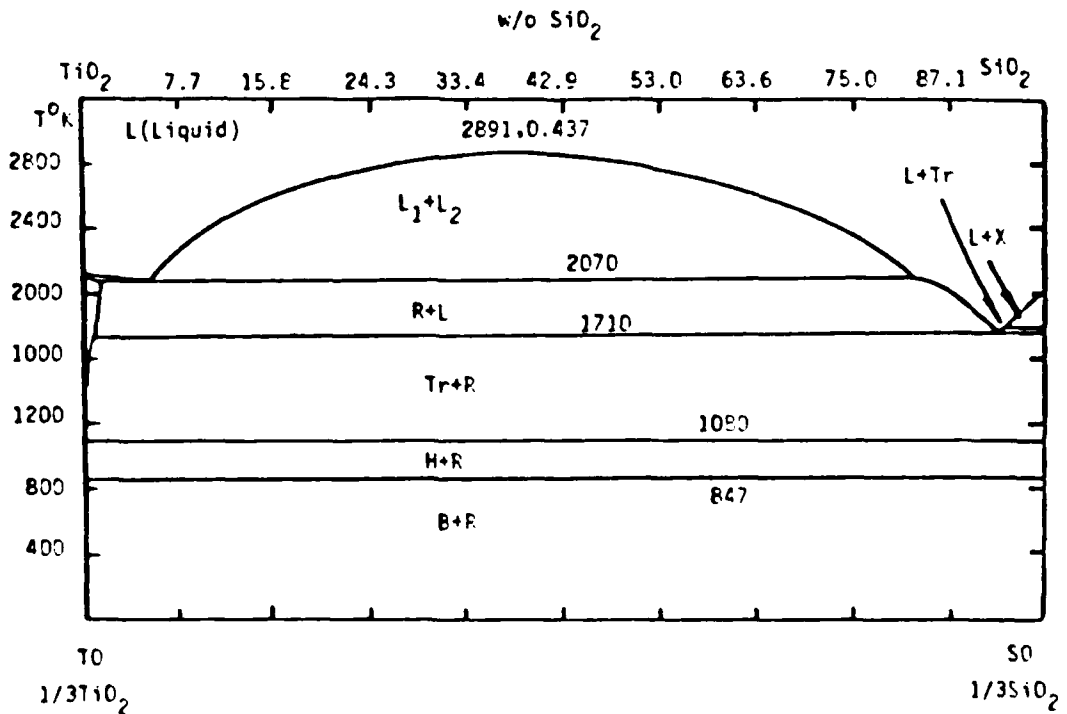


Figure 2. Calculated TiO₂-SiO₂ Phase Diagram

X = Cristoballite
 Tr = Tridymite
 H = Quartz
 B = Quartz

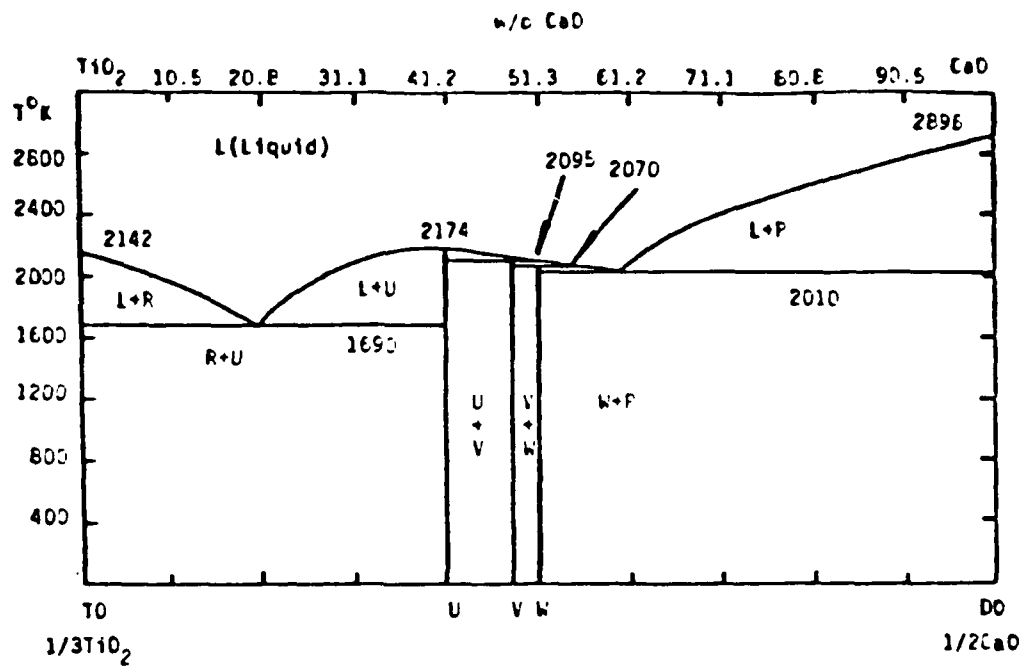


Figure 3. Calculated TiO₂-CaO Phase Diagram.

$$U = TO_{.6}DO_{.4} = 1/5(TiO_2 \cdot CaO)$$

$$V = TO_{.529}DO_{.471} = 1/17(3TiO_2 \cdot 4CaO)$$

$$W = TO_{.5}DO_{.5} = 1/12(2TiO_2 \cdot 3CaO)$$

w/o Y₂O₃

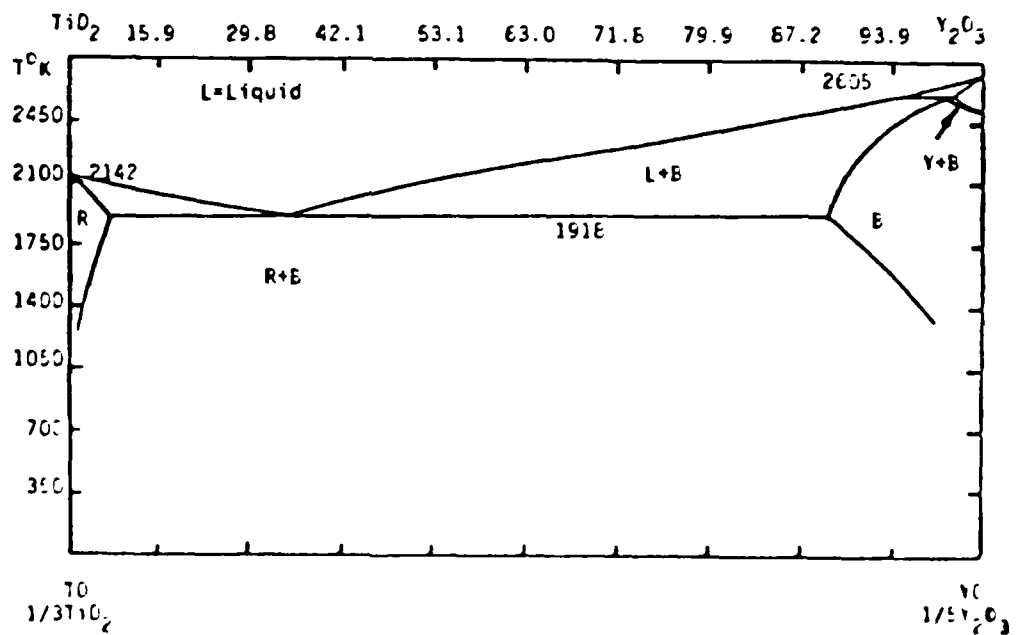


Figure 4. Calculated TiO₂-Y₂O₃ Phase Diagram.

Figures 5-20. In each case the component quasi-binary systems are arranged in the appropriate ternary orientation to permit interpretation of the ternary sections. Thus the analysis of the TO-AO-MO case begins with Figure 5 showing the component quasi-binary systems. The calculated isothermal sections for this system between 3000°K and 900°K are shown in Figures 6-8. Figures 713 and 714 (8) show experimental results which are in good agreement with the calculations. In particular the minimum melting point is shown at 1843K in the experimental diagram in the TO rich part of the TO-MO edge in excellent agreement with the calculated results shown in Figure 7. In addition, Figure 6 shows the calculated Gibbs energy changes defining the subsolidus stability of the various compounds in the system. The extension of the binary description into the ternary is performed along the lines suggested by Equations (7) - (11) in reference (4). Tables 3 and 5 contain all of the required descriptive data. Reference to Table 5 shows that in most cases the counterphase parameter is equal to zero. This is true in the TO-AO-MO, AO-TO-SO AND AO-TO-HO cases. The values for F, V and W in MO-SO-TO were chosen to agree with experimental results. Figures 9-12 show the AO-TO-SO calculations which are dominated by the miscibility gap in the liquid at high temperatures and the compound interactions at low temperatures. The Gibbs energy change calculated for the interactions between the M+R and D+T pairs is shown in Figure 12 defining 1707K as the critical temperature. The calculated results are in good agreement with the experimental findings shown in Figures 771-775 (9). The calculated sections for TO-AO-HO are shown in Figures 13-16 which display the lowest temperature for liquid stability near the TO corner on the TO-AO edge just below 1900K. Experimental description of TO-AO-ZO in Figures 773-774 (9) shows similar behavior at 1853K. The final set of ternary calculations are presented in Figures 17-20 for the MO-SO-TO system. Extensive experimental data have been reported for this system in Figures

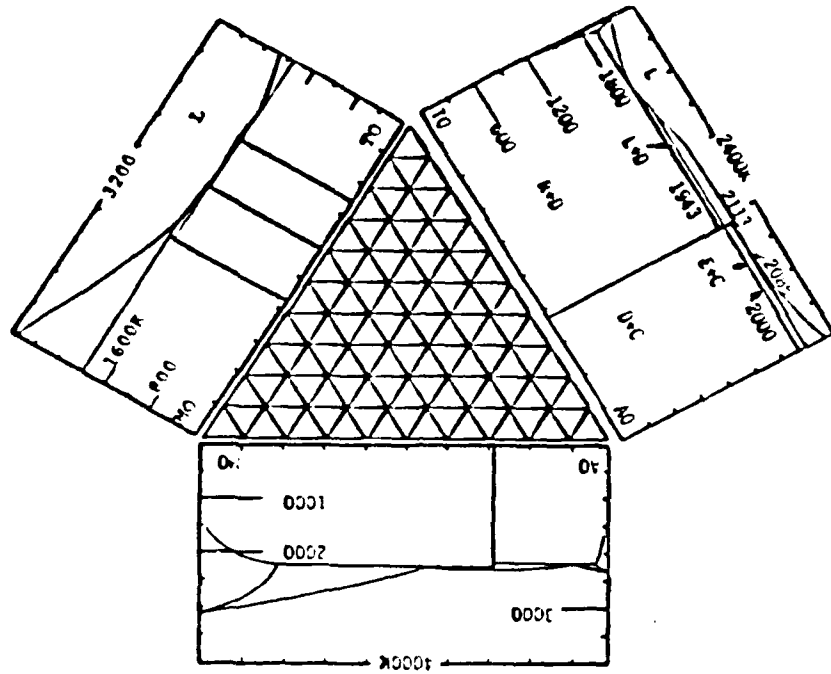


Figure 5 Calculated Isothermal Sections in the $TO(1/3 TiO_2) - AO(1/5 Al_2O_3) - MO(1/2 MgO)$ system.

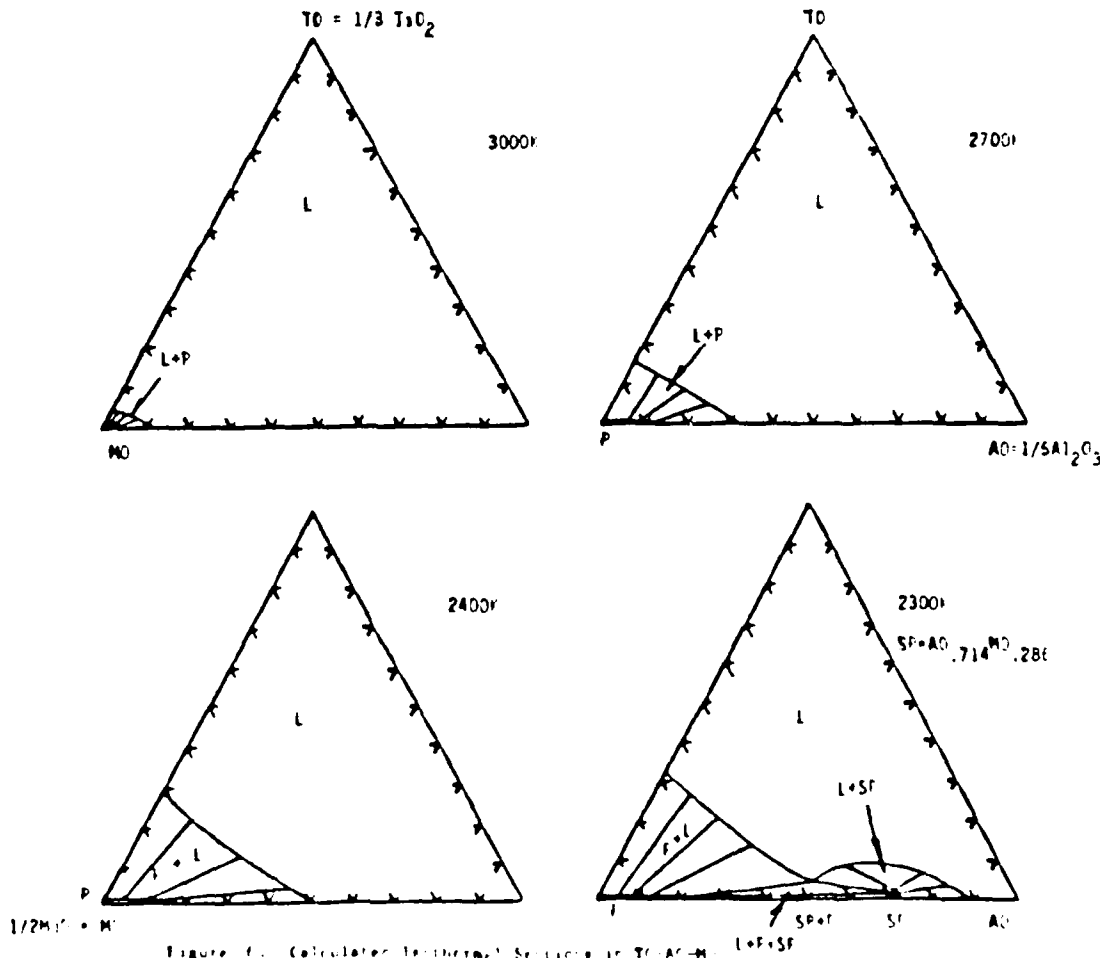


Figure 6. Calculated Isothermal Sections in Ti-AO-M

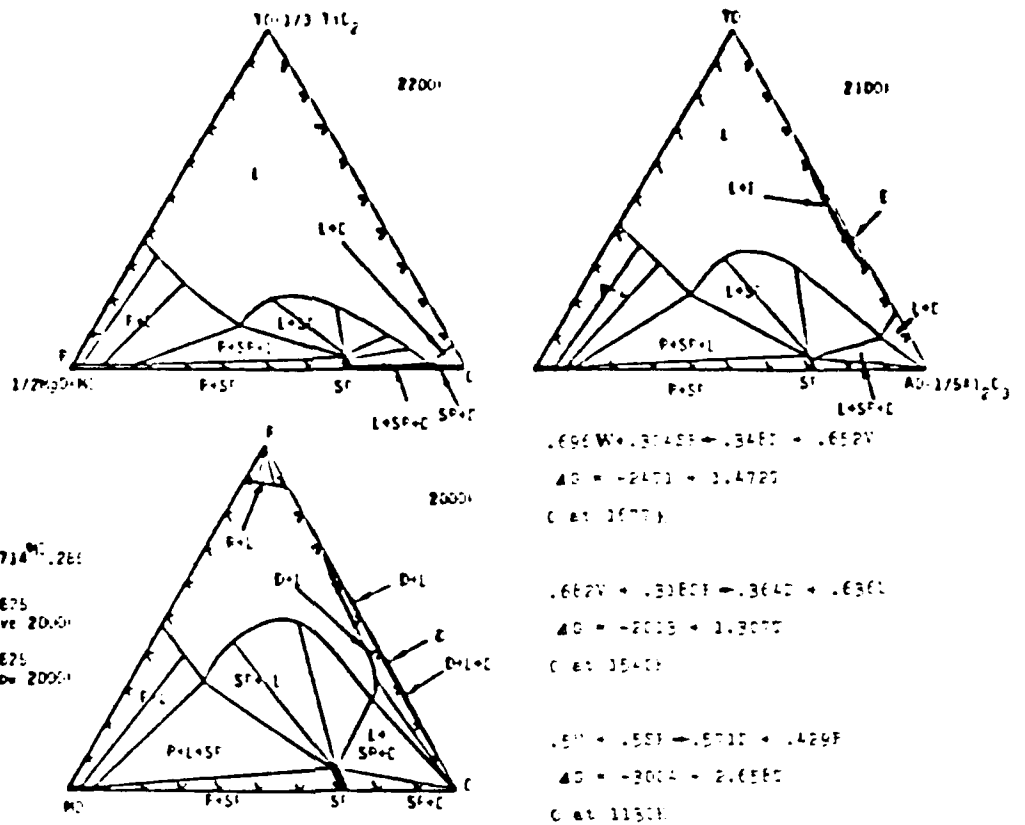


Figure 7. Calculated Isothermal Sections in TO-AC-MO

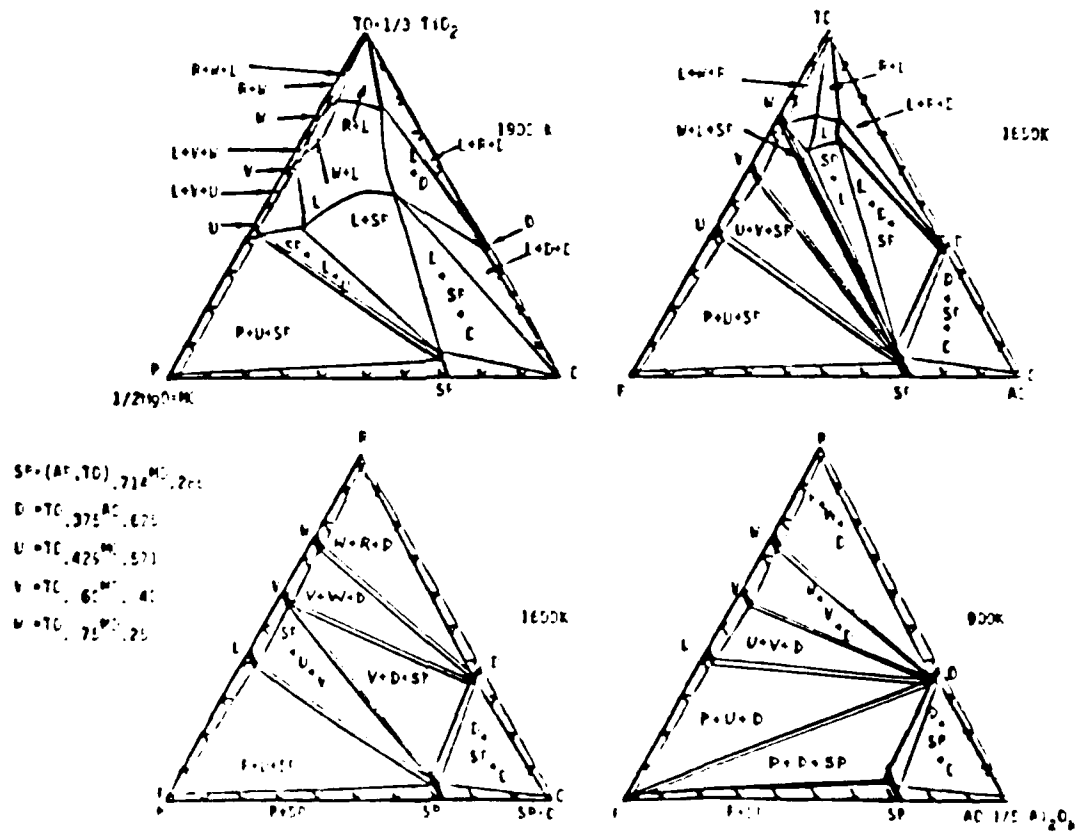


Figure 8. Calculated Isothermal Sections in TO-AC-P

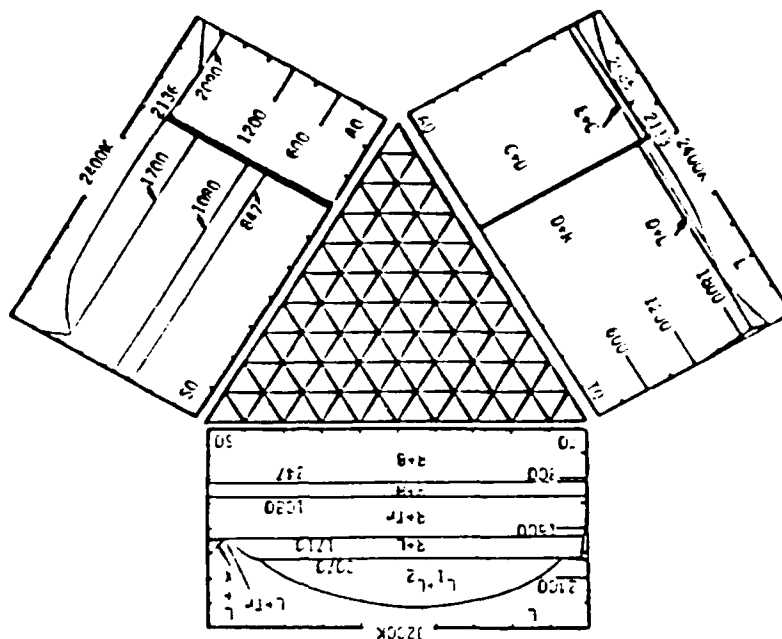


Figure 9. Calculated Isothermal Sections in the $AO(1/5 Al_2O_3) - TO(1/3 TiO_2) - SO(1/3 SiO_2)$ system.

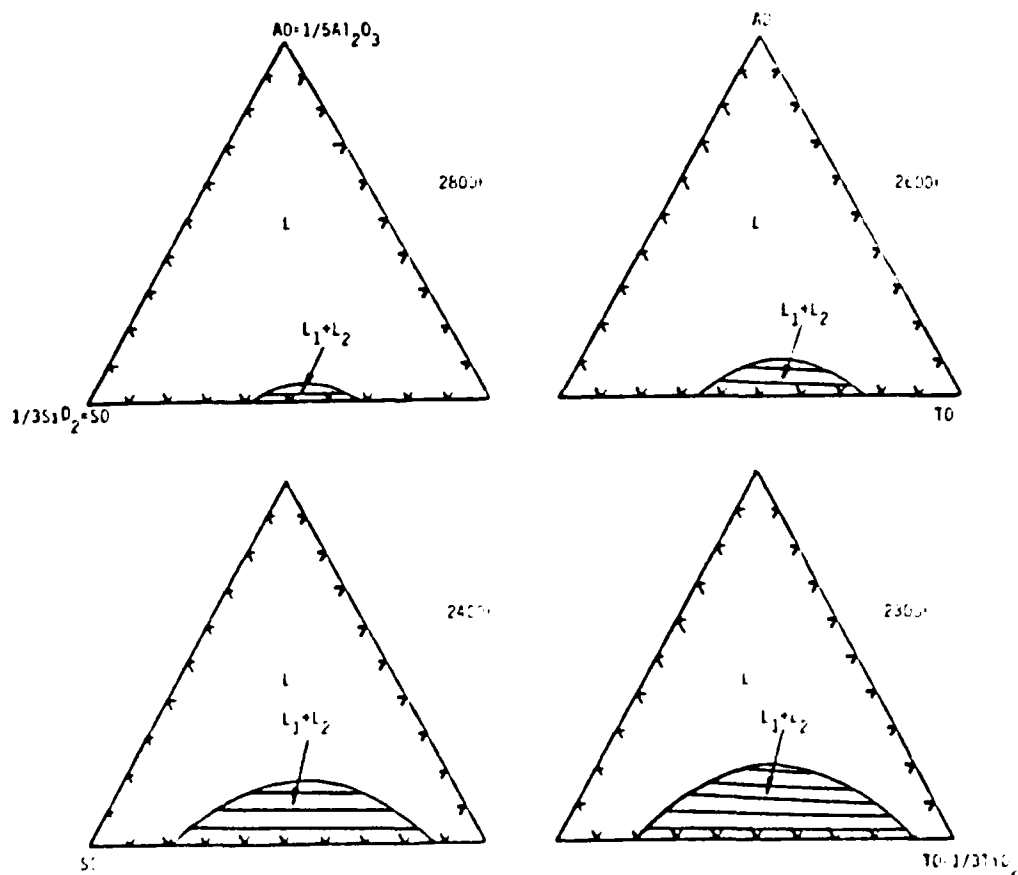


Figure 10. Calculated Isothermal Sections in AO-TO-SO

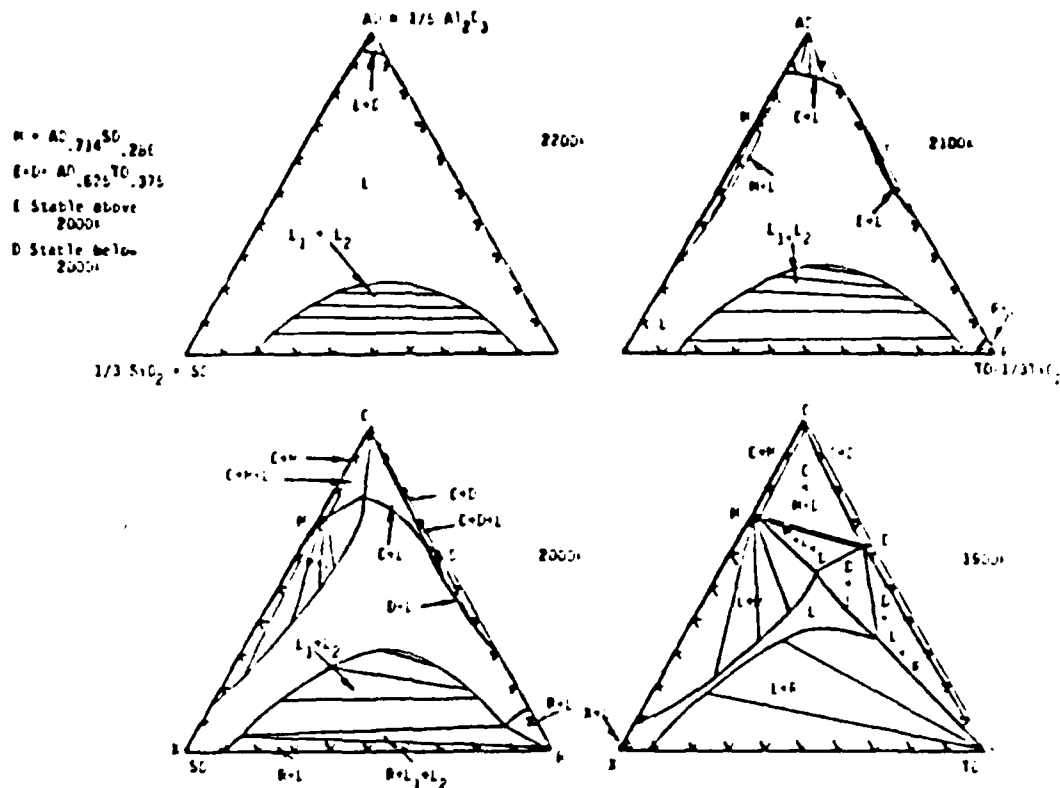


Figure 11. Calculated Isothermal Sections in AD-TG-SC

$.7M = .3E = .2C = .2T$
 $AD = -65E5 + 3.E57C$
 O at 1707°

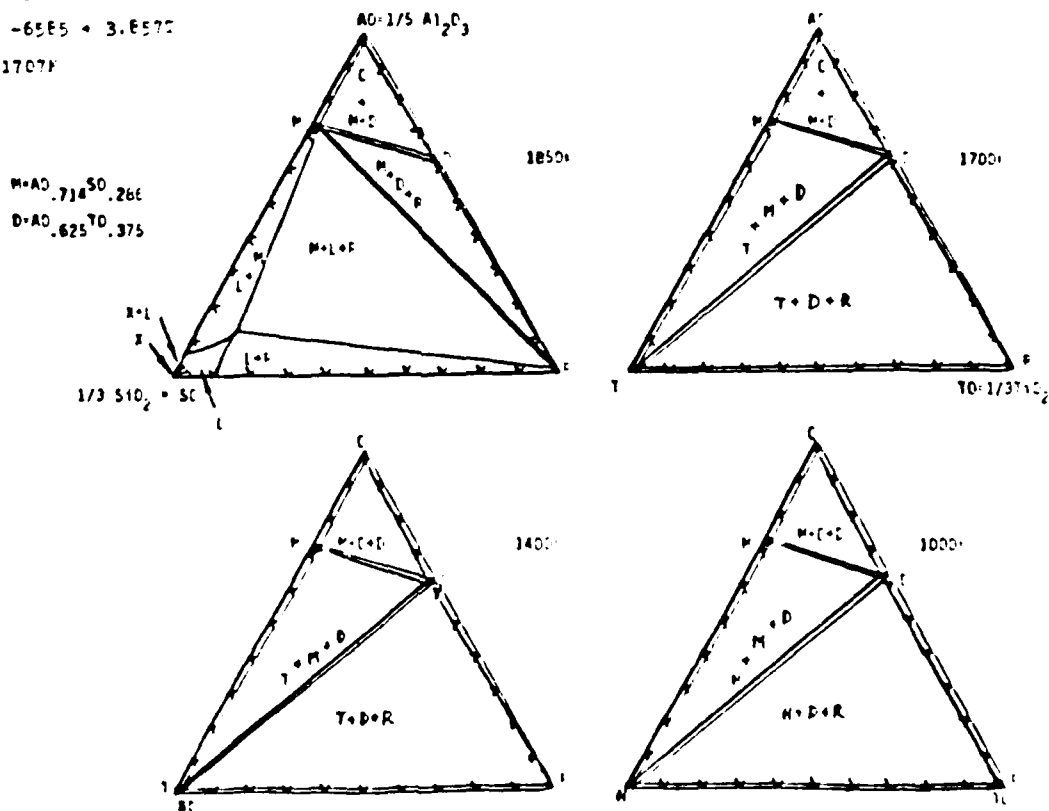


Figure 12. Calculated Isothermal Sections in AD-TG-SC

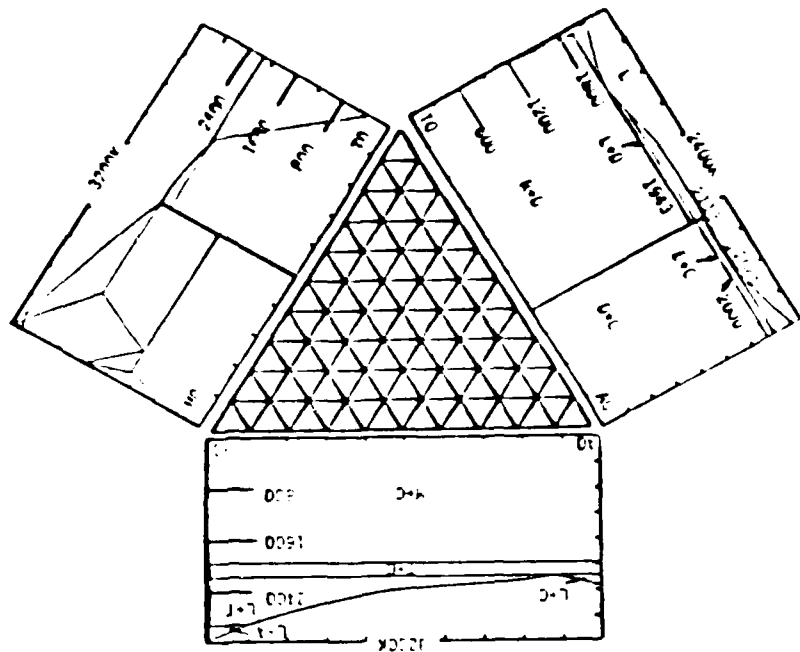


Figure 16. Calculated Isothermal Sections in the $TiO_2 - 1/3 TiO_2 - Al_2O_3 - HfO_2$ system.

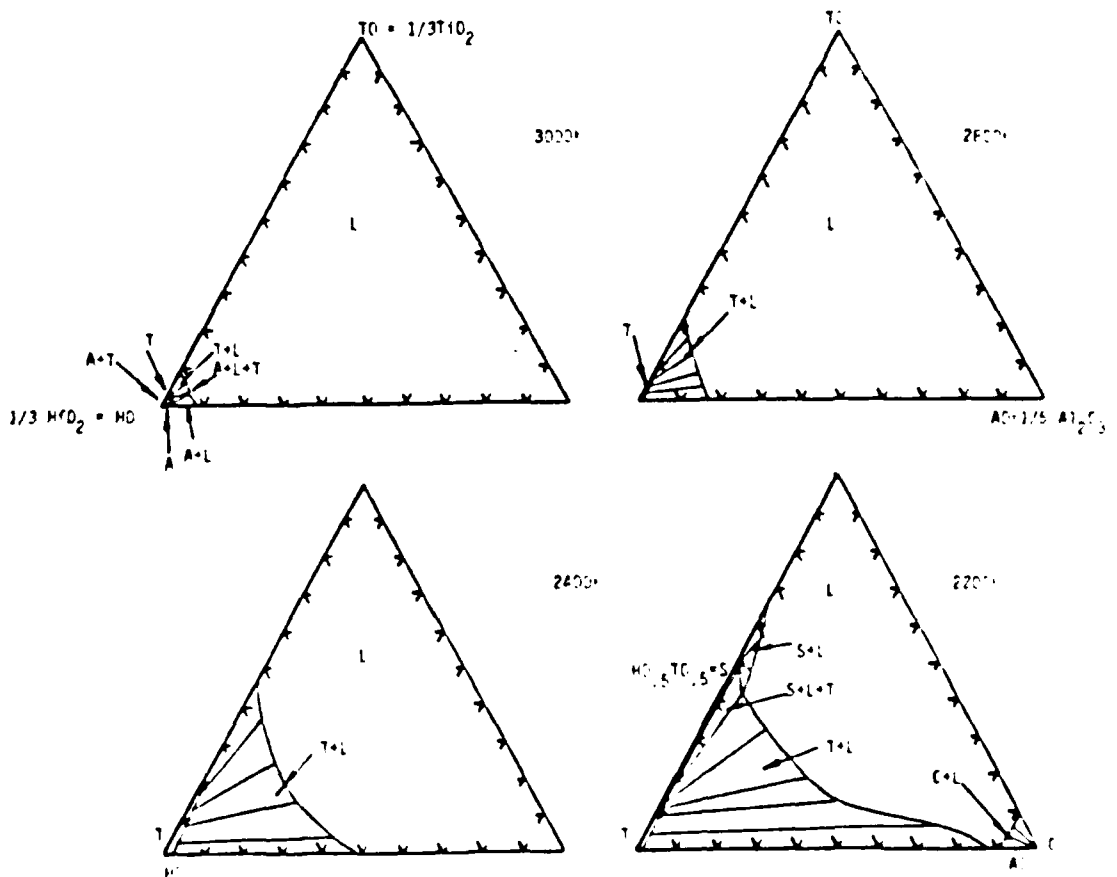
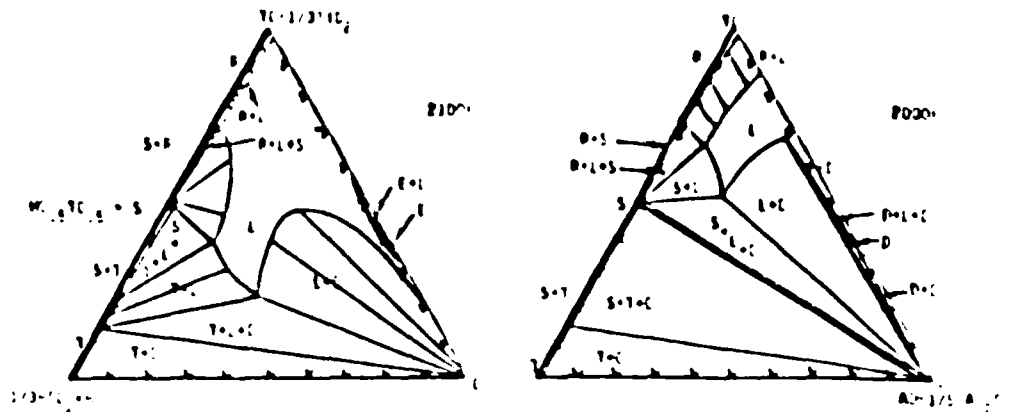


Figure 17. Calculated Isothermal Sections in $TiO_2 - Al_2O_3 - HfO_2$.



$E=TC, .375AC, .625$
 $F=TC, .375AC, .625$
 E Stable below 2000°
 F Stable above 2000°

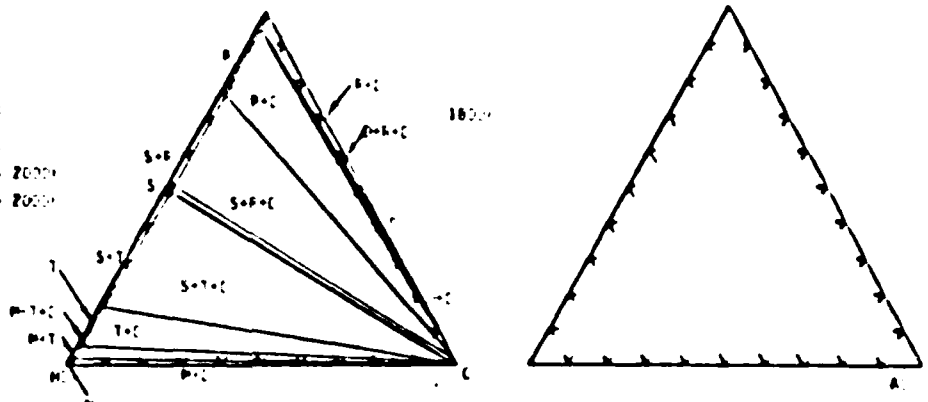
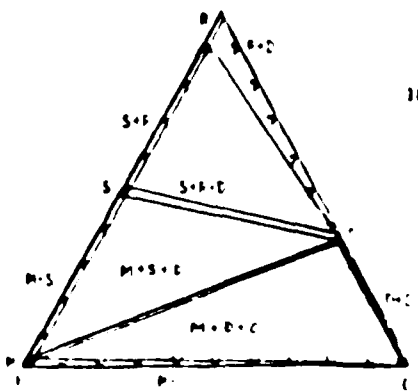
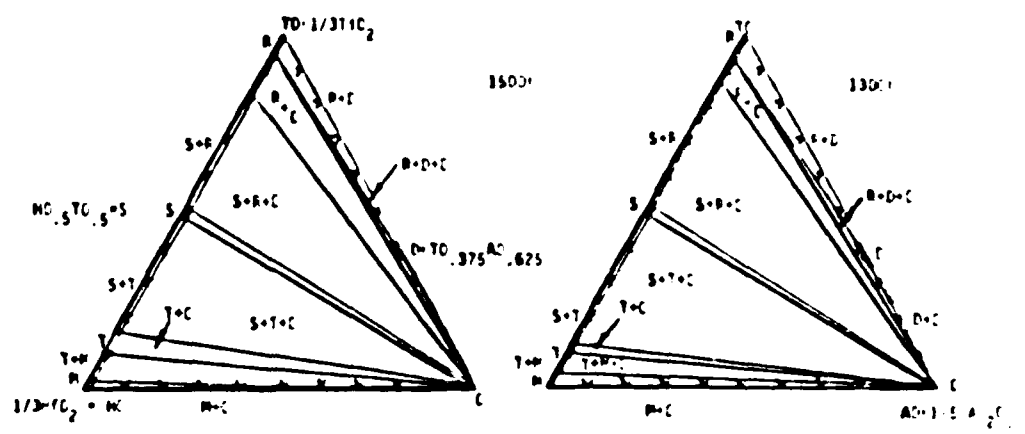


Figure 15. Calculated Isothermal Sections in TO-AC-MC



$$.545S + .455C = .727D + .273T$$

$$\Delta G = -6274 + 5.43T$$

0 at 1155°

Figure 16. Calculated Isothermal Section at 1000°

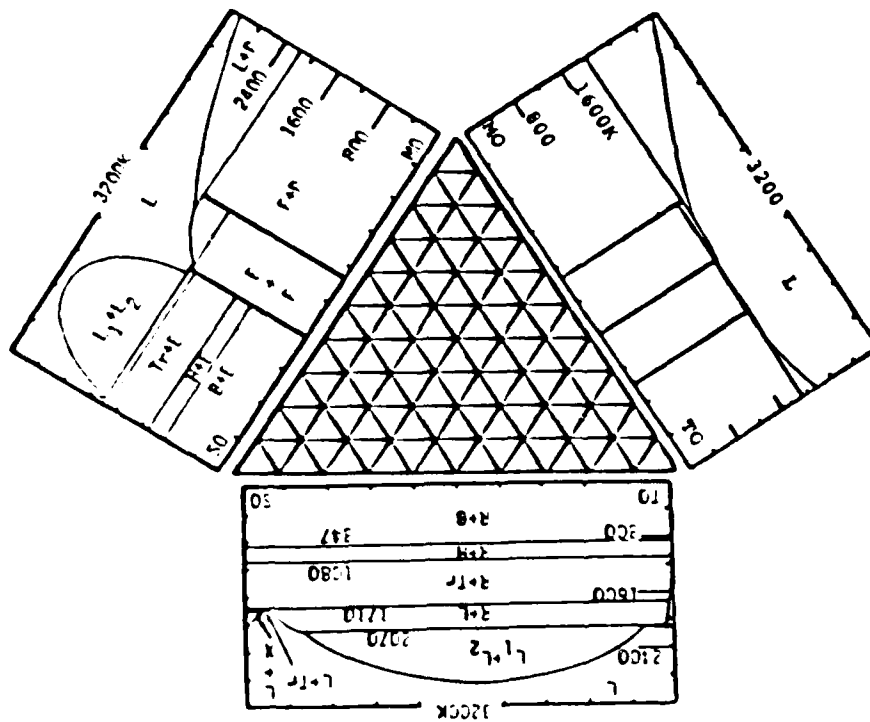


Figure 17 Calculated Isothermal Sections for the $MnO(1/2MnO) - TO(1/3TiO_2) - SC(1/3SnO_2)$ System

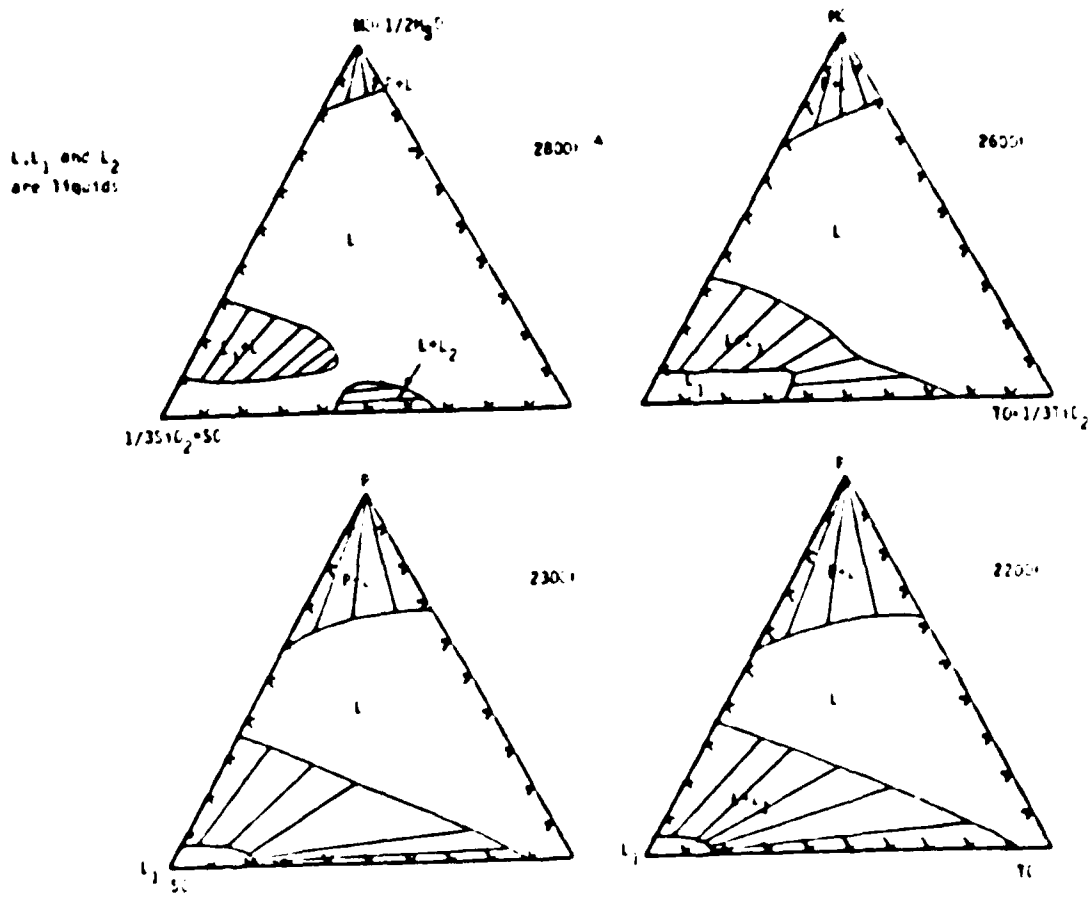


Figure 18 Calculated Isothermal Sections for Mn, TO, S

F-M .573 SC .026
 F-M .6 SC .6
 U-M .573 TC .026
 U-M .6 TC .6
 W-M .25 TC .75

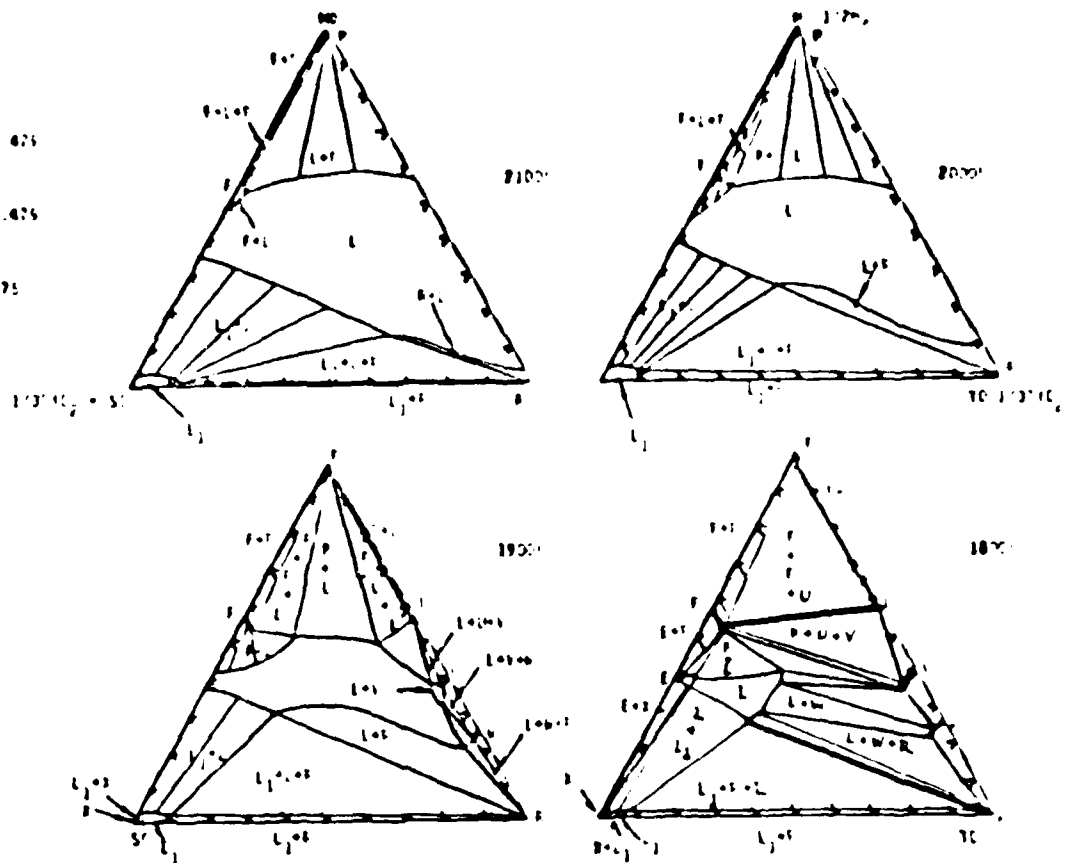


Figure 19. Calculated isothermal sections for Mg-TC-SC

F-MC .573 SC .026
 F-MC .6 SC .6
 U-MC .573 TC .026
 U-MC .6 TC .6
 W-MC .25 TC .75

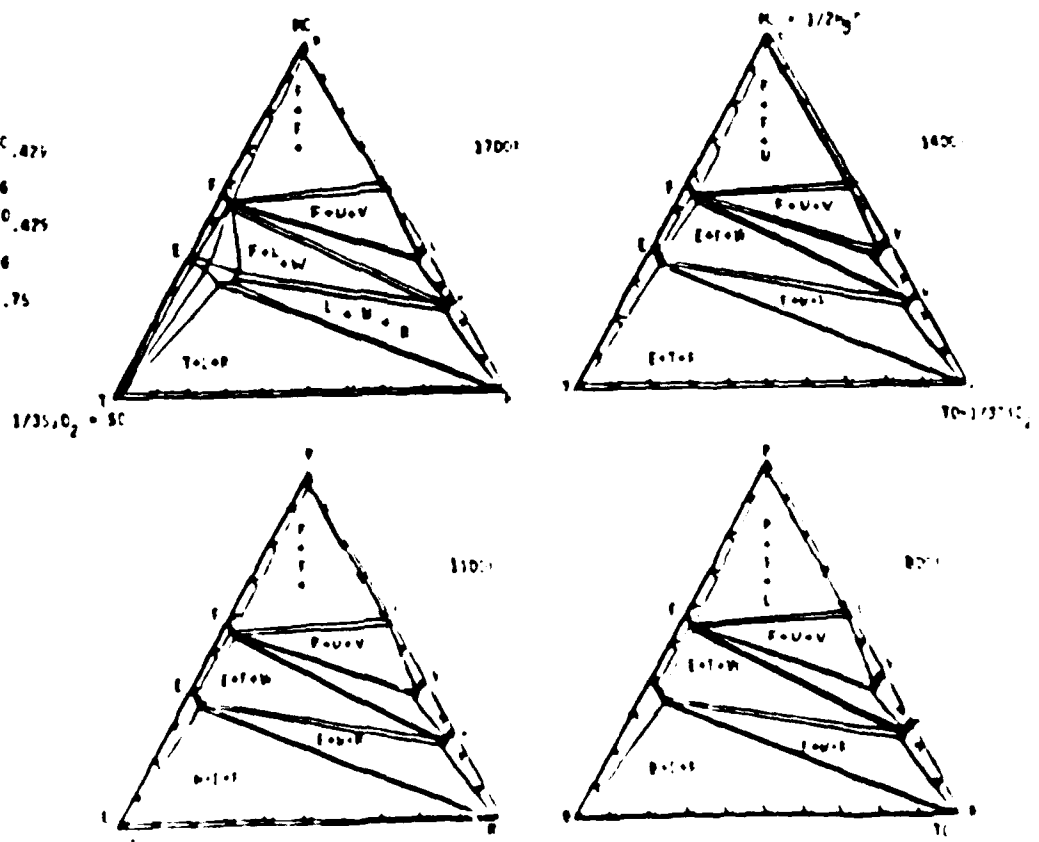


Figure 20. Calculated isothermal sections for Mg-TC-SC

723, 2542, 4573 and 4574 of (9). The minimum liquid temperature is reported at 1663°K which compares favorably with the calculated section at 1700°K in Figure 20. At high temperatures the equilibria is dominated by the interaction between the liquid miscibility gaps emanating from the MO-SO and SO-TO edges.

SUMMARY

The forgoing set of binary and ternary examples show how model calculations of ceramic phase diagrams can be performed to guide development of new structural systems and to evaluate existing experimental data. It also provides a means for planning future experimental studies.

ACKNOWLEDGEMENT

This research was sponsored by the Air Force Office of Scientific Research, Bolling Air Force Base, D.C. 20332 under Contract F49620-84-C-0078.

REFERENCES

1. L. Kaufman and H. Nesor, CALPHAD 2 (1978) 35.
2. L. Kaufman and H. Nesor, CALPHAD 3 (1979) 27.
3. L. Kaufman and H. Nesor, CALPHAD 3 (1979) 279.
4. L. Kaufman, F. Hayes, F. D. Hinnie, D., CALPHAD 5 (1981) 163.

5. L. Kaufman, F. Hayes, D. Birnie, D., High Temperatures - High Pressures 14 619 (1982).
6. L. Kaufman, User Application of Phase Diagrams pp. 147-178 (1978) ASM-International, Metals Park, Ohio.
7. S. T. Gulati, J. N. Hansson and J. D. Helfinstine, Metal Progress p. 21 Feb. 1984.
8. G. Kubaschewski, C. F. Alcock, C.F. "Metallurgical Thermochemistry Pergamon Press, Oxford (1979).
9. E. M. Levin, C. R. Robbins and H. F. McMurdie, "Phase Diagrams for Ceramists", American Ceramics Society, Columbus, Ohio (1964), (1969), (1975).
10. R. S. Roth, T. Negas, T. and L. Cook, "Phase Diagrams for Ceramists," American Ceramics Society, Columbus, Ohio (1981).
11. E. Fitzner, S. Neumann, and J. Slichting, Glastechn. Ber. (1983).
12. J. Slichting and S. Neumann, Jnl. of Non-Crystalline Solids 48 (1982) 185.
13. J. Lorentz, H. L. Lukas, H. L., E. F. Hucke, E. E. and L. J. Gaukler, CALPHAD 7 (1983) 125.

V. CALCULATION OF METAL-OXYGEN, METAL-CARBONITRIDE AND CERAMIC PHASE DIAGRAMS WITH THE THERMOCALC SYSTEM

The THERMOCALC system is a databank for thermochemistry and metallurgy developed at the division of Physical Metallurgy of the Royal Institute of Technology (KTH) in Stockholm. Using the facilities of THERMOCALC one can tabulate thermodynamic data, calculate the heat change of chemical reactions and their driving force, evaluate equilibria for chemical systems and phase transformations and calculate various types of multicomponent phase diagrams by an automatic mapping procedure. The databank is quite general and can be applied to all systems where data assessed by a model implemented in the databank are available [1]. Examples of applications include nine component tool steels, metal carbide and nitride systems as well as binary and multicomponent alloy systems. The present work was directed toward illustrating the application to metal-oxygen carbonitride and oxide systems. Copies of the THERMOCALC system were provided for this exercise by the division of Physical Metallurgy at KTH in Stockholm and stored on VAX computers at the Massachusetts Institute of Technology in Cambridge, Massachusetts and the National Bureau of Standards in Gaithersburg, Maryland. These installations were accessed remotely using IBM-PC and AT models via modem and telephone. Tables 1-4 and Figures 1-14 show the results obtained in the course of this study which covered the Fe-Ni-C, Fe-Cr-C, Ti-C-N and Al_2O_3 - Y_2O_3 - ZrO_2 systems.

Table 1 and Figure 1 display the results for the Fe-Ni-C system [2] at 1877. Table 1 contains the THERMOCALC description modeled after reference 2 while Figure 1 shows the output depicting the phase diagram as a function of oxygen pressure (ordinate) and nickel/(nickel + iron) ratio (abscissa). The THERMOCALC output is shown in the left while the output generated at the FACIT (Facility for Chemical Thermodynamics) at Ecole Polytechnique in Montreal is shown in the right. The lower panels show the tie lines defining the phase boundaries of the three phase fields as well as those covering the two phase fields in the ternary. The abscissa is nickel/(nickel + iron).

TABLE 1
THERMOCALC DATA FOR THE Fe-Ni-O SYSTEM

```

***** THERMOCALC ENERGY SYSTEM ON GAS OPS 178          1-71 60- 5- 0

ALL DATA IN SI UNITS
FUNCTIONAL VALUES FOR 258.15 TO 6000.00 K UNLESS OTHER LIMITS STATED

ELEMENT STATE ELEMENT REFERENCE  MASS      MISE-HI    SIZE
C  S  AVALUUM                    0.00000E+00  0.00000E+00  0.00000E+00
O  T  100                        5.01367E+01  0.00000E+00  0.00000E+00
Ni  S  FCC                        5.01367E+01  0.00000E+00  0.00000E+00
O  S  1/2 MOLE O2                 1.50683E+01  0.00000E+00  0.00000E+00

SPECIES
1  FE
2  NI
3  O
4  O2

STOICHIOMETRY
FE
NI
O
O2

EQU
EQUATION MODEL IS FE1.000+NI0.000+O0.000
CONSTITUENTS: FE,NI

O FE1.000+NI0.000+O0.000-HOSE FCC,FE10 * +0.00000E
O FCC,NI10-HOSE FCC,NI10 * 0.0
O FE1.000+NI0.000 * -16954.1+0.010000*T**2-4.18851E-05*T**3
O FCC,FE,NI10 * +16460.0+0.014017*T**2+0.001174E-05*T**3

FIND 1 MIX
O S: LATTICES, SITES 1 : 1
CONSTITUENTS: FE,NI : 0

O FE1.0,NI1.0,FE:O:O-HOSE FCC,FE:O-HOSE 1/2 MOLE GAS,O:O * +0.00000E
+0.00000E+0.00000E
O FE1.0,NI1.0,NI:O:O-HOSE FCC,NI:O-HOSE 1/2 MOLE GAS,O:O * +0.00000E
+0.00000E

HEMITE
O S: LATTICES, SITES 2 : 3
CONSTITUENTS: FE : 0

O HEMITE,FE:O:O-HOSE FCC,FE:O-HOSE 1/2 MOLE GAS,O:O *
0.00000E+0.00000E-16954.1+0.010000*T**2-4.18851E-05*T**3

SPECIES
EQUATION MODEL IS FE1.000+NI0.000+O0.000
O S: LATTICES, SITES 3 : 3
CONSTITUENTS: FE : FE,NI : O

O SPINEL,FE:FE:O:O-HOSE FCC,FE:O-HOSE 1/2 MOLE GAS,O:O
+0.00000E+0.00000E+0.00000E+0.00000E
O SPINEL,FE:NI:O:O-HOSE FCC,FE:O-HOSE 1/2 MOLE GAS,O:O
+0.00000E+0.00000E+0.00000E+0.00000E
O SPINEL,FE:NI:O:O-HOSE FCC,NI:O-HOSE 1/2 MOLE GAS,O:O
+0.00000E+0.00000E+0.00000E+0.00000E

MAGNET
O S: LATTICES, SITES 4 : 4
CONSTITUENTS: FE : O

O MAGNET,FE:O:O-HOSE FCC,FE:O-HOSE 1/2 MOLE GAS,O:O *
+0.00000E+0.00000E

SPECIES
STATUS VALUE/FUNCTION
1  FE  0.000000  0.3144800E+00
2  NI  0.000000  0.3144800E+00
3  O2  0.000000  0.3144800E+00
4  O  0.000000  0.3144800E+00
*****

```

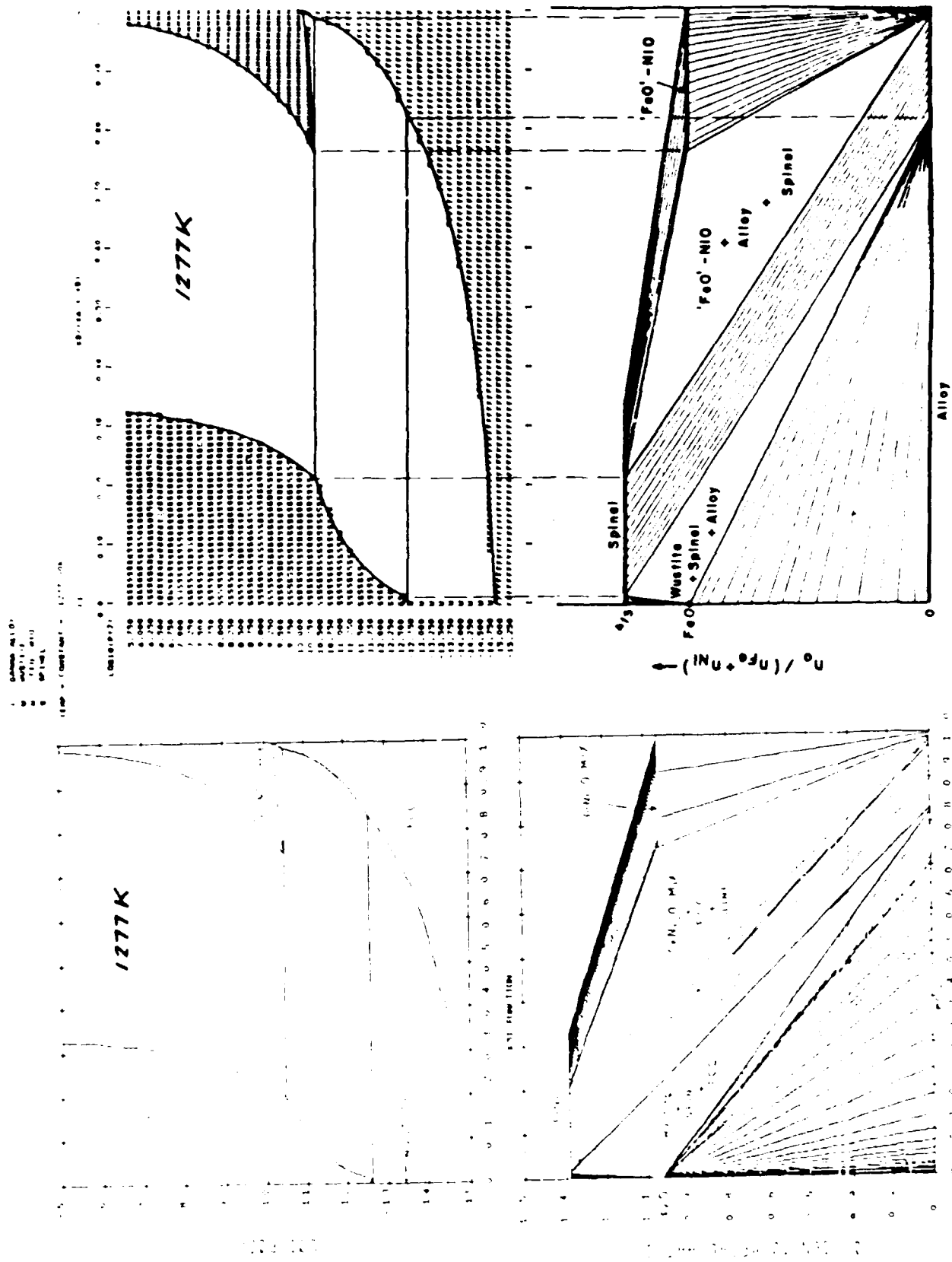


Figure 1. Thermocalc Output for Fe-Ni-O (left) compared with FACT Output (right)

TABLE 2
THERMOCALC DATA FOR THE Fe-Cr-O SYSTEM

```

EXTRACT FROM COMBUSTION ENERGY SYSTEM ON 04/20/85 12:48
DATE EC- 5- 7

ALL DATA IN SI UNITS
FUNCTIONS VALUE FOR 298.15 K 6000.00 K UNLESS OTHERWISE SPECIFIED

ELEMENT STABLE ELEMENT REFERENCE MASS MOLE-WEIGHT EDSE
C CR 12.0107 0.0000E+00 0.0000E+00 0.0000E+00
O O 16.00 0.0000E+00 0.0000E+00 0.0000E+00
FE FE 55.845 0.0000E+00 0.0000E+00 0.0000E+00
GAS 1.0000E+00 0.0000E+00 0.0000E+00 0.0000E+00
1/2 MOLE GAS 0.5000E+00 0.0000E+00 0.0000E+00 0.0000E+00

SPECIES STOICHIOMETRIES
1 CR CR
2 O O
3 FE FE
4 GAS C
5 1/2 MOLE GAS C

FOO
EXCESS MODEL IS FEILICH-HIESTER-MUGGIAND
CONSTITUENTS: CR,FE

G(FOO,CR;O)-M2SE(FOO,CR;O) = +10400-6.076*T
G(FOO,FE;O)-M2SE(FOO,FE;O) = +9100FE
G(FOO,CR,FE;O) = +7400-6.076*T

FE2O4
2 SUBLATTICES, SITES 1 : 1
CONSTITUENTS: FE : O

G(FE2O4,FE;O;O)-M2SE(FOO,FE;O)-M2SE(1/2 MOLE GAS,O;O) = -(0000)
+20.0014*T-9100FE

WEMATITE
EXCESS MODEL IS FEILICH-HIESTER-MUGGIAND
2 SUBLATTICES, SITES 2 : 3
CONSTITUENTS: CR,FE : C

G(WEMATITE,CR;O;O) - 2 M2SE(FOO,CR;O) - 3 M2SE(1/2 MOLE GAS,O;O) =
500.00 T - 2000.00 - 3129700+265.24*T-5.445*T^2+LOG(T)
G(WEMATITE,FE;O;O) - 2 M2SE(FOO,FE;O) - 3 M2SE(1/2 MOLE GAS,O;O) =
500.00 T - 2000.00 - 823010+240.51*T-11.585*T^2+LOG(T)

SPINEL
EXCESS MODEL IS FEILICH-HIESTER-MUGGIAND
3 SUBLATTICES, SITES 1.666666 : 1.333333 : 1.333333
CONSTITUENTS: CR,FE : FE : O

G(SPINEL,CR;FE;O;O)-0.666666 M2SE(FOO,CR;O)-0.333333 M2SE(FOO,FE;O)
-1.333333 M2SE(1/2 MOLE GAS,O;O) =
298.15 T - 2000.00 + 0.333333*9100FE
G(SPINEL,FE;FE;O;O)-0.555555 M2SE(FOO,FE;O)-1.333333 M2SE(1/2 MOLE GAS,O;O)
-1.333333 M2SE(1/2 MOLE GAS,O;O) = -358540+20.006*T-5.322*T^2+LOG(T)-9100FE

LUCIFER
2 SUBLATTICES, SITES 1 : 1
CONSTITUENTS: LI : O

G(LUCIFER,FE;O;O)-M2SE(FOO,FE;O)-M2SE(1/2 MOLE GAS,O;O) = -264800
+01.0014*T-9100FE

SPECIES STATUS VALUE/FUNCTION
1 CR 0.000000 0.31448000E+00
2 O 0.000000 +9.7420005.800000E-01*(*)
3 FE 0.000000
4 GAS 0.000000
5 1/2 MOLE GAS 0.000000 +3451.7000-0.074475*T*(*)-1.1E-04*T^2+3.0.05434E-07*T^3
6 CR 0.000000 +0.00E+00-3.4018*T-1.0074T^2+3.0-5.1004E-06*T^3
7 O 0.000000 +0.00E+00-5.4970-0.000000*T^2+0.0000E-07*T^3+3
8 CR 0.000000
9 O 0.000000 +1447700-200.80*T-4.0000*T^2+LOG(T)

```

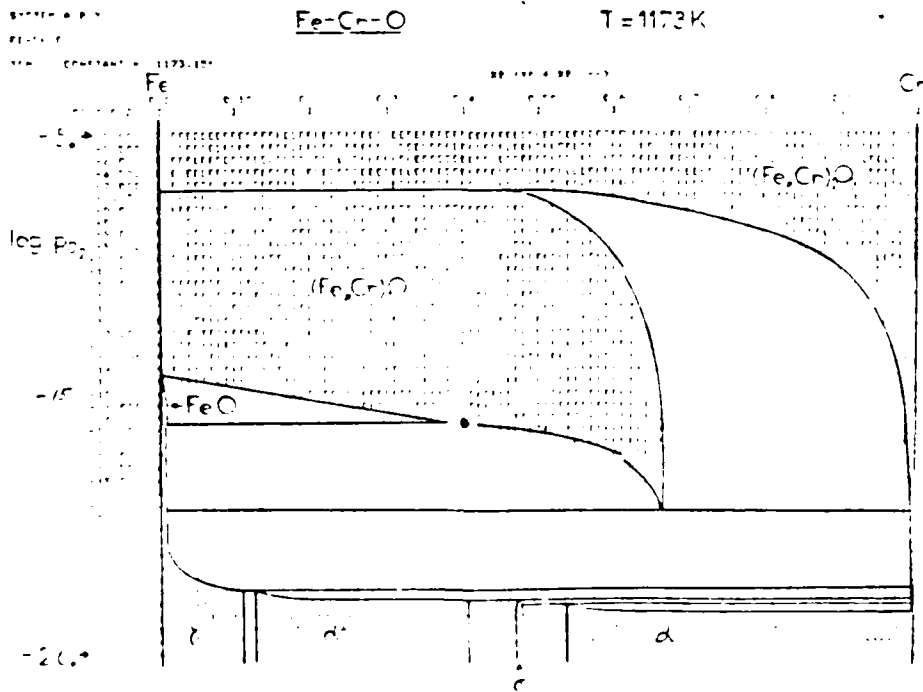
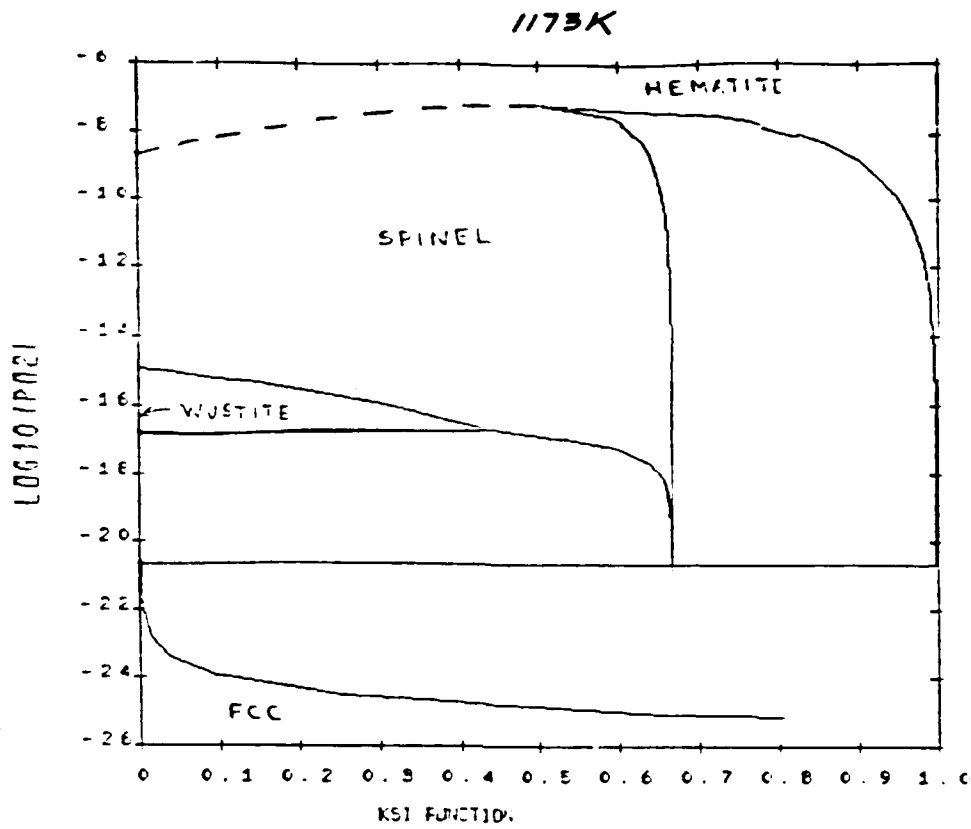


Figure 2. Thermocalc Output for fcc, Hematite, Spinel and Wustite (above) compare with FACT Output (below)

TABLE 3
THERMOCALC DATA FOR THE Ti-C-N SYSTEM

OUTPUT FROM EISEE ENERGY SYSTEM ON VAX/VMS KTH DATE 87- 6-12

ALL DATA IN SI UNITS
FUNCTIONS VALID FOR 298.15 TO 6000.00 K UNLESS OTHER LIMITS STATED

ELEMENT	STABLE	ELEMENT	REFERENCE	MASS	H298-H0	S298
0 VA	VACUUM			0.0000E+00	0.0000E+00	0.0000E+00
1 C	GRAPHITE			1.2011E+01	0.0000E+00	0.0000E+00
2 N	1/2MOLE_GAS			1.4007E+01	0.0000E+00	0.0000E+00
3 TI	HCF			4.7880E+01	0.0000E+00	0.0000E+00

SPECIES	STOICHIOMETRY
1 C	C
2 N	N
3 TI	TI
4 VA	VA

GRAPHITE

CONSTITUENTS: C

$$G(\text{GRAPHITE}, \text{C}; 0) - \text{H298}(\text{GRAPHITE}, \text{C}; 0) = 0.0$$

NITROGEN

CONSTITUENTS: N

$$G(\text{N2}, \text{N}; 0) - \text{H298}(\text{1/2MOLE_GAS}, \text{N}; 0) = 0.0$$

TiCN

2 SUBLATTICES, SITES 2 + 1

CONSTITUENTS: TI + N

$$G(\text{TiCN}, \text{TI}; 0) - \text{H298}(\text{1/2MOLE_GAS}, \text{N}; 0) - 2 \text{H298}(\text{HCF}, \text{TI}; 0) = -504976 + 18.1678T$$

Ti FCC

EXCESS MODEL IS REDLICH-HISTER_MUGGIANDU

2 SUBLATTICES, SITES 1 + 1

CONSTITUENTS: TI + C, N, VA

$$G(\text{Ti FCC}, \text{TI}; 0) - \text{H298}(\text{GRAPHITE}, \text{C}; 0) - \text{H298}(\text{HCF}, \text{TI}; 0) = -163979 + 10.5778T$$

$$G(\text{Ti FCC}, \text{TI}; 0) - \text{H298}(\text{1/2MOLE_GAS}, \text{N}; 0) - \text{H298}(\text{HCF}, \text{TI}; 0) = -333323 + 2.62148T$$

$$G(\text{Ti FCC}, \text{TI}; \text{VA}; 0) - \text{H298}(\text{HCF}, \text{TI}; 0) = 3347.2$$

$$G(\text{Ti FCC}, \text{TI}; \text{C}, \text{VA}; 0) = -62358 + 1.50628T$$

$$G(\text{Ti FCC}, \text{TI}; \text{C}, \text{VA}; 1) = -162343 + 46.158T$$

$$G(\text{Ti FCC}, \text{TI}; \text{C}, \text{N}; 0) = -22073$$

$$G(\text{Ti FCC}, \text{TI}; \text{N}, \text{VA}; 0) = -10460 + 18.418T$$

Ti FCC

EXCESS MODEL IS REDLICH-HISTER_MUGGIANDU

2 SUBLATTICES, SITES 1 + 2

CONSTITUENTS: TI + C, N, VA

$$G(\text{Ti FCC}, \text{TI}; 0) - 2 \text{H298}(\text{GRAPHITE}, \text{C}; 0) - \text{H298}(\text{HCF}, \text{TI}; 0) = +20936.8 + 2.05678T$$

$$G(\text{Ti FCC}, \text{TI}; \text{N}; 0) - 3 \text{H298}(\text{1/2MOLE_GAS}, \text{N}; 0) - \text{H298}(\text{HCF}, \text{TI}; 0) = -466203 + 1.7788T$$

$$G(\text{Ti FCC}, \text{TI}; \text{VA}; 0) - \text{H298}(\text{HCF}, \text{TI}; 0) = +4351 - 3.76568T$$

$$G(\text{Ti FCC}, \text{TI}; \text{C}, \text{VA}; 0) = -4184.1$$

$$G(\text{Ti FCC}, \text{TI}; \text{C}, \text{VA}; 1) = -8768.1$$

Ti FCC

EXCESS MODEL IS REDLICH-HISTER_MUGGIANDU

2 SUBLATTICES, SITES 2 + 1

CONSTITUENTS: TI + C, N, VA

$$G(\text{Ti FCC}, \text{TI}; 0) - \text{H298}(\text{1/2MOLE_GAS}, \text{N}; 0) - 2 \text{H298}(\text{HCF}, \text{TI}; 0) = -393046 + 1.7788T$$

$$G(\text{Ti FCC}, \text{TI}; \text{VA}; 0) - \text{H298}(\text{HCF}, \text{TI}; 0) = 0.0$$

$$G(\text{Ti FCC}, \text{TI}; \text{C}, \text{VA}; 0) = -41770 - 14.3928T$$

Ti FCC

EXCESS MODEL IS REDLICH-HISTER_MUGGIANDU

2 SUBLATTICES, SITES 1 + 1

$$G(\text{Ti FCC}, \text{TI}; 0) - \text{H298}(\text{GRAPHITE}, \text{C}; 0) = +114210.2 - 27.1968T$$

$$G(\text{Ti FCC}, \text{TI}; \text{N}; 0) - \text{H298}(\text{1/2MOLE_GAS}, \text{N}; 0) = -8890.168 + 66.860328T$$

$$G(\text{Ti FCC}, \text{TI}; \text{VA}; 0) - \text{H298}(\text{HCF}, \text{TI}; 0) = +10564.92 - 12.13368T$$

$$G(\text{Ti FCC}, \text{TI}; \text{C}, \text{VA}; 0) = +52000.47 - 9328T$$

$$G(\text{Ti FCC}, \text{TI}; \text{C}, \text{VA}; 1) = +107679.4 - 97168T$$

$$G(\text{Ti FCC}, \text{TI}; \text{C}, \text{N}; 0) = +102379.71 - 768T$$

$$G(\text{Ti FCC}, \text{TI}; \text{C}, \text{N}; 1) = +107479.4 - 71368T$$

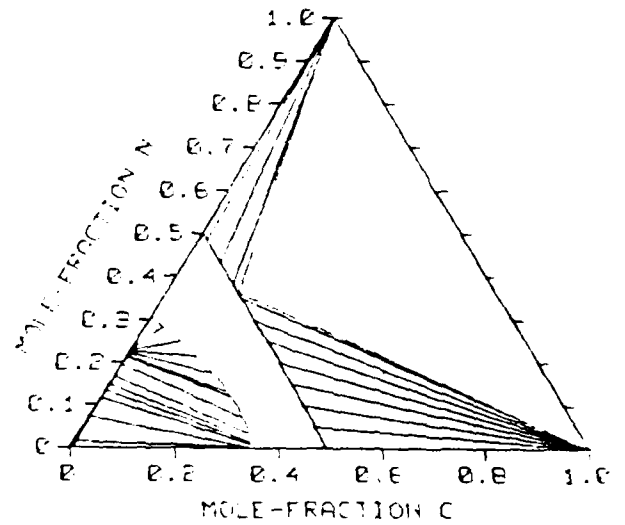
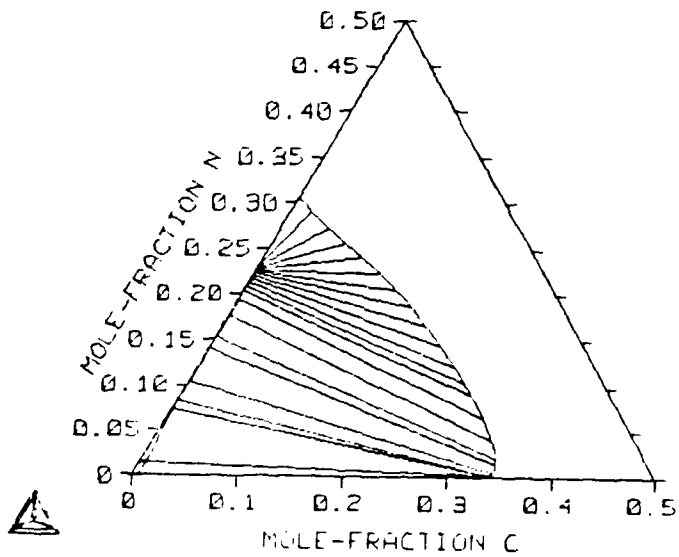
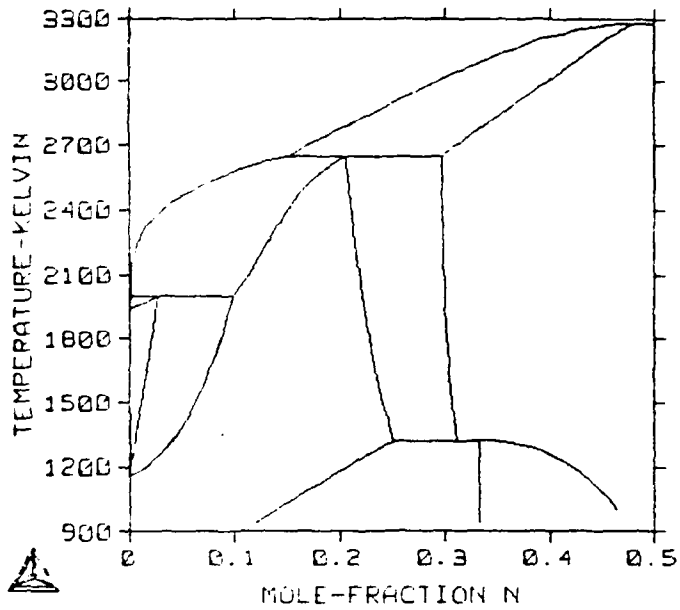


Figure 3. Calculated Ti-N Phase Diagram and Ti-N-C Isothermal Section at 1600K from the Thermocalc System.

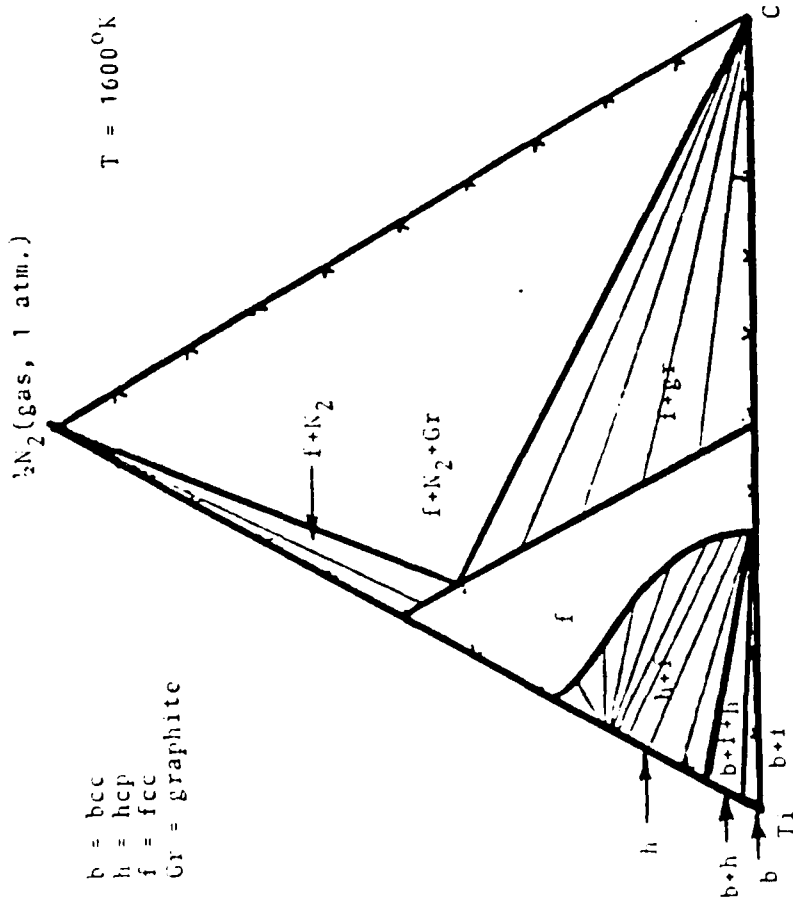
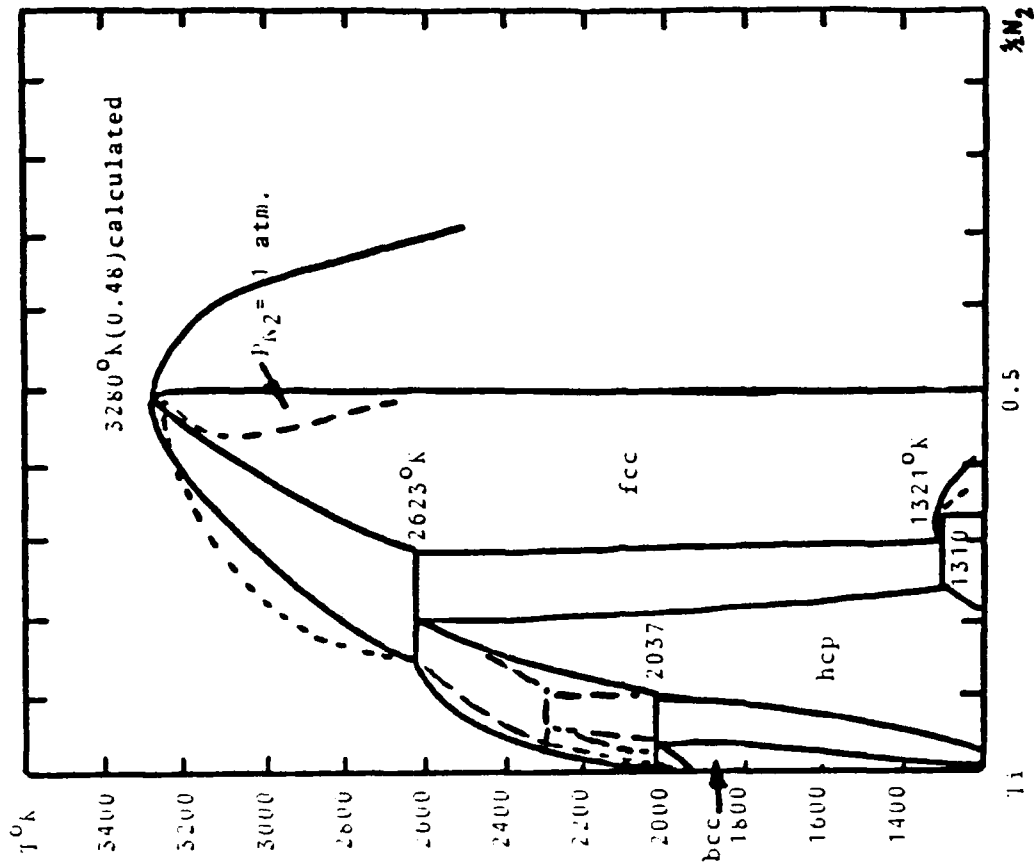


Figure 4. Calculated Ti-N and Ti-N-C Isothermal section at 1600K
From the ManJabs System.

TABLE 4

SUMMARY OF LATTICE STABILITY, SOLUTION AND COMPOUND
PHASE PARAMETERS FOR THE CALCULATION OF AO-ZO-YO

Summary of Lattice Stability Parameters, T in Kelvins

(All units in Joules per gram atom (mole of atoms), T in Kelvins)

AO=(1/5) Al₂O₃, ZO=(1/3) ZrO₂, YO=(1/5) Y₂O₃, L= Liquid

C= Corundum, Y=high temperature (hexagonal) Y₂O₃, B=bcc

(Mn₂O₃) Y₂O₃, A=ZrO₂ cubic, T=ZrO₂ Tetragonal, M=ZrO₂ Monoclinic

ZOZOLA=(1/3) ZrO₂ (liquid)-(1/3) ZrO₂ (CaF₂) Cubic

AOAOLC=23640-10.209T

AOAOLA= - 9.832T

AOAOLT= -10.586T

ZOZOAT=1987-0.753T

ZOZOTM=2008-1.381T

ZOZOLA=29008- 9.832T

ZOZOLC= -10.209T

ZOZOLY=17991- 8.368T

ZOZOLB=24853- 9.205T

YOYOLY=22694- 8.368T

YOYOLB=26878-10.042T

YOYOLA=22615- 9.832T

YOYOAT=-8368- 0.753T

YOYOTM=-8368- 1.381T

Summary of Solution and Compound Phase Parameters

(All units in Joules per gram atom (mole of atoms), T in Kelvins)

LZCAO=17573, LAOZO=39748, TZCAO=TAOZO=AZCAO=AAOZO=62760

CAOZO=CZCAO=62760

Solution Phases

LZOYO= 14016 + 4.184T

LYOZO= 14016 + 4.184T

BZOYO= 2929 + 8.368T

BYOZO= 2929 + 8.368T

AZOYO=-12552 +11.297T

AYOZO= 837 + 4.602T

YZOYO= 2929 + 8.368T

YYOZO= 2929 + 8.368T

TZOYO=-12552 + 11.297T

TYOZO= 837 + 4.602T

MZOYO= 4184 + 11.297T

MYOZO= 837 + 4.602T

Compound Phase = P = (1/19) (3ZrO₂·2Y₂O₃)=(1/19) Z_{0.9}Y_{0.10}

Z_{0.474}Y_{0.526}, Base =A, Compound Parameter C= 31798 +

11.097T, Gibbs Energy of Formation from (1/3) ZrO₂ (L) and

(1/5) Y₂O₃ (B), $\Delta G_f = -286 - 2.86T$

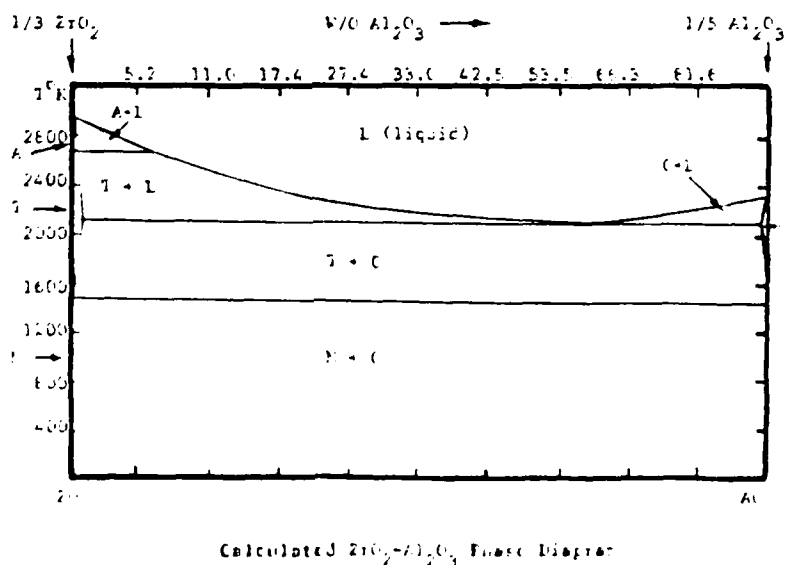
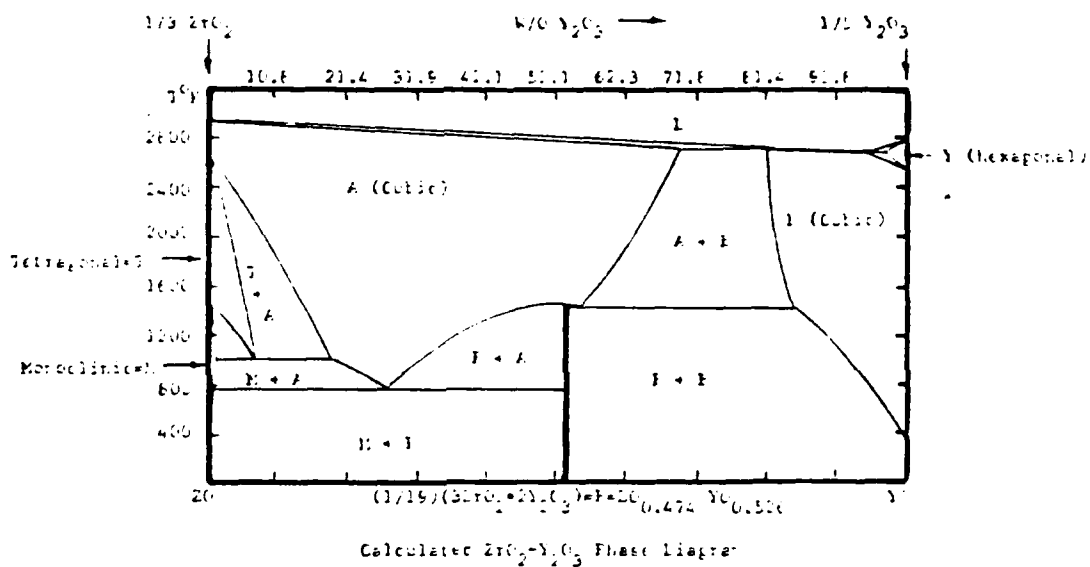
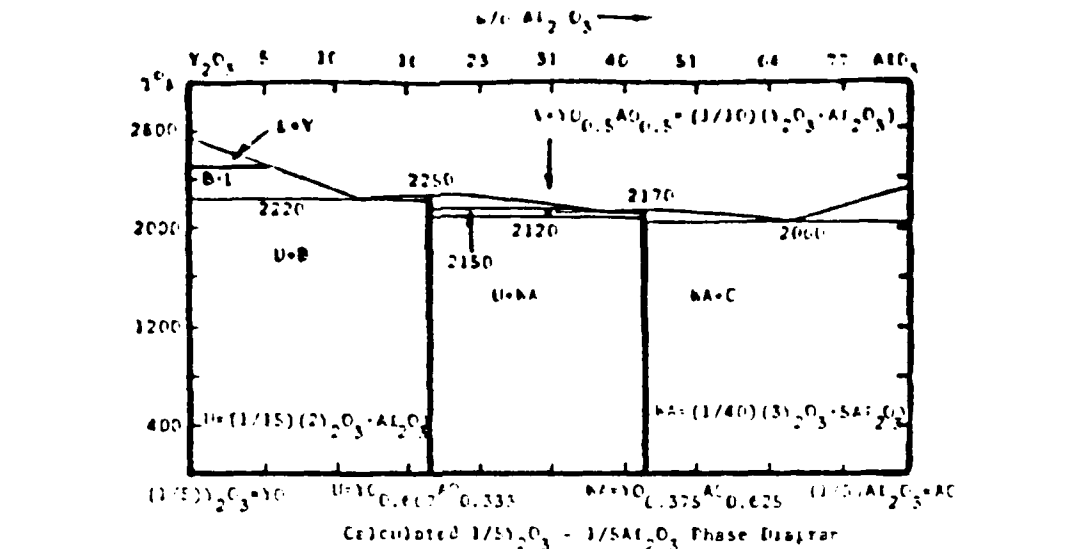


Figure 5. Calculation of the YO-AO, ZO-YO and ZO-AO Phase Diagrams on the ManLabs System.

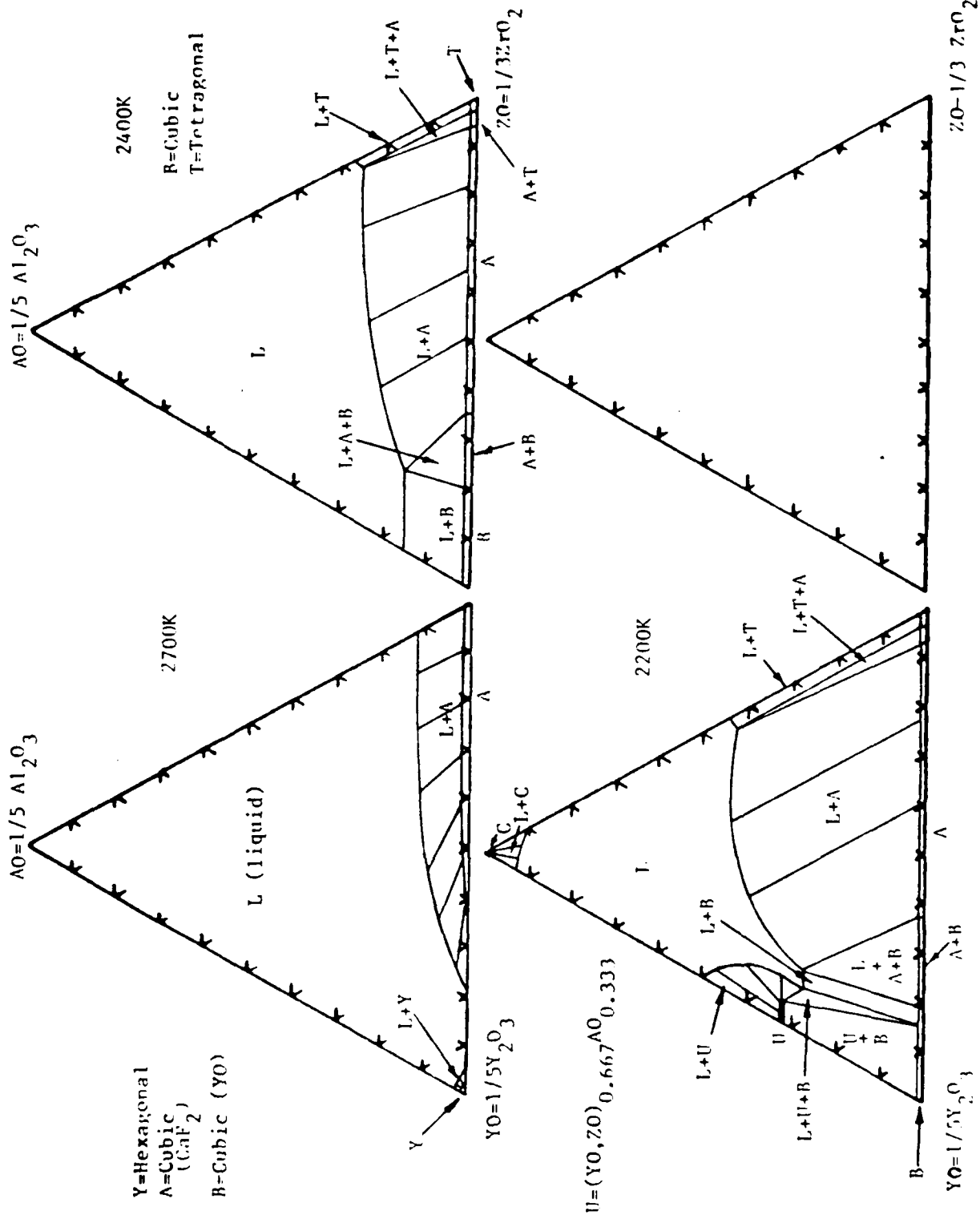


Figure 6. Calculated isothermal sections in the $Al_2O_3-ZrO_2-Y_2O_3$ system (ManLabs System).

$W = (Y_0, Z_0) 0.375 \text{ Al}_2\text{O}_3, 0.625 \text{ Y}_2\text{O}_3$
 $U = (Y_0, Z_0) 0.667 \text{ Al}_2\text{O}_3, 0.333 \text{ Y}_2\text{O}_3$

L = Liquid
 C = Corundum
 A = Cubic (CaF_2)
 H = Cubic
 I = Tetragonal

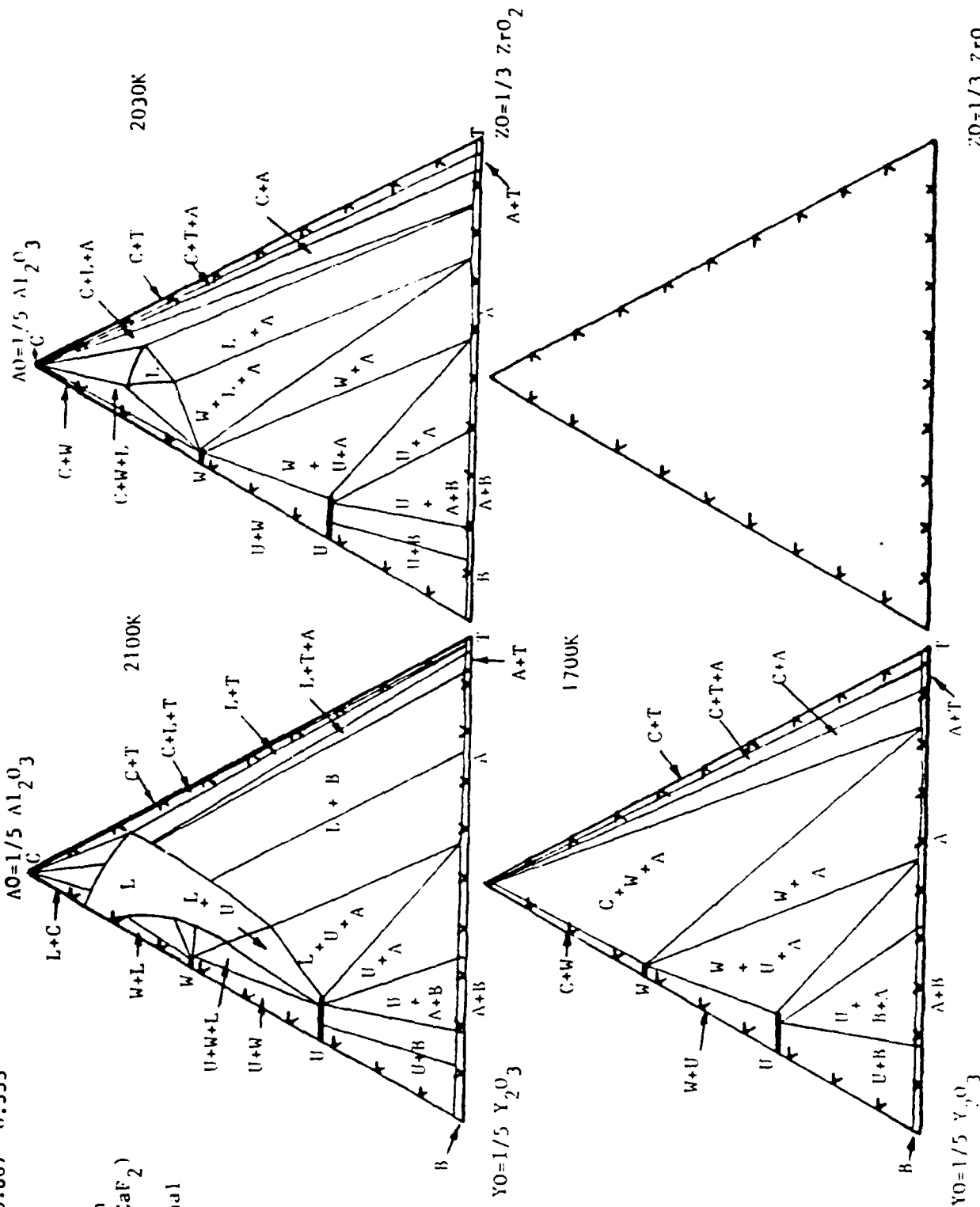


Figure 7: Calculated Isothermal Sections in the $\text{Al}_2\text{O}_3\text{-ZrO}_2\text{-Y}_2\text{O}_3$ System (ManLabs System).

TABLE 5

SUMMARY OF LATTICE STABILITY, SOLUTION AND COMPOUND PHASE PARAMETERS
FOR THE CALCULATION OF THE AM-ZM-YM SYSTEM (Joules, °K)

AM=1/2Al₂O₃, ZM=ZrO₂, YM = 1/2Y₂O₃

C=Corundum, Y=high temperature (hexagonal), B=bcc (Mn₂O₃)Y₂O₃

A=ZrO₂ cubic, T=ZrO₂ Tetragonal, M=ZrO₂ Monoclinic

LATTICE STABILITY PARAMETERS

AMAMLC=59100-25.5T	ZMZMAT=5961-2.26T
AMAMLA= -24.58T	ZMZMTM=6024-4.14T
AOAOLT= -24.47T	
	YMYMLY=56735-20.92T
ZMZMLA=87024-29.50T	YMYMLB=67195-25.11T
ZMZMLC= -30.63T	TMTMLA=56538-24.58T
ZMZMLY=53973-25.10T	YMYMAT=-20920-1.88T
ZMZMLB=74559-27.61T	YMYMTM=-20920-3.45T

SOLUTION PHASE PARAMETERS

LZMYM=-1674-37.66T	LYMZM=63178-37.66T	LZMAM=LAMZM=4184
BZMYM=-18410-25.10T	BYMZM=46442-31.38T	TZMAM=TZMAN=41840
AZMYM=-26778-33.47T	AYMZM=38074-39.75T	AZMAM=AMZM=41840
TZMYM=-26778-33.47T	TYMAM=38074-39.75T	CZMAM=CAMZM=41840
YZMYM=-18410-25.10T	YYMZM=46442-31.38T	
MZMYM=7950-33.47T	MYMZM=38074-39.75T	
LYMAM=-66944	LAMYM=-66944	
YYMAM=-20920	YAMYM=-20920	
BYMAM=-20920	BAMYM=-20920	
CYMAM=-20920	CAMYM=-20920	

COMPOUND PARAMETERS

P=ZM_{.429}YM_{.571}=1/7(3ZrO₂·2Y₂O₃); Base phase=A; C=84308-17.99T

U=YM_{.677}AM_{.333}=1/6(2Y₂O₃·Al₂O₃); Base phase=B; C=67362+17.49T

V=YM_{.5}AM_{.5}=1/4(Y₂O₃·Al₂O₃); Base phase=C; C=24058+60.25T

W=YM_{.375}AM_{.625}=1/16(5Y₂O₃·3Al₂O₃); Base phase=C; C=135980-2.89T

$Y_O = 1/5 \quad Y_2 \quad O_3$
 $Y_M = 1/2 \quad Y_2 \quad O_3$
 $A_O = 1/5 \quad Al_2 \quad O_3$
 $A_M = 1/2 \quad Al_2 \quad O_3$

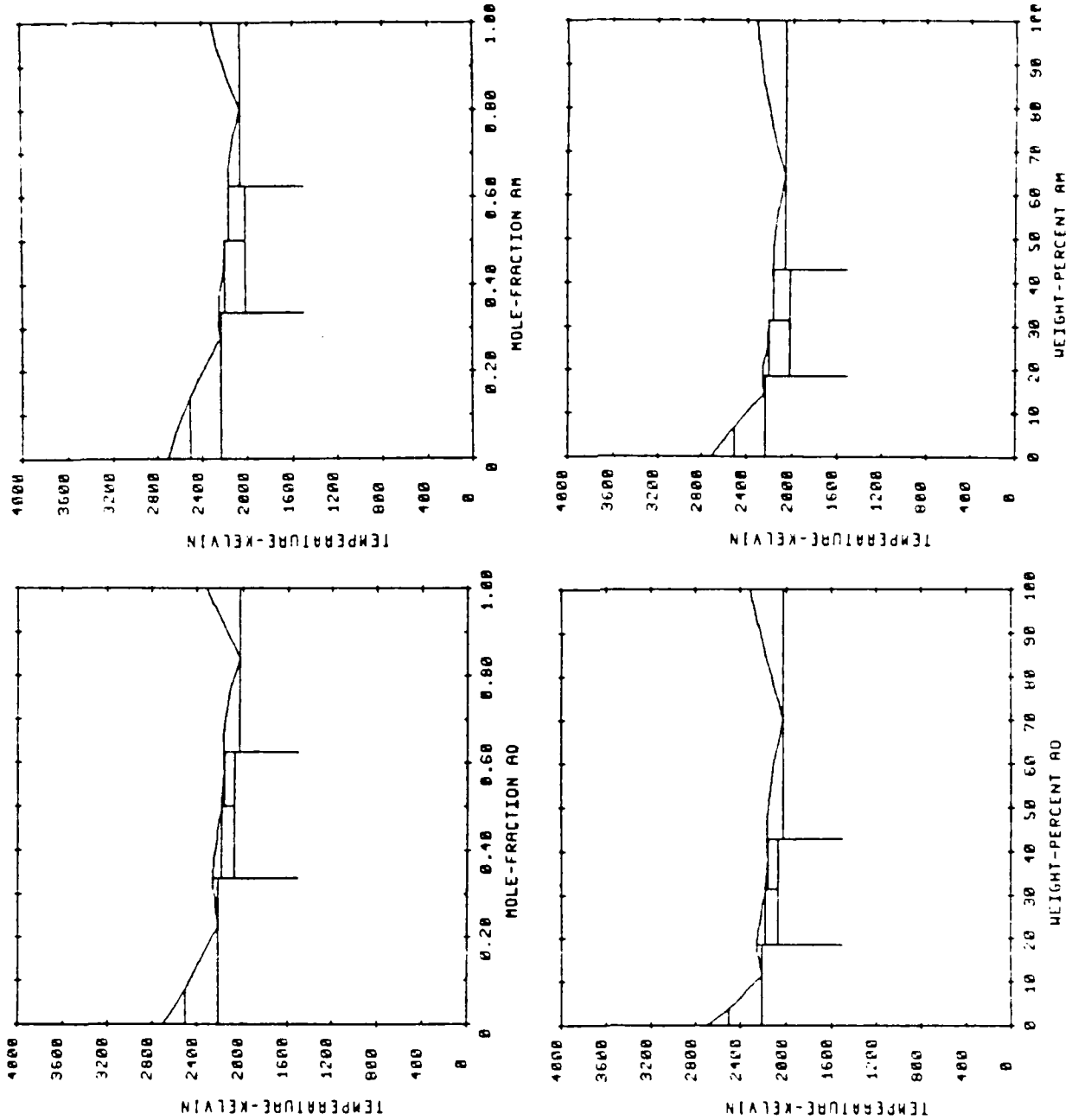


Figure 8. Thermocalc output for calculation of YO-AO and YM-AM Systems as a function of mol fraction and weight percent AO and AM (see Figure 5)

$$ZO = 1/3 \text{ Zr O}_2$$

$$ZM = \text{Zr O}_2$$

$$YO = 1/5 \text{ Y}_2 \text{ O}_3$$

$$YM = 1/2 \text{ Y}_2 \text{ O}_3$$

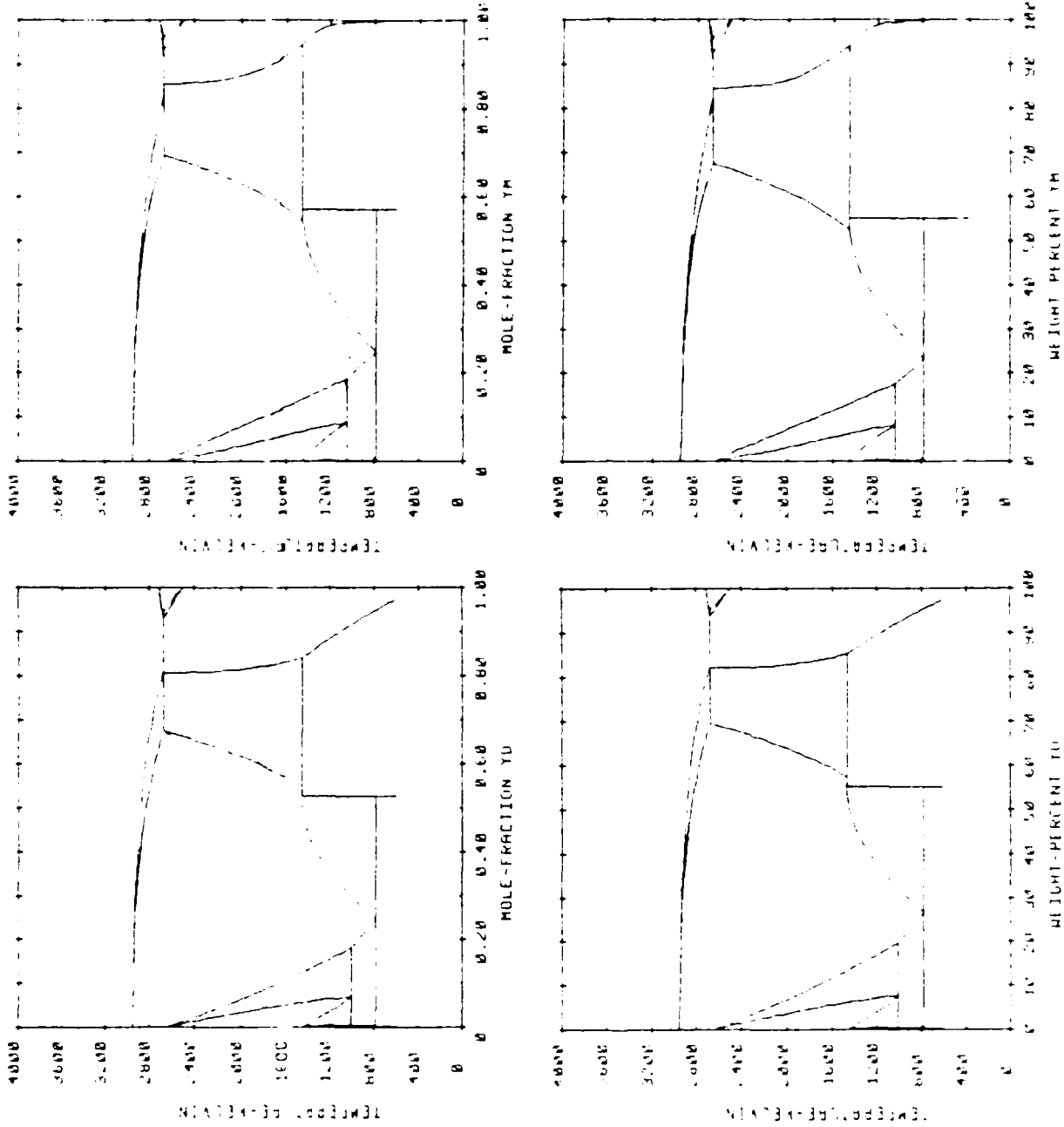


Figure 9. Thermocalc output for calculation of ZO-YO and ZM-YM

as a function of mol fraction and weight percent

YO and YM. (See Figure 5)

ZO = 1/3 ZrO₂
 ZM = ZrO₂
 AO = 1/5 Al₂O₃
 AM = 1/2 Al₂O₃

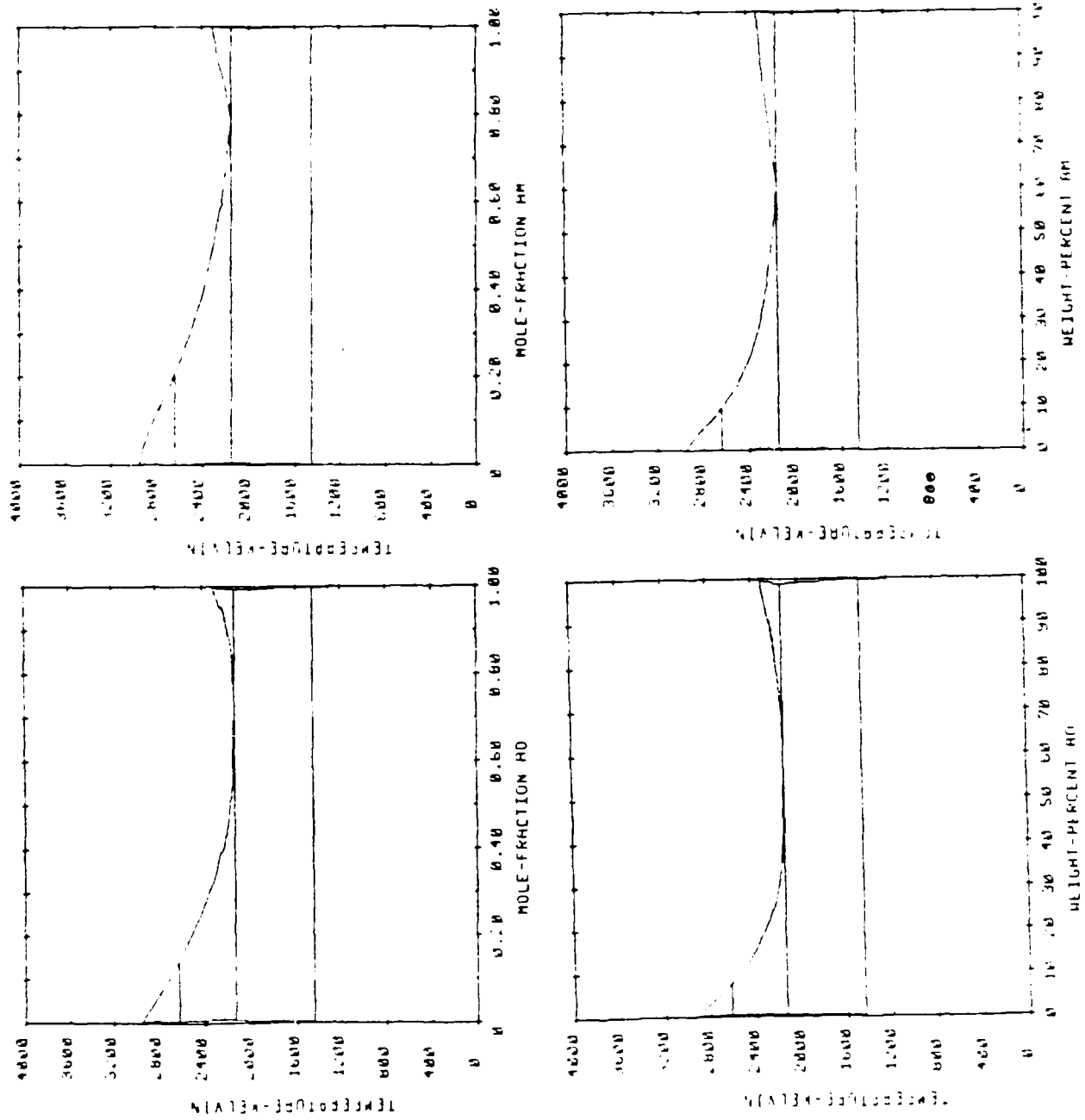


Figure 10 Thermocalc Output for calculation of ZO-AO and ZM-YM as a function of mol fraction and weight percent AO and AM (See Figure 5).

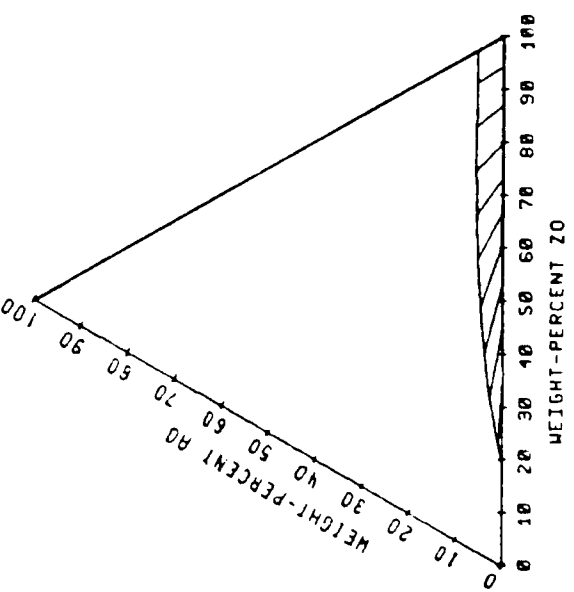
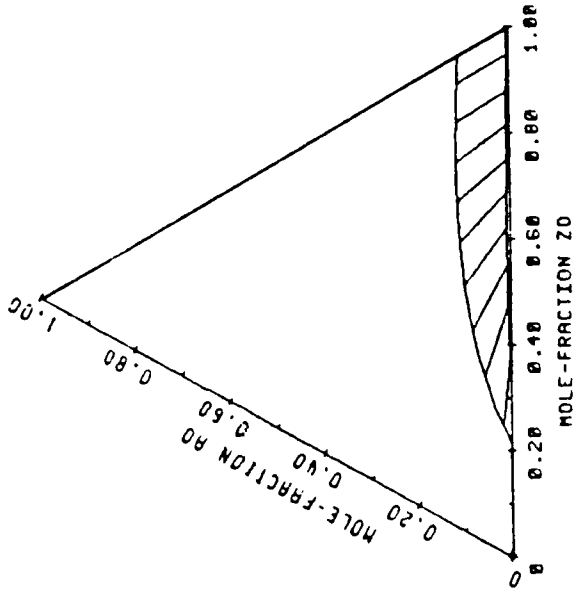
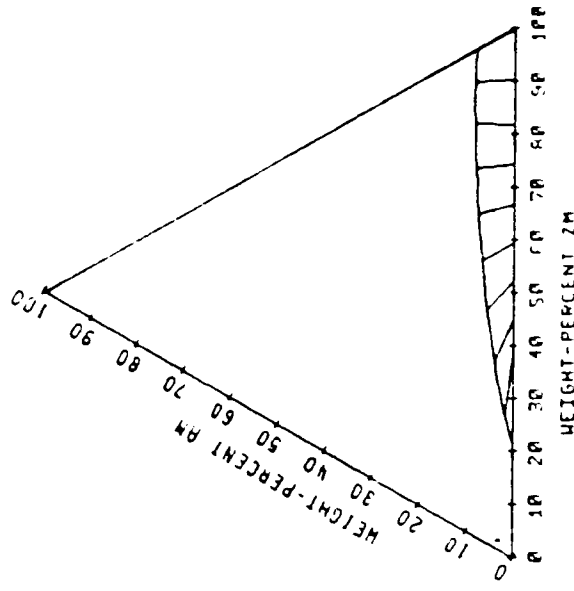
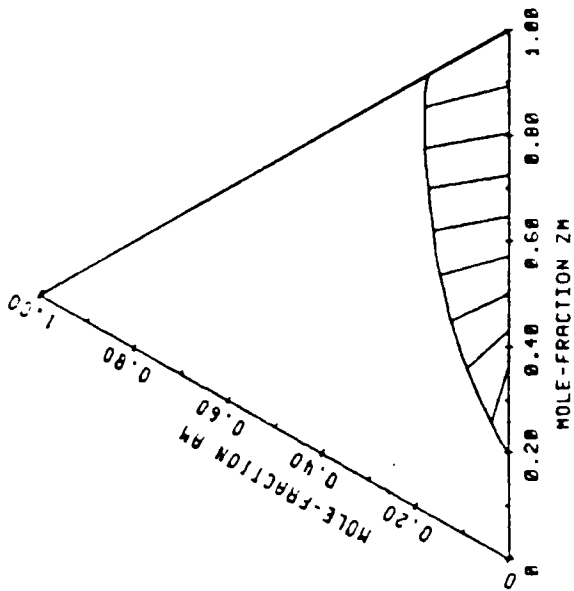


Figure 11 Thermocalc output for AO-ZO-YO and AM-ZM-YM at 2700K
(See Figure 6)

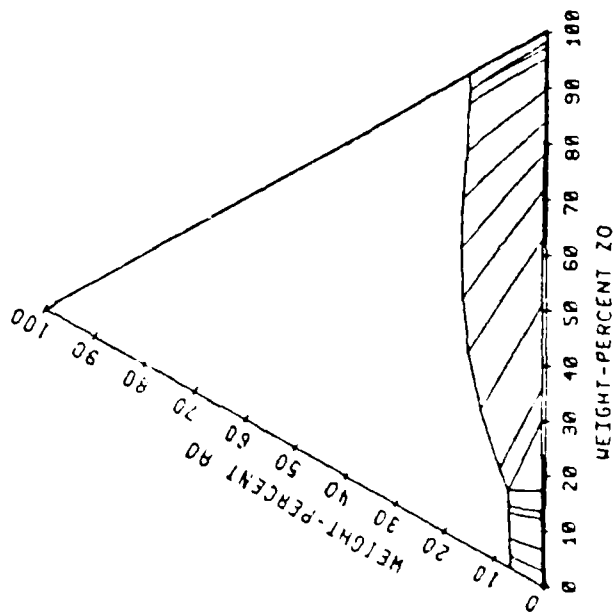
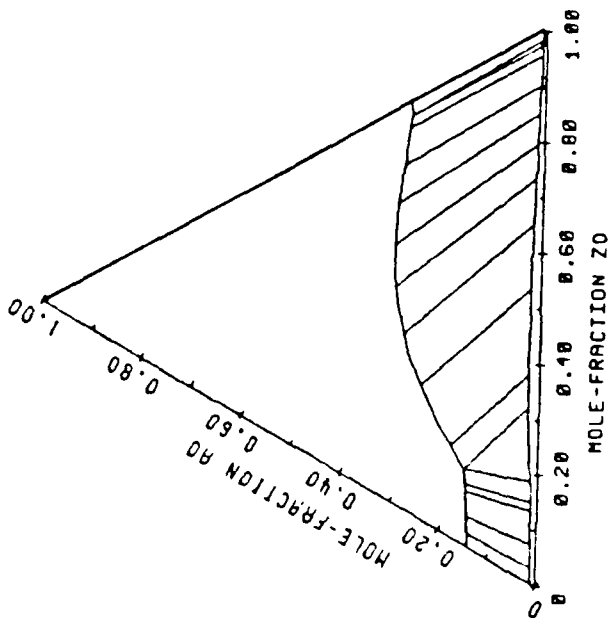
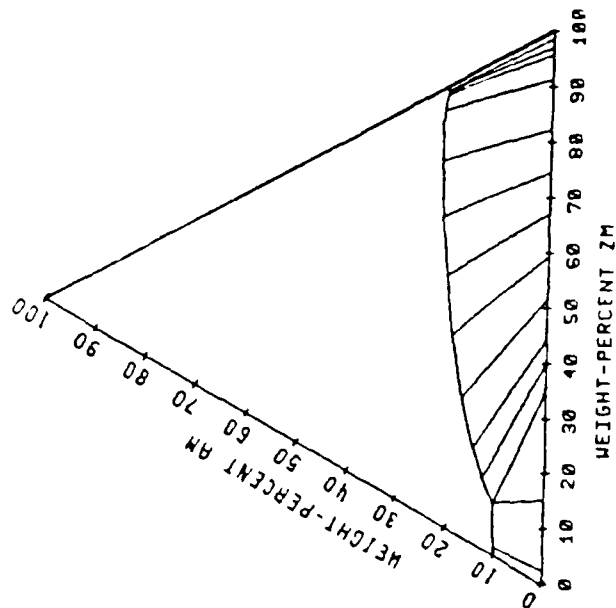
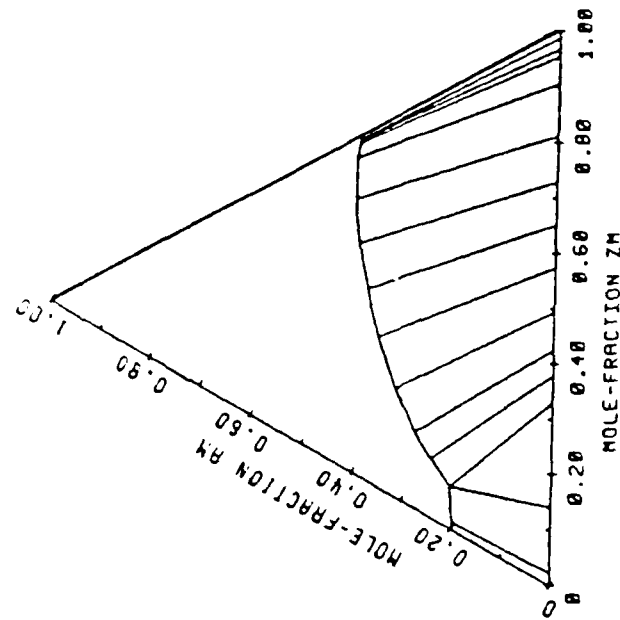


Figure 12 Thermocalc Output for A0-Z0-Y0 and AM-ZM-YM at 2400K

(See Figure 6)

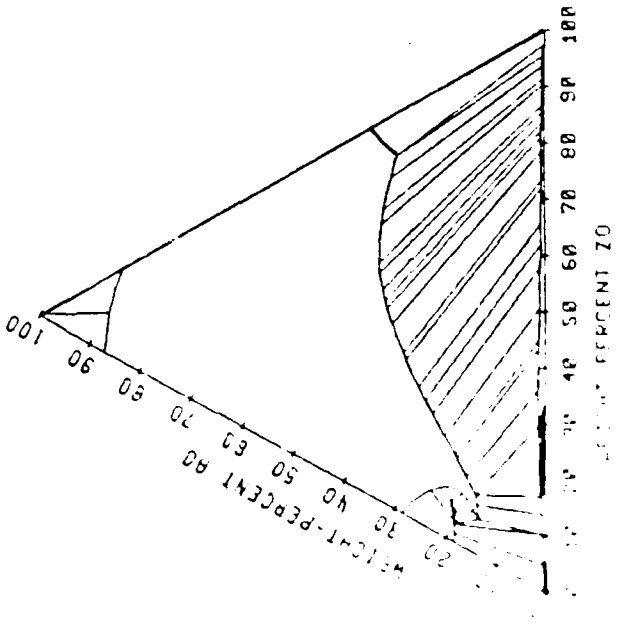
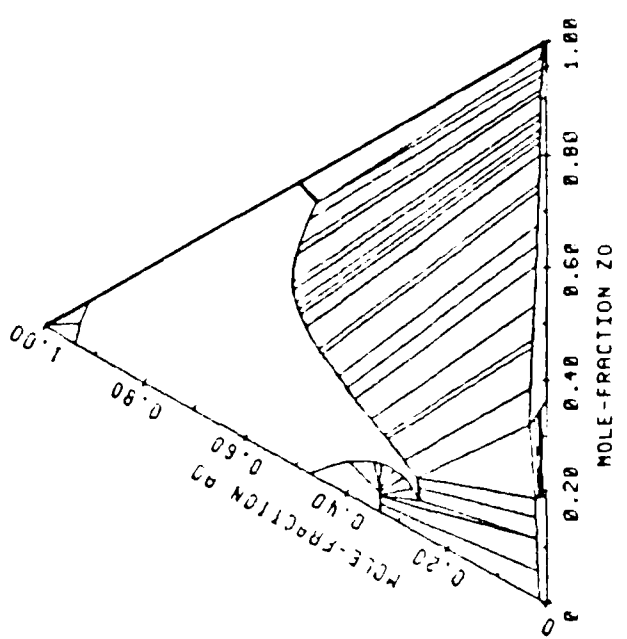
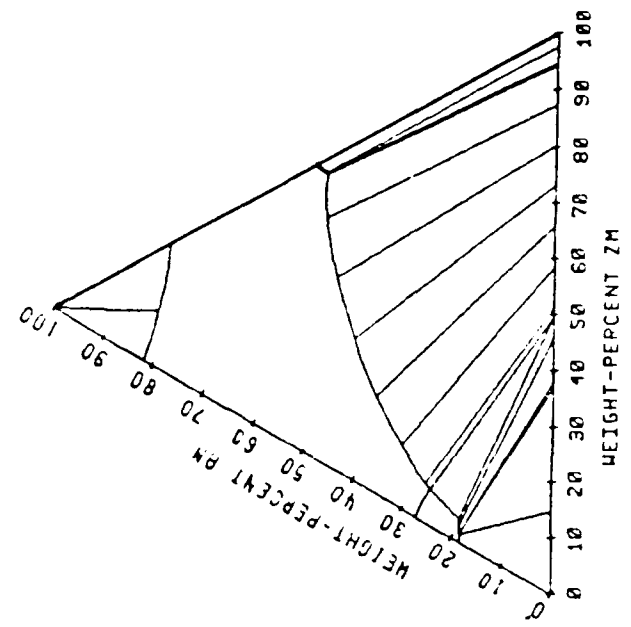
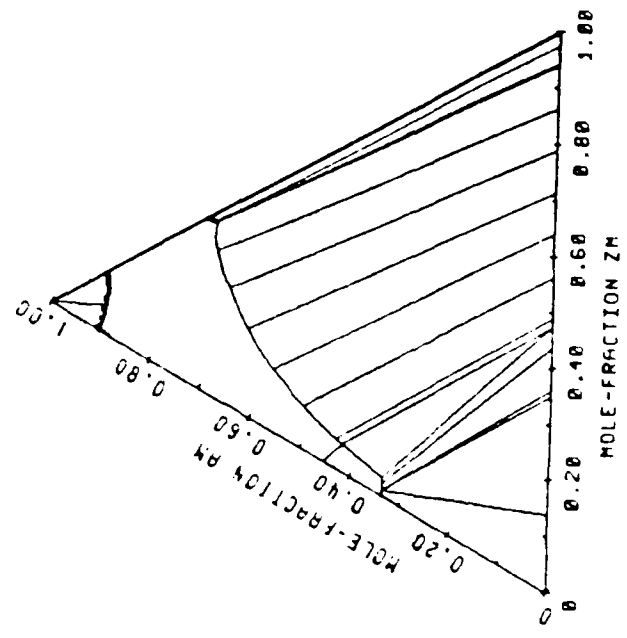


Figure 7) Thermocouple Output for A0-Z0-Y0 and AM-ZM-YM at 2200K

AD-A183 174

APPLICATION OF COMPUTER METHODS FOR CALCULATION OF
MULTI COMPONENT PHASE. (U) MANLABS INC CAMBRIDGE MASS
L KAUFMAN 31 JUL 87 AFOSR-TR-87-0920 F49620-84-C-0078

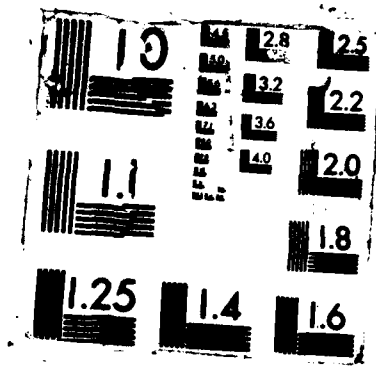
2/2

UNCLASSIFIED

FFG 11/2

NL





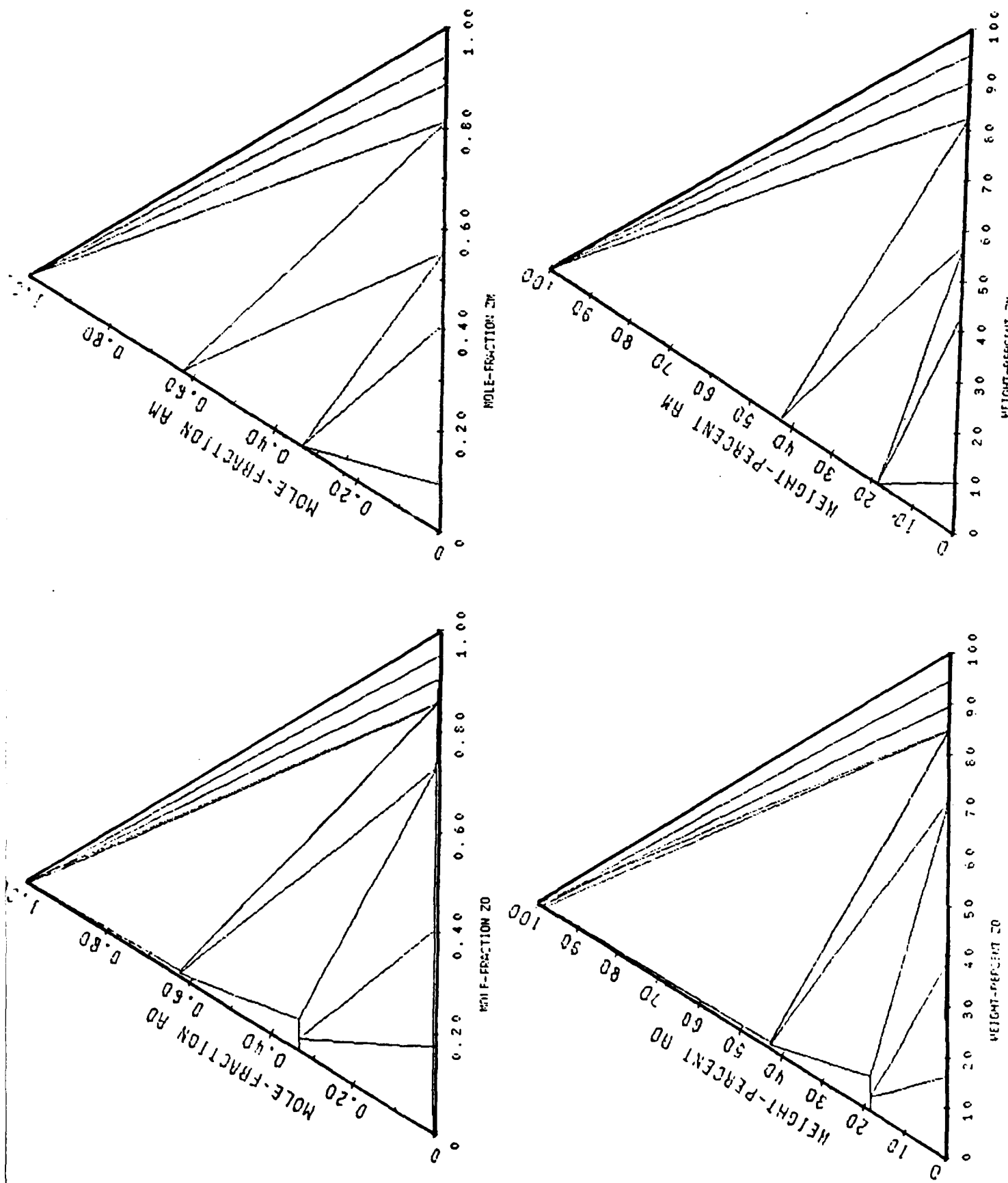


Figure 14 Thermocalc Output for AO-ZO-YO- and AM-ZM-YM at 1700K (See Figure 6)

Table 2 and Figure 2 show a similar exercise for the Fe-Cr-O system. The only difference being that the fcc metallic phase (γ) is the only one included in the THERMOCALC description while the FACT description (2) also contains the sigma (σ) and bcc (α) phases which emanate from the Fe-Cr edge. The Fe-Ni-O and Fe-Cr-O examples shown above demonstrate how this system can be employed to compute metal-metal-oxygen phase diagrams. Table 3 and Figures 3 and 4 show a similar exercise performed in a calculation of the Ti-C-N system at 1600K comparing the ManLabs system (Figure 4) and the THERMOCALC system (Figure 3) The fcc phase is the monocarbide Ti(C,N). The dashed lines in Figure 4 are the experimental phase boundaries in the Ti-1/2N₂ phase diagram. Table 3 and Figures 3 and 4 show how the THERMOCALC system can readily be applied to treating hard metal carbonitride systems.

The final example selected for the study is the Al₂O₃-ZrO₂-Y₂O₃ system which is shown in Table 4 and Figures 5-7. In this case the system is model as AO-ZO-YO ie 1/5 Al₂O₃-1/3 ZrO₂-1/5 Y₂O₃. Table 4 summarizes the lattice stability, solution and compound phase parameters along the lines described earlier in Sections III and IV. The systems in question have been recalculated on a mole metal basis ie as AM-ZM-YM where AM=1/2 /Al₂O₃, ZM=ZrO₂ and YM=1/2 Y₂O₃ on the basis of Table 5 by matching the Gibbs energies of each of the phases in the systems of interest. Table 5 summarizes the AM-ZM-YM description while Figures 8-14 show the results derived with THERMOCALC. Figure 8 shows YO-AO and YM-AM in mol and weight percent. The upper left panel in Figure 8 compares directly with the upper panel in Figure 5. Figures 9 and 10 show comparable results for ZO-YO, ZM-YM, ZO-AO and ZM-YM. Finally Figures 11-14 show isothermal sections at 2700, 2400, 2200 and 1700. Comparison of the weight percent ternary sections shows little difference between the gram atom model and the mole-metal model. These results illustrate the general utility of the THERMOCALC system!

REFERENCES

1. B. Sundman, B. Jansson and J.O. Andersson, CALPHAD 9 153(1985).
2. A.D. Pelton and H. Schmalzreid, Met. Tr. 4 1395.

Approved for public release;
distribution unlimited.

AIR FORCE OFFICE OF SCIENTIFIC AND TECHNICAL SERVICES
NOTICE OF DISSEMINATION RIGHTS
This document contains information that is not to be disseminated
outside the Department of Defense without the approval of the
Director, Office of Scientific and Technical Services, AFOSI/AIR 190-12.
MATTHEW J. LAMPER
Chief, Technical Information Division

END

9-87

Dtic